Algemeen Relativistische Plasma Dynamica

een wetenschappelijke proeve op het gebied van de
Natuurwetenschappen, Wiskunde en Informatica

PROEFSCHRIFT

ter verkrijging van de graad van doctor
aan de Radboud Universiteit Nijmegen
op gezag van de Rector Magnificus prof. dr. C.W.P.M. Blom,
volgens besluit van het College van Decanen
in het openbaar te verdedigen op maandag 8 mei 2006
des namiddags om 1.30 uur precies
door
Joachim Benedictus Moortgat
geboren op 15 juni 1977
te Keulen, Duitsland.

Promotor:

Prof. dr. J. Kuijpers

Manuscript commissie:

Prof. dr. N.P. Landsman (voorzitter)
Subfaculteit Wiskunde

Prof. dr. A. Achterberg
Sterrekundig Instituut
Universiteit Utrecht

Dr. M. Marklund
Department of Physics
University of Umeå

Prof. dr. D.B. Melrose
School of Physics
University of Sydney

Prof. dr. R.A.M.J. Wijers
Sterrenkundig Instituut 'Anton Pannekoek'
Universiteit van Amsterdam

ISBN-10: 90-9020493-8
ISBN-13: 978-90-9020493-2

Dit proefschrift is mede tot stand gekomen dankzij financiële steun van de Nederlandse Onderzoekschool voor Astronomie, NOVA.

General Relativistic Plasma Dynamics

A Scientific Essay in Physics and Astronomy

DOCTORAL THESIS

to obtain the degree of doctor
from Radboud University Nijmegen
on the authority of the Rector, Prof. C.W.P.M. Blom,
according to the decision of the Council of Deans
to be defended in public on Monday, 8 May 2006
at 1.30 p.m. precisely
by
Joachim Benedictus Moortgat
born in Cologne, Germany
on 15 June 1977.

Doctoral supervisor:

Prof. dr. J. Kuijpers

Members of the Doctoral Thesis Committee:

Prof. dr. N.P. Landsman (chair)
Subfaculty of Mathematics

Prof. dr. A. Achterberg
Astronomical Institute
Utrecht University

Dr. M. Marklund
Department of Physics
University of Umeå

Prof. dr. D.B. Melrose
School of Physics
University of Sydney

Prof. dr. R.A.M.J. Wijers
Astronomical Institute 'Anton Pannekoek'
University of Amsterdam

ISBN-10: 90-9020493-8
ISBN-13: 978-90-9020493-2

This doctoral thesis was made possible in part by funding from the Netherlands Research School for Astronomy, NOVA.

Contents

List of Figures

List of Tables

Acknowledgements

First of all, I would like to thank my supervisor Jan Kuijpers and congratulate him for setting up a successful new astrophysics department in Nijmegen: in only the four years that I was a PhD student here we grew from a group of only three to over twenty members. My time at the department was made more fruitful and enjoyable by the new faculty members Paul and Gijs N. who organised seminars and colloquia followed by departmental drinks, by the new PhD students Gijs R., Sven and my local paranimph Stijn with whom I organised many clandestine drinks, haute cuisine dinners in the coffee room and barbecues on the roof of our new building, and by the rest of the department who each contributed their own particular characters to the institute.

On the international front, I would like to thank my colleagues at the Aristotle University in Thessaloniki, Greece, for their generous hospitality during a very pleasant and productive workshop. At Caltech, USA, I owe gratitude to prof. Sterl Phinney for inviting me for an extended visit to the TAPIR group, and to profs. Thorne, Kamionkowski, Piran, Kulkarni and the rest of the department for many interesting weekly meetings and discussions. I especially appreciated my collaboration with Mattias Marklund, during his visit to Nijmegen and my subsequent stay at his institute in Umeå, Sweden, where I also thank Gert Brodin and the entire department for their hospitality.

During the past years my academic life was balanced by frequent dinner parties, pub crawls and trips with my friends in Utrecht. I would like to thank in particular my second paranimph Hylke Koers who proof-read all my papers and thesis, Sandra, Jeroen, Ytsen, Vincent, Esther, Job, Jasmijn, Morag, Guiot, Hans, Teffie and several more for always being there for me.

None of this would have been possible without the support offered by my parents Michael and Elisabeth, from the financial to the psychological and practical and by my sister Judith. Finally, my biggest support in the past nine years has been my fiancé Suzanne with whom I shared both the pleasures and occasional frustrations of our PhD projects, alternated with as much travelling as we could get away with to refresh our minds.

CHAPTER 1

Introduction

GRAVITY is the weakest of the fundamental forces and, not surprisingly, gravitational waves (GW) have proven to be the most elusive signals in astronomy. In fact, now that almost every electromagnetic frequency window is observable and even cosmic ray and neutrino astronomy are becoming a reality, the first direct detection of gravitational waves still has to be made. With the development of advanced resonant bar and in particular interferometric GW detectors, this will most likely happen within the next one or two decades.

The same property of GW that makes them so hard to detect is their main advantage as a diagnostic of the Universe: because GW hardly interact with anything, the entire Universe is transparent to them. The planned Laser Interferometer Space Antenna, LISA[1] expects to detect the signal from merging supermassive black holes out to any distance and the Laser Interferometer Gravitational-wave Observatory, LIGO[2], which has recently achieved design sensitivity, could for instance probe the central engines of gamma-ray bursts (GRBs) which are opaque to all electromagnetic radiation.

In general, electromagnetic and GW observations are very complimentary and an electromagnetic counterpart to any GW signal and vice versa is invaluable. As an example: with electromagnetic observations it is very difficult to determine the inclination of a binary system, whereas this could be easily measured from the polarization of a GW signal (Schutz 1996). On the other

[1] LISA website: `http://lisa.jpl.nasa.gov/`
[2] LIGO website: `http://www.ligo.caltech.edu/`

hand, the amplitude of a GW measured on earth does not allow a unique determination of the distance and the intrinsic strain at the source (which can be determined only from the chirp of the system). When the distance can be determined electromagnetically from the red-shift, this uncertainty can readily be removed.

Rather than studying different types of GW sources and trying to find accompanying electromagnetic processes, we investigate in this thesis whether the GW *themselves* produce an electromagnetic signal when they propagate through the magnetohydrodynamic (MHD) plasma in which many GW sources are embedded. In particular, one can think of rapidly spinning neutron stars with a small asymmetry, low-mass X-ray binaries, neutron stars with an r-mode instability, asymmetric supernova core collapse and bounce (GRB with afterglow), newly born neutron stars that boil and oscillate (magnetars) and coalescing compact binaries (short GRB candidates). Gravitational waves interact already to linear order with media that have an anisotropic stress-energy tensor. Interaction is therefore possible with a magnetized MHD plasma and not, for instance, with dust or an isotropic hydrodynamic ideal fluid.

An entirely different arena where the dynamical properties of gravity play an important role is in *cosmological models*. During the radiation era, the Universe was filled with a hot homogeneous plasma but since then somehow structure must have formed on all scales since we see stars, galaxies and clusters of galaxies. A clue to the origin of this structure is provided by the *cosmic microwave background* (CMB). As the Universe expanded, the plasma eventually cooled to $\simeq 3000$ K, allowing the electrons and protons to recombine to neutral hydrogen. At that time the photons that were previously coupled to the matter by Thomson scattering could escape and since then have been free-streaming and cooling adiabatically to the currently observed ~ 3 K CMB radiation. The recent results of WMAP[3] have shown, however, that the CMB is *not* completely homogeneous but shows a scale-free spectrum of temperature (or equivalently density) perturbations in accordance with the predictions of *inflation theory*.

These density fluctuations are best described by general relativistic, gauge-invariant covariant perturbation theory. In the final chapter of this thesis we extend this theory to a two-component plasma where the species have different temperatures. We study the thermal effects on scalar perturbations of a Friedmann-Lemaître-Robertson-Walker (FLRW) Universe.

1.1 Outline

The thesis is set up as follows. Chapters 3–6 comprise the main content and closely follow four refereed journal papers (Moortgat and Kuijpers 2003, 2004, 2006; Moortgat and Marklund 2006), the references to which are given at the

[3] WMAP website: `http://www.gsfc.nasa.gov/`

beginning of each chapter. In the independent Chapter 2, the theoretical background of differential geometry, gauge-invariance, the 3+1-split and tetrads is given in some more detail than in the published papers. In this way, the treatment in this thesis is made more self-consistent, yet clearly separates personal contributions from more standard theory. The remaining chapters are heavily cross-referenced with the theoretical backbone in Chapter 2.

Chapter 3 presents our first exploration of the effect of a gravitational wave propagating through a magnetized plasma. A GW interacts only directly with the magnetic field, and the geodesic deviations caused by a GW are in its transverse plane. Hence, we first consider a GW propagating *perpendicularly* to a uniform magnetic field and neglect the gas pressure. We present numerical estimates that show that indeed the GW are converted into MHD waves in the plasma. These results are generalized in Chapter 4 were we include the gas pressure, both polarizations of the GW and arbitrary angles with respect to the magnetic field. We find that Alfvén as well as slow and fast magnetosonic waves can be excited and study their properties and back-reaction on the GW. In Chapter 5 we investigate whether the MHD waves that are excited at the kiloHertz GW frequencies, can inverse-Compton scatter to observable radio emission at ~ 100 MHz.

The application of the same techniques to the influence of temperature effects on *cosmological* scalar perturbations and structure formations are considered in Chapter 6, and we end with a summary of our contributions and conclusions in Chapter 7.

1.2 Units

Throughout Chapters 3–4, Gaussian geometrized units with $G = c = 1$ are adopted in the equations but the numerical results are given in standard units (for instance in Section 3.6). Chapters 5–6 use standard geometrized units.

Latin indices $a \ldots e$ stand for $0, 1, 2, 3$ as a reminder that we consider tensors as abstract geometrical objects living on a curved space time, rather than vectors and tensor *components* on a flat space-time. For the latter, as in Special Relativity, we use the Greek alphabet, for instance in Chapter 5.

CHAPTER 2

Theoretical framework: Differential Geometry

EINSTEIN'S theory of general relativity (GR) is a *geometrical* theory. The gravitational *force* of Newton –acting at a distance– is replaced by a *dynamical space-time* where in the proximity of massive objects more space is created and clocks tick slower. Many physical problems can be described more elegantly and even more intuitively in this picture but this comes at a cost. Simple concepts that one is accustomed to but that depend on a flat *Euclidean* geometry, fail in a curved space-time. For example, parallel lines can intersect, the shortest distance between two points is not necessarily 'straight' and there is no unique way to define a global coordinate system in which to describe physics.

Already in the Special Theory of Relativity is was necessary to define *tensor* quantities corresponding to pre-relativity physical quantities. Tensors are defined as quantities that have the same form in every inertial frame. When one specifies to a particular coordinate system one can calculate the tensor *components* that resemble those of vectors or matrices. Products and sums of tensors can then be found by manipulating the indices assigned to the tensors just as in standard linear algebra.

However, an essential consequence of General Relativity is that measured values of a physical quantity are not only different in different inertial frames but also depend on the (arbitrary) choice of coordinates. Therefore, *modern* general relativity describes physics in the mathematical framework of *differential geometry* where the tensors are abstract objects living on a curved manifold, and the specification to a particular coordinate system is avoided as

much as possible. The tensor indices now do not refer to components but to the number of (dual) vectors it can act on, and to keep track of commutations which are non-trivial in GR.

Treatments of differential geometry as a tool for GR can be found in many textbooks, such as Ohanian and Ruffini (1994); Misner et al. (1973); Wald (1984); Hawking and Ellis (1973); Stewart (1990), listed here in order from the most physically to the most mathematically oriented. In this chapter we will largely follow the first chapter of Stewart (1990) because it gives the most rigorous yet compact overview of the definitions, theorems and lemmas that are explicitly or implicitly assumed in the rest of this thesis. Most of the definitions related to differential geometry can also be found in a more prosaic form in Part I and Appendices A–C of Wald (1984) and sometimes we will use his formulation. For a more extensive review of the 3+1 and tetrad formalisms we refer to Ellis and van Elst (1999b) (or Weinberg (1972)).

This chapter will be of a rather mathematical nature and stands separate from the independent research presented in the next four chapters. It serves as a self-consistent justification of many of the concepts used in this thesis that are not easy to find in many of the older textbooks on GR. Chapters 3–6 closely follow published papers but are supplemented with many references to the theoretical background laid out in this chapter.

2.1 Coordinates on a curved manifold

The physicist's concept of a coordinate system is called a chart by mathematicians and is defined as follows:

Definition 2.1.1. *A **chart** or **coordinate system** on a given topological space M is a* 1-1 *map $\phi : M \to R^n$ from an open subset $U \subset M$ to an open subset $\phi(U) \subset R^n$.*

Definition 2.1.2. *The **(maximal) atlas**, A, is the collection of (all) charts that are C^∞-related, such that both the map*

$$\phi_2 \circ \phi_1^{-1} : \phi_1(U_1 \cap U_2) \to \phi_2(U_1 \cap U_2) \tag{2.1}$$

and its inverse are C^∞ and every point of the space M lies in the domain of at least one chart.

Figure 2.1 shows how the domains of two charts ϕ_1 and ϕ_2 are required to mesh smoothly through the map $\phi_2 \circ \phi_1^{-1}$, by Definition 2.1.2.

These definitions are needed to define one of the most important concepts in GR: the *manifold* which is the mathematical description of the 4-dimensional continuum that is a dynamical space-time.

Definition 2.1.3. *A C^∞-**differential manifold** of **dimension** n is the set (M, A) of a space M and its maximal atlas A in which for each chart in the atlas the map $\phi : U \to R^n$ is of the same n.*

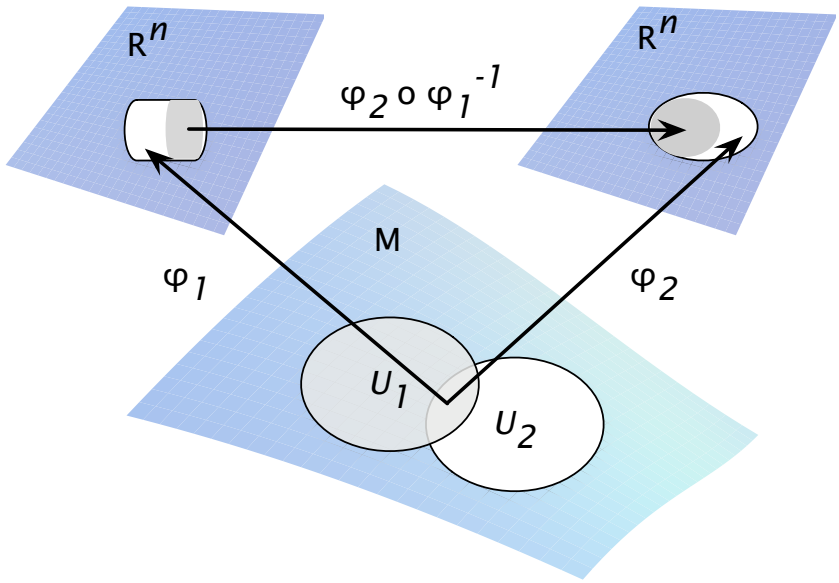

Figure 2.1: Illustration of the map $\phi_2 \circ \phi_1^{-1}$ relating two overlapping coordinate neighborhoods.

2.2 Vectors as directional derivatives

In a curved space-time, the simple interpretation of vectors as 'arrows' fails since the 'arrows' would point out of the physical space-time. Vectors can only be defined as tangents to curves that lie in the manifold.

Definition 2.2.1. *A C^∞-**curve** in a manifold M is a map λ of the open interval $I = (p, q) \in R \to M$ such that $\phi \circ \lambda : I \to R^n$ is a C^∞ map for any chart ϕ.*

Definition 2.2.2. *The **tangent vector** $\dot{\lambda}_p = \frac{d\lambda}{dt}\big|_p$ at the point p on the curve $\lambda(t)$ is the map*

$$\dot{\lambda}_p(f) = \dot{\lambda}_p : f \to (f \circ \lambda)^{\cdot}_p \tag{2.2}$$

from the set of real functions f defined in a neighborhood of p to R.

*The **components** of $\dot{\lambda}_p$ with respect to the chart ϕ with coordinates x^i are*

$$(f \circ \lambda)^{\cdot}_p = \frac{d}{dt} x^i(\lambda(t))\bigg|_p . \tag{2.3}$$

2.3 Bases of tangent spaces

Theorem 2.3.1. *The **tangent space** $T_p(M)$, which is the set of tangent vectors at p, is a vector space of dimension n if the space M is n-dimensional.*

Definition 2.3.2. *Let ϕ be a chart with coordinates x^i, then the tangent vectors $(\partial/\partial x^i)_p$ is a linearly independent **basis** that spans $T_p(M)$.*

Definition 2.3.3. *The **dual space** $T_p^*(M)$ of $T_p(M)$ is the vector space of linear maps $\lambda : T_p(M) \to R$. Elements of the dual space are **1-forms** or **covectors**.*

Definition 2.3.4. *The **differential** or **gradient** $df \in T_p^*(M)$ of any function f on M is the map $df : T_p(M) \to R$ with*

$$df(X_p) = X_p f \tag{2.4}$$

of a tangent vector $X_p \in T_p(M)$ to a scalar.

Lemma 2.3.5. *Given a chart ϕ with coordinates x^i, then the coordinate gradients dx^i form the **dual basis** for $T_p^*(M)$ with*

$$\left\langle dx^i, \left(\frac{\partial}{\partial x^j}\right)_p \right\rangle = dx^i(\partial/\partial x^j|_p) = \delta^i{}_j \ . \tag{2.5}$$

Or more generally, for any basis (e_a) of $T_p(M)$ and any dual basis (ω^a) of $T_p^*(M)$ one has $< \omega^a, e_b >= \delta^a{}_b$.

2.4 Covariance and contravariance

Definition 2.4.1. ***Covariant** quantities are 1-forms that transform like*

$$\hat{\omega}^i = A^i{}_j \omega^j \tag{2.6}$$

under a change of basis $\omega^a \mapsto \hat{\omega}^a$. In particular for a coordinate transformation $x^i \to y^i(x^j)$, one has $dy^i = A^i{}_j dx^j$ with $A^i{}_j = \left(\frac{\partial y^i}{\partial x^j}\right)_p$.

Definition 2.4.2. ***Contravariant** quantities are tangent vectors that transform like*

$$\hat{e}_i = (A^{-1})_i{}^j e_j \tag{2.7}$$

under a change of basis $e_a \mapsto \hat{e}_a$.

In particular for a coordinate transformation $x^i \to y^i(x^j)$, one has $\left(\frac{\partial}{\partial y^i}\right)_p = (A^{-1})_j{}^i \left(\frac{\partial}{\partial x^j}\right)_p$ with $(A^{-1})_i{}^j = \left(\frac{\partial x^i}{\partial y^j}\right)_p$.

2.5 Tensors, vector fields and commutators

Definition 2.5.1. *A (1,2)* ***tensor*** S *on* $T_p(M)$ *is a map*

$$S : T_p(M) \times T_p(M) \times T_p^*(M) \to R \ , \tag{2.8}$$

which is linear in each argument and is determined by its components ${S_{ab}}^c$ *with respect to a basis. Let again* (e_a), (ω^a) *be dual bases, then the tensor components are defined by*

$${S_{ab}}^c = S(e_a, e_b, \omega^c) \in R \ . \tag{2.9}$$

And when the tensor acts on two general vectors and a 1-form with components $X = X^a e_a$, $Y = Y^b e_b$ and $\lambda = \lambda_c \omega^c$, respectively, one has $S(X, Y, \lambda) = X^a Y^b \lambda_c {S_{ab}}^c$ and equivalently for any (r, s) tensor (the set of which forms a vector space).

This leads to the pictorial interpretation in Misner et al. (1973) of a tensor as a linear machine with *slots* that eats s vectors and r 1-forms and spits out one number.

The **symmetrization** and **antisymmetrization** operations for a tensor are respectively given by

$${S_{(ab)}}^c = \frac{1}{2}({S_{ab}}^c + {S_{ba}}^c) \ , \quad {S_{[ab]}}^c = \frac{1}{2}({S_{ab}}^c - {S_{ba}}^c) \ , \tag{2.10}$$

and similarly for any subset of its indices.

Definition 2.5.2. *A* ***vector field*** *on* M *is a map* $X : M \to T(M)$ *such that* $X(p) = X_p$ *is a vector in* $T_p(M)$ *for each point* p *on the manifold* M*.*

The *components* X_p^i of X with respect to a coordinate system x^i and corresponding basis $(\partial/\partial x^i)_p$ for each tangent space $T_p(M)$ are given by the vector X_p acting on the function x^i with

$$X_p = X_p^i \left(\frac{\partial}{\partial x^i} \right)_p , \quad X_p^i = X_p(x^i) \ . \tag{2.11}$$

Definition 2.5.3. *The* ***commutator*** $[X, Y]$ *is a vector field defined by two vector fields* X *and* Y *such that*

$$[X, Y]_p f = X_p(Yf) - Y_p(Xf) \quad \forall f \ , \tag{2.12}$$

with components

$$[X, Y]^i = X^j {Y^i}_{,j} - Y^j {X^i}_{,j} \ . \tag{2.13}$$

Similar to the commutator of quantum operators (like creation and annihilation) it is defined by its action on a function. As usual, the commutator is linear and satisfies $[X, Y] = -[Y, X]$ and the *Jacobi identity* $[[X, Y], Z] + [[Y, Z], X] + [[Z, X], Y] = 0$.

2.6 Maps of manifolds

Definition 2.6.1. *A map $h : M \to N$ that maps the manifold M to another manifold N (not necessarily of the same dimension!), is C^∞ if for every C^∞ function $f : N \to R$ the function $fh : M \to R$ is also C^∞.*

For each such map h, there is the induced linear ***push forward*** *map*[1] *$h_\star : T_p(M) \to T_{h(p)}(N)$ that maps the tangent vector of a curve γ at the point $p \in M$ to the tangent vector of the curve $h(\gamma)$ at $h(p) \in N$.*

When acting on a C^∞ function $f : N \to R$ one has $(h_* X_p)f = X_p(f \circ h)$.

Definition 2.6.2. *The map between covectors on two manifolds appears to be in the reverse direction. The linear* ***pull-back*** *map $h^* : T^*_{h(p)}(N) \to T^*_p(M)$ for $\omega \in T^*_{h(p)}(N)$ is induced by the push-forward map for the vector $X_p \in T_p(M)$ as*

$$(h^*\omega)(X_p) = \omega(h_* X_p) \ . \tag{2.14}$$

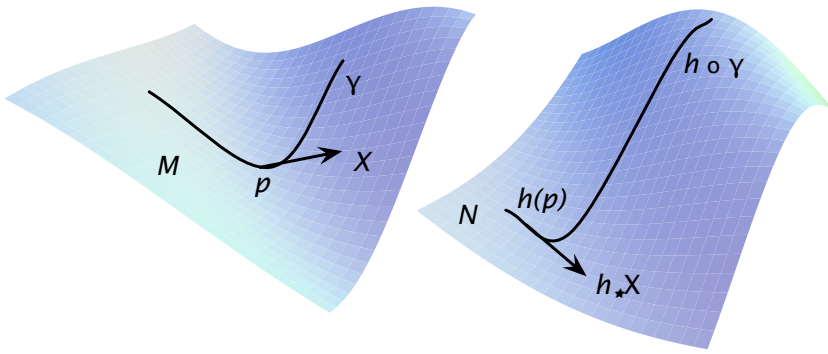

Figure 2.2: The **push-forward** $h_\star$, corresponding to the map $h : M \to N$, maps tangent vectors of curves in M to tangent vectors of curves in N.

Theorem 2.6.3. *For each smooth vector field X there is a unique local integral curve γ through each point p such that $\gamma(0) = p$. For a local coordinate chart x^i with x^i_p the coordinates of p, this integral curve follows from $dx^i(t)/dt = X^i(x^j(t))$ with initial conditions $x^i(0) = x^i_p$.*

[1] See also Appendix C of Wald (1984). We will again use the notation of Stewart (1990), note the differences: in Wald both h^* and h_* are called pull-back and the notation is the opposite $h^* \leftrightarrow h_*$.

Lemma 2.6.4. *If X is a smooth vector field with $X_p \neq 0$, then there exists a coordinate system x^i defined in a neighborhood U of p such that in U, $X = \partial/\partial x^0$.*

Definition 2.6.5. *A **congruence** is the set of **complete** integral curves that exist for all t.*

Definitions 2.6.1, 2.6.3 allow the definition of a useful 1-parameter Abelian group[2]of transformations of the space M to itself.

Definition 2.6.6. *The transformation $h_s : M \to M$ maps each point $p \in M$ to a point $h_s(p)$ which lies a parameter distance s further along the unique integral curve $\gamma(t)$ of a smooth vector field X through p, i.e. $h_s(\gamma(t_0)) = \gamma(t_0 + s)$. In General Relativity, the parameter s is usually called the* affine parameter.

Theorem 2.6.7. *A **geometrical representation of the commutator** $[X, Y]$ of two smooth vector fields X, Y is given in terms of their two induced groups g_t and h_s by trying to make a small quadrilateral $pqrv$ (or $pqru$). Let $p \in M$ be the starting point, then $q = g_{dt}(p)$ is a point on the integral curve of X a distance dt from p and similarly $r = h_{ds}(p)$ is a point on the integral curve of Y. Next, move from q to $u = h_{ds}(q)$ along the integral curve of Y and from r to $v = g_{dt}(r)$ along the integral curve of X. Then the missing piece from u to v is given by the map k_{dtds} induced by the commutator $[X, Y]$ along its integral curve:*

$$v = k_{dtds}(u) + \mathcal{O}(ds^3, dt^3) \ , \tag{2.15}$$

and a quadrilateral is completed iff the commutator vanishes (as in Figure 7 in Hawking and Ellis (1973)).

On a curved manifold, the differentiation of (co)vectors is far from trivial. (Co)vectors at different space-time points cannot be compared by ordinary differentiation since they lie in different tangent vector spaces. It is, however, possible to compare with an additional smooth vector field X.

Definition 2.6.8. *The **Lie derivative of a real function** $f : M \to R$ is defined in a manifestly coordinate invariant way in terms of a smooth vector field X, a point p on its integral curve γ and its induced 1-parameter group of transformations h_t by*

$$(\pounds_X f)_p = \lim_{dt \to 0} \left[\frac{f(h_{dt}(p)) - f(p)}{dt} \right] \ . \tag{2.16}$$

*Similarly, the **Lie derivative of a smooth vector field** Z with respect to X at p is again a well defined vector at p, given by:*

$$(\pounds_X Z)_p = \lim_{dt \to 0} \left[\frac{Z_p - (h_{dt})_* Z_{h_{-dt}(p)}}{dt} \right] \ . \tag{2.17}$$

[2]An Abelian group has $h_{t+s} = h_{s+t}$, an identity element h_0 and inverse $h_s^{-1} = h_{-s}$

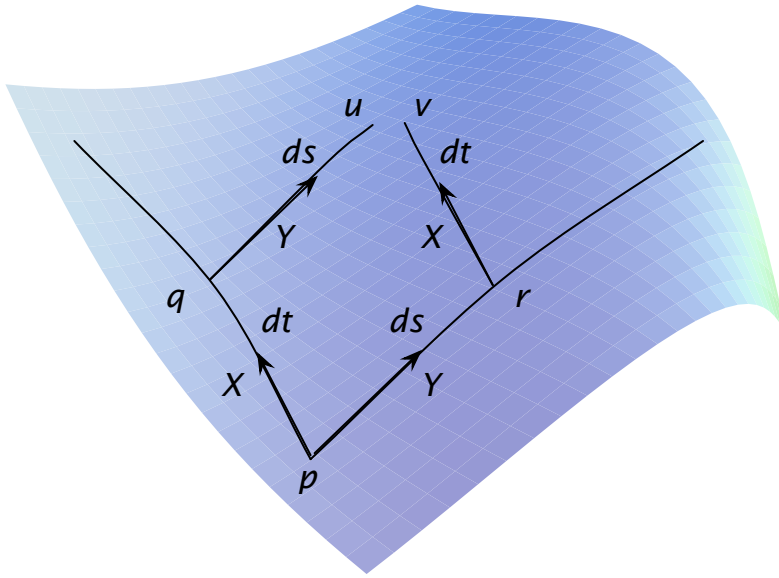

Figure 2.3: Geometrical representation of the commutator.

More suitable formulae for the computation of Lie derivatives are given by:

Theorem 2.6.9. *For any function f on M or smooth vector field Y, the Lie derivative with respect to a smooth vector field X is given by*

$$(\pounds_X f)_p = X_p f \ , \tag{2.18}$$
$$(\pounds_X Y)_p = [X, Y]_p \ . \tag{2.19}$$

The use of Lie derivatives is essential in the formulation of Lorentz transformations, the Poincaré invariance group of special relativity and in the linear perturbation theory on manifolds which is the basis of the final chapter of this thesis.

2.7 Gauge-invariant perturbation theory

Let M_ϵ be a 1-parameter family of smooth non-intersecting 4-dimensional manifolds that are embedded in a smooth 5-dimensional manifold N. These M_ϵ could be perturbations of a specific manifold M_0, and points on M_ϵ are identified with corresponding points on M_0 by a *point identification map* given by

the integral curves of a vector field V on N that is everywhere transverse to the M_ϵ and is scaled such that the induced map h_ϵ maps M_0 to M_ϵ. The **gauge freedom** common in general relativity is the freedom to choose a particular vector field V.

Definition 2.7.1. ***Linear perturbations*** *on a (curved) manifold are defined as follows. If F_0 is some quantity on M_0 and F_ϵ the perturbed quantity, e.g. the corresponding quantity on M_ϵ, one can perform a Taylor expansion of the field F in N along each integral curve of V and only keep the linear term:*

$$F_\epsilon = h_{\epsilon\star}[F_0 + \epsilon(\pounds_V F_\epsilon)_{\epsilon=0}] + \mathcal{O}[\epsilon^2] \ , \tag{2.20}$$

with $h_{\epsilon\star} : T_p(M_0) \to T_{h_\epsilon(p)}(M_\epsilon)$ the push-forward map defined in Definition 2.6.2 and induced by $h_\epsilon : M_0 \to M_\epsilon$.

Definition 2.7.2. *A linearized perturbation of F is **gauge invariant** iff the Lie derivative of F_0 vanishes for every 4-vector X on M_0, which is the case if $F_0 = 0$, F_0 is a constant scalar field or F_0 is a linear combination of Kronecker deltas with constant coefficients.*

This simple but far-reaching statement is also referred to as the Stewart & Walker Lemma (Stewart and Walker 1974) and is the basis of many of the derivations in Chapter 6.

2.8 Covariant derivatives and connections

Definition 2.8.1. *The **covariant derivative** of a smooth vector field Y with respect to X is defined in terms of the **linear connection** ∇ on M, which is a map that sends every pair of smooth vector fields (X, Y) to a new vector field $\nabla_X Y$ with the following properties:*

$$\nabla_X(aY + Z) = a\nabla_X Y + \nabla_X Z \ , \tag{2.21a}$$
$$\nabla_X(fY) = f\nabla_X Y + (Xf)Y \ , \tag{2.21b}$$
$$\nabla_{X+fY} Z = (\nabla_X Z + f\nabla_Y Z) \ , \tag{2.21c}$$
$$\nabla_X f = Xf \ , \tag{2.21d}$$

for constant scalars a and functions f.

*Note that the **covariant derivative of** Y is given by the map ∇Y from X to $\nabla_X Y$ and is a $(1,1)$ tensor since it is linear in X (unlike the Lie derivative).*

Definition 2.8.2. *The **components of the connection** are given in a particular basis (e_a) for vector fields as*

$$\nabla_{e_b} e_a = \Gamma^c{}_{ab} e_c \qquad \Leftrightarrow \qquad \Gamma^c{}_{ab} = e^c{}_i \, e_b{}^j \, \nabla_j e_a{}^i \tag{2.22}$$

(i.e. $\Gamma^c{}_{ab}$ is the c-component of the covariant derivative in the b-direction of the a-vector). In terms of the connection and $X = X^a e_a$ et cetera, the components of the covariant derivative ∇Y, $Y^c_{;b}$ can be evaluated as

$$\nabla_X Y = [X(Y^c) + \Gamma^c{}_{ab} X^b Y^a] e_c \ , \tag{2.23a}$$

$$Y^c_{;b} X^b = [e_b(Y^c) + \Gamma^c{}_{ab} Y^a] X^b \ . \tag{2.23b}$$

In a basis induced by coordinates x^i , such that $e_i = \partial/\partial x^i$, Eq. 2.23b reduces to the familiar definition of the covariant derivative in general relativity:

$$Y^i_{;j} = Y^i_{,j} + \Gamma^i{}_{kj} Y^k \ . \tag{2.24}$$

In words, the connection coefficient $\Gamma^c{}_{ab}$ gives the c-component of the covariant derivative in the b-direction of the a-vector (pg. 18 in Ellis and van Elst (1998)).

Definition 2.8.3. *A vector Y is **parallelly transported** with respect to a vector field X when $\nabla_X Y = 0$.*

Definition 2.8.4. *The covariant derivative of a **covector** η can be derived by applying Leibniz' rule for differentiation to the function $\eta(Y)$. In a particular dual basis (ω^c) with $\eta = \eta_c \omega^c$ et cetera, the components of the covariant derivative of the covector are given by:*

$$(\nabla_{e_a} \eta)_b = e_a(\eta_b) - \Gamma^c{}_{ba} \eta_c \ , \tag{2.25}$$

and since e_a and ω^b are orthogonal,

$$\nabla_{e_a} \omega^b = -\Gamma^b{}_{ca} \omega^c \ . \tag{2.26}$$

If we define $\eta_{i;j} \equiv (\nabla_{e_j} \eta)_i$ in a coordinate basis, Eq. 2.25 reduces to

$$\eta_{i;j} = \eta_{i,j} - \Gamma^k{}_{ij} \eta_k \ . \tag{2.27}$$

Definition 2.8.5. *For a (1,1) tensor T, the coordinate free expression for the covariant derivative is given by*

$$(\nabla_{e_a} T)^c{}_b = e_a(T^c_b) + \Gamma^c{}_{da} T^d_b - \Gamma^d{}_{ba} T^c_d \ . \tag{2.28}$$

2.9 Geodesics: acceleration or geodesic deviation

Definition 2.9.1. ***Geodesics** are defined by the integral curves of a vector field X which satisfies $\nabla_X X = 0$, i.e. its tangent vector is parallel transported along itself. Geodesics are the equivalent to a 'straight line' or shortest distance on flat space.*

Theorem 2.9.2. *There is exactly one geodesic through a given point $p \in M$ in a given direction X_p. In a particular coordinate system x^i it is given by the solutions of*

$$\frac{d^2x^i(t)}{dt^2} + \Gamma^i{}_{jk}(x(t))\frac{dx^j}{dt}\frac{dx^k}{dt} = 0 \ , \tag{2.29}$$

with initial conditions $x^i(0) = x^i_p$ the coordinates of p and $(dx^i/dt)_0 = X^i_p$ a tangent vector at p.

The geodesic equation (2.29) *has a freedom in the* ***affine parameter*** *on the curve since it is only defined up to a change of origin and scale: a parameter $s(t) = at + b$ with a, b constant has $\ddot{s} = 0$ and preserves the form of Eq. 2.29.*

Definition 2.9.3. *Let p be a fixed point on M, $X_p \in T_p(M)$ some vector at p and (e_a) a basis for this vector space. The* ***exponential map*** *maps each vector X_p to the point which lies a unit parameter distance along the unique geodesic through p with tangent vector X_p. It has an inverse in a small* ***normal neighborhood*** *U of p such that $q \in U$ implies $q = \exp(X_p) = \exp(X^a_p e_a)$ with X^a_p the* ***normal coordinates*** *of q.*

Expressed in terms of normal coordinates, the symmetric part of each connection coefficient vanishes at a point p:

$$\Gamma^i{}_{(jk)} = 0 \ , \tag{2.30}$$

Definition 2.9.4. *Any pair of smooth vector fields X and Y define a* $(1,2)$ ***torsion tensor*** *field T given by*

$$T(X,Y) = (\nabla_X Y - \nabla_Y X - [X,Y]) \ . \tag{2.31}$$

In terms of a basis (e_a) we can define the scalar ***commutator coefficients*** *$\gamma^a{}_{bc}$ satisfying*

$$[\, \boldsymbol{e}_a, \boldsymbol{e}_b \,] = \gamma^c{}_{ab}(x^i)\, \boldsymbol{e}_c \qquad \Rightarrow \qquad \gamma^a{}_{bc}(x^i) = -\gamma^a{}_{cb}(x^i) \ . \tag{2.32}$$

that vanish if the basis $(\boldsymbol{e}_a)$ is coordinate induced: that is, there exist coordinates x^i such that $\boldsymbol{e}_a = \delta_a{}^i\, \partial/\partial x^i$, iff $[\, \mathbf{e}_a, \boldsymbol{e}_b \,] = 0 \Leftrightarrow \gamma^a{}_{bc} = 0$.

The components of the torsion are given in a basis (e_a) and using Eq. 2.22 by

$$T(e_a, e_b) = [\Gamma^c{}_{ba} - \Gamma^c{}_{ab} - \gamma^c{}_{ab}]e_c \ , \tag{2.33a}$$

$$T^c{}_{ab} = -2\Gamma^c{}_{[ab]} - \gamma^c{}_{ab} \ . \tag{2.33b}$$

In the theory of general relativity all derivative operators are required to be torsion free (vanishing torsion tensor).

Definition 2.9.5. *The* $(1,3)$ ***Riemann curvature tensor*** *field is defined by*

$$R(X,Y)Z = \nabla_Y \nabla_X Z - \nabla_X \nabla_Y Z + \nabla_{[X,Y]} Z \ . \tag{2.34}$$

The components of R in a basis (e_a) with $X = e_c$, $y = e_d$ and $Z = e_b$ are defined by $R(e_c, e_d)e_b = R^a{}_{bcd}e_a$ and follow from

$$\begin{aligned} R(e_c, e_d)e_b &= [e_d(\Gamma^a{}_{bc}) - e_c(\Gamma^a{}_{bd}) \\ &+ \Gamma^f{}_{bc}\Gamma^a{}_{fd} - \Gamma^f{}_{bd}\Gamma^a{}_{fc} + \gamma^f{}_{cd}\Gamma^a{}_{bf}\Big] e_a \ . \end{aligned} \tag{2.35}$$

In a coordinate induced basis the commutator coefficients vanish and the components of R are written succinctly as

$$\frac{1}{2}R^i{}_{jkl} = \Gamma^i{}_{j[k,l]} - \Gamma^i{}_{m[k}\Gamma^m_{|j|l]} \ . \tag{2.36}$$

The notation in the last term indicates that the antisymmetrization operation is only on the indices k and l.

Definition 2.9.6. *Let the components of $\nabla\nabla X$ in a coordinate induced basis be defined by $X^i{}_{;jk} = (X^i{}_{;j})_{;k}$. The commutation of the two connections are given by the **Ricci identity** in terms of the Riemann tensor field: $X^i{}_{;[jk]} = \frac{1}{2}R^i{}_{ljk}X^l$.*

Definition 2.9.7. *The **Ricci curvature tensor** is a $(0,2)$ tensor field defined by the contraction of the Riemann tensor:*

$$R_{ab} = R^c{}_{acb} \ . \tag{2.37}$$

Theorem 2.9.8. *The torsion T and curvature R vanish in a simply connected region U iff there exists a coordinate system in which the connection coefficients vanish everywhere in U.*

Definition 2.9.9. *A **connecting vector** Z of a congruence (Definition 2.6.5) of curves with tangent vector X is defined such that $[X, Z] = 0$.*

Definition 2.9.10. *In the absence of torsion, the **acceleration** of a connecting vector Z for a congruence of geodesics with tangent vector X satisfies the equation of **geodesic deviation***

$$\nabla_X \nabla_X Z = -R(X, Z)X \ , \tag{2.38}$$

given in component notation and in terms of the affine parameter T along the geodesics by

$$\frac{d^2 Z^a}{dt^2} = -R^a{}_{bcd}X^b X^c Z^d \ . \tag{2.39}$$

The equations of geodesic deviation describe the deviation in the separation of test mirrors in gravitational wave interferometer detectors such as LIGO and LISA. Furthermore, Definition 2.9.10 will be used in Chapters 4 (Eq. (4.12)) and 5 to study the effect of a passing gravitational wave on the particles and fields in a strongly magnetized plasma.

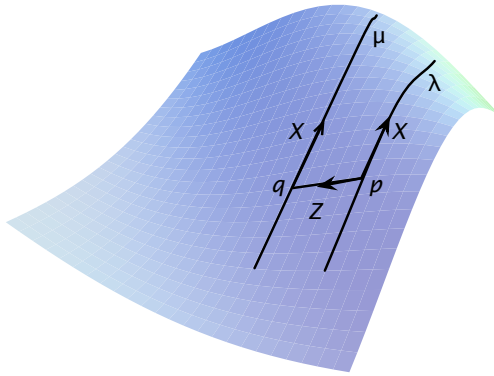

Figure 2.4: The **connecting vector** Z is tangent to the infinitesimal curve pq that joins points at the same affine parameter on the neighboring geodesics $\lambda(t)$ and $\mu(t)$ of a congruence with tangent vector field X.

Theorem 2.9.11. *In the absence of torsion the Riemann tensor has the following symmetries:*

$$R^a{}_{bcd} = \frac{2}{3}(R^a{}_{(bc)d} - R^a{}_{(bd)c}) \ , \tag{2.40a}$$

$$R^a{}_{[bcd]} = R^i{}_{j[kl;m]} = 0 \ . \tag{2.40b}$$

The last expression defines the ***Bianchi identities****.*

From these symmetries it follows that Riemann can be determined completely from measurements of geodesic deviation (even though Eq. 2.38 only determines $R^a{}_{(bc)d}$).

2.10 Metric tensor

Definition 2.10.1. *The* $(0,2)$ *symmetric* ***metric tensor*** g *at a point* p *in* M *defines for each vector* X *in the vector space* $T_p(M)$ *the* ***magnitude***

$$m(X) = \sqrt{|g(X,X)|} \ , \tag{2.41}$$

and between any two vectors X, Y *the* ***angle***

$$a(X,Y) = \arccos\left[\frac{g(X,Y)}{m(X)m(Y)}\right] \ . \tag{2.42}$$

Definition 2.10.2. ***Properties of the metric tensor***

- *The components of g with respect to a basis (e_a) are $g_{ab} = g(e_a, e_b)$,*
- *The vectors X, Y are **orthogonal** if $g(X, Y) = 0$,*
- *A curve with tangent vector X has a **length** between s_1 and s_2 defined by $L(s_1, s_2) = \int_{s_1}^{s_2} m(X)ds$.*
- *The metric is **non-degenerate** if $g(X, Y) = 0$ for all Y iff $X = 0$.*
- *If g is non-degenerate, we can define the $(2, 0)$ inverse metric tensor with components g^{ab} satisfying $g^{ac}g_{cb} = \delta^a{}_b$.*
- *The metric provides a non-natural isomorphism between the dual spaces $T_p(M) \leftrightarrow T_p^*(M)$ and the dual (co)vectors $\eta \leftrightarrow X$ by*

$$X^a = g^{ab}\eta_b \ , \tag{2.43}$$

$$\eta_a = g_{ab}X^b \ . \tag{2.44}$$

- *On the basis of this isomorphism both covectors and vectors can be called X and similarly for tensors $T^{ab} \leftrightarrow T_{ab} \leftrightarrow T^a{}_b \leftrightarrow T_a{}^b$.*
- *The **signature** of a metric is the difference between the number of positive and negative eigenvalues. In a **Riemannian** metric the signature is positive definite and equals the number of dimensions n, while in a **pseudo-Riemannian** or **Lorentzian** metric the signature is $\pm(n-2)$.*

Theorem 2.10.3. *If a manifold possesses a metric g then there is a unique metric (or **Levi-Civita**) connection such that $\nabla g = 0$.*
In a basis (e_a) we find

$$\Gamma_{abc} = g(e_a, \nabla_c e_b) = g_{ab}\Gamma^d{}_{bc} \tag{2.45a}$$

$$= \frac{1}{2}\left[e_b(g_{ac}) + e_c(g_{ba}) - e_a(g_{cb}) \right. \tag{2.45b}$$

$$+ \left. \gamma^d{}_{cb}g_{ad} + \gamma^d{}_{ac}g_{bd} - \gamma^d{}_{ba}g_{cd} \right] \ . \tag{2.45c}$$

2.11 Christoffel symbols, Ricci rotation coefficients and Einstein tensor

Definition 2.11.1. *If the basis is coordinate induced, the basis vectors commute and the last three terms vanish defining the **Christoffel symbols** as*

$$\Gamma^i{}_{jk} = \frac{1}{2}g^{il}\left[g_{kl,j} + g_{jl,k} - g_{jk,l}\right] \ . \tag{2.46}$$

These definitions can also be found from Eq. (8.24b) in Misner et al. (1973).

Definition 2.11.2. *In an orthonormal tetrad basis (Section 2.15) the metric is locally Minkowskian and the first three terms vanish defining the* ***Ricci rotation coefficients symbols*** *by* (2.45c).

Definition 2.11.3. *On a metric manifold two more curvature quantities are defined:*

$$R = g^{ab} R_{ab} \tag{2.47}$$

is the ***Ricci scalar*** *and*

$$G_{ab} = R_{ab} - \frac{1}{2} R g_{ab} \tag{2.48}$$

is the ***Einstein curvature tensor****. Using Eq.* (2.40b) *we find that the Einstein curvature tensor satisfies the* ***twice-contracted Bianchi identities***

$$\nabla_a G^a{}_b = \nabla_a R^a{}_b - \frac{1}{2} e_b(R) = 0 \ . \tag{2.49}$$

Theorem 2.11.4. *The Riemann tensor associated with a metric connection has the additional symmetries*

$$R_{(ab)cd} = 0 \ , \tag{2.50}$$

$$R_{abcd} = R_{cdab} \ , \tag{2.51}$$

with $R_{abcd} = g_{ae} R^e{}_{bcd}$.

2.12 Special relativistic Minkowski space

Since we will consider gravitational waves as a field living on a flat space-time, we introduce the postulates of special relativity as follows. space-time is a smooth 4-dimensional manifold M with a Lorentzian flat metric η_{ab} of signature 2, as defined in Definitions 2.10.2. In a specific **inertial coordinate system** the metric has components[3]

$$\eta_{ab} = \mathrm{diag}(-1, 1, 1, 1) \ . \tag{2.52}$$

In this metric $\eta(X, X) = 0$ no longer implies that $X = 0$. Only *null cones* of η that describe the propagation of light in vacuum have $\eta(X, X) = 0$. Vectors that have $\eta(X, X) < 0$ correspond to the geodesics of freely falling observers and the **proper time** measured by such observers is given by

$$\int d\tau = \int \sqrt{\eta_{ab} x^a x^b} = \int \frac{dt}{\sqrt{1 - v^2}} \ , \tag{2.53}$$

where $\gamma = \sqrt{1 - v^2}$ is the Lorentz factor.

[3] Note that this differs by a minus sign from the metric chosen in Stewart (1990) and Jackson (1975) but agrees with Wald (1984) and Misner et al. (1973). See the cover in Misner et al. (1973) for sign conventions in other literature.

2.13 General relativity

Einstein's field equations can be derived heuristically by requiring that general relativity agrees locally with special relativity as in Section 2.12, explains the deflection of light by masses, implies a family of preferred relatively accelerated worldlines corresponding to free-fall and defines a tidal field tensor representing gravity which is consistent with Newton's or Poisson's law.

Definition 2.13.1. ***Einstein's field equations*** *(*EFE*) are given by*

$$G_{ab} = 8\pi G T_{ab} \ , \tag{2.54}$$

where the energy-momentum tensor T_{ab} will be defined in Section 2.14.

2.14 3+1 split

Given a congruence of preferred worldlines, for example defined by the average bulk motion of a fluid, the most convenient covariant description of space-time is in the so-called $3+1$ split.

Let x^i be a local coordinate chart, then the worldlines are a solution of

$$u^i(x^j(\tau)) = \frac{dx^i(\tau)}{d\tau} \ , \tag{2.55}$$

or $u = \partial/\partial\tau$ with τ the proper time along the fundamental worldlines following from Lemma 2.6.4. The 4-velocity is time-like with $u^a u_a = -1$ and Theorem 2.6.3 guaranties that for a given preferred worldline, it is unique.

Definition 2.14.1. *Associated with the 4-velocity vector are the two unique* ***projection tensors*** *with components:*

$$U^a{}_b \equiv -u^a u_b \ , \tag{2.56a}$$
$$h_{ab} \equiv g_{ab} + u_a u_b \ , \tag{2.56b}$$

that project parallel and orthogonal to the u^a, respectively. Properties of these projection tensors are:

$$\begin{array}{lllllll} U^a{}_c U^c{}_b & = & U^a{}_b & , & h^a{}_c h^c{}_b & = & h^a{}_b \ , \\ U^a{}_a & = & 1 & , & h^a{}_a & = & 3 \ , \\ U_{ab} u^b & = & u_a & , & h_{ab} u^b & = & 0 \ . \end{array} \tag{2.57}$$

If T_p is the tangent vector space at a point $p \in M$, N is the space of all vectors proportional to u and W is the space of all vectors orthogonal to u, then Eqs. (2.56) *define the maps $U : T_p(M) \to N$ and $h : T_p \to W$.*

Definition 2.14.2. *In the* 3+1 *split we define two additional derivatives. The* ***covariant time derivative along the fundamental worldlines*** *is given for any* $(2,2)$ *tensor with components* $T^{ab}{}_{cd}$ *by*

$$\dot{T}^{ab}{}_{cd} = u^e \nabla_e T^{ab}{}_{cd} \ . \tag{2.58}$$

The ***fully orthogonally projected covariant derivative*** $\tilde{\nabla}$ *has components*

$$\tilde{\nabla}_e T^{ab}{}_{cd} = h^a{}_f h^b{}_g h^p{}_c h^q{}_d h^r{}_e \nabla_r T^{fg}{}_{pq} \ , \tag{2.59}$$

where $\tilde{\nabla}$ *is a proper* 3*-dimensional covariant derivative only if the* ***vorticity*** *of* u^a *vanishes.*

Definition 2.14.3. *Orthogonal projections of vectors and the orthogonally projected symmetric trace-free part of tensors are denoted by angle brackets, which we will also use for the orthogonal projections of Eq.* (2.58) *called* ***Fermi derivatives***

$$\begin{array}{rclcrcl} v^{<a>} & = & h^a{}_b v^b & , & T^{<ab>} & = & [h^{(a}{}_c h^{b)}{}_d - \frac{1}{3} h^{ab} h_{cd}] T^{cd} \ , \\ \dot{v}^{<a>} & = & h^a{}_b \dot{v}^b & , & \dot{T}^{<ab>} & = & [h^{(a}{}_c h^{b)}{}_d - \frac{1}{3} h^{ab} h_{cd}] T^{cd} \ . \end{array} \tag{2.60}$$

Note that since $g^{ac} g_{cb} = \delta^a{}_b$, $U^a{}_b + h^a{}_b = -u^a u_b + (\delta^a{}_b + u^a u_b) = \delta^a{}_b$.

These definitions allow a full decomposition in *time* (which runs in the direction of u) and *space* (which is the 3-dimensional *hypersurface* orthogonal to u), which is still coordinate and basis independent (except for the temporal basis vector). The *tetrad description* of space-time that we will discuss shortly, is coordinate independent but also specifies the spatial basis vectors.

Definition 2.14.4. *In terms of the two derivatives defined above we can split the covariant derivative of* u^a *in its irreducible parts by*

$$\begin{array}{rcl} \nabla_a u_b & = & -u_a \dot{u}_b + \tilde{\nabla}_a u_b \\ & = & -u_a \dot{u}_b + \frac{1}{3} \Theta h_{ab} + \sigma_{ab} + \omega_{ab} \ . \end{array} \tag{2.61}$$

- *The volume rate of* ***expansion*** *of the fluid is determined by the trace* $\Theta = \tilde{\nabla}_a u^a$*,*
- *the distortion of the fluid flow is described by the trace-free symmetric rate of* ***shear tensor*** $\sigma_{ab} = \tilde{\nabla}_{<a} u_{b>}$ *and has the properties* $\sigma_{ab} = \sigma_{(ab)}$*,* $\sigma_{ab} u^b = 0$ *and* $\sigma^a{}_a = 0$*,*
- *the rotation of the fluid with respect to a Fermi-propagated (non-rotating) right-handed spatial basis is determined by the skew-symmetric* ***vorticity tensor*** $\omega_{ab} = \tilde{\nabla}_{[a} u_{b]}$ *with the properties* $\omega_{ab} = \omega_{[ab]}$ *and* $\omega_{ab} u^b = 0$*,*
- *the* ***relativistic acceleration vector*** $\dot{u}^a$ *measures the combined effect of all forces other than gravity and inertia.*

When the vorticity and the acceleration vanish, the fluid flow is called hypersurface-orthogonal and there exist a global function t such that $u_a = -\nabla_a t$. Furthermore, the metric on the orthogonal 3-dimensional (spatial) manifolds is given by h_{ab}.

Matter energy-momentum tensor

Definition 2.14.5. *The **matter energy-momentum tensor** T_{ab} can be decomposed with respect to u^a as*

$$T^{(\mathrm{m})}_{ab} = \mu u_a u_b + p h_{ab} + \pi_{ab} + 2q_{(a}u_{b)} \ , \tag{2.62}$$

which defines

- *the non-electromagnetic **relativistic energy density**: $\mu = T_{ab}u^a u^b$,*
- *the **isotropic pressure**: $p = \frac{1}{3}T_{ab}h^{ab}$,*
- *the trace-free **anisotropic pressure** or **stress**: $\pi_{ab} = T_{cd}h^c{}_{<a}h^d{}_{b>}$, which satisfies $\pi_{ab} = \pi_{(ab)}$, $\pi_{ab}u^b$ and $\pi^a{}_a = 0$,*
- *and the **relativistic momentum density** or **energy flux**: $q^a = -T_{bc}u^b h^{ca}$, which satisfies $q_a u^a = 0$.*

For a *perfect fluid* the heat flux q_a and anisotropic pressure π_{ab} vanish and the energy-momentum tensor reduces to

$$T_{ab} = \mu u_a u_b + p h_{ab} \ . \tag{2.63}$$

Note, however, that two fluid species that move at different bulk velocities with respect to a fundamental observer and behave like ideal fluids in their own rest-frame will together still behave as an imperfect fluid with stress-energy tensor Eq. (2.62) (see Marklund et al. (2003)).

Maxwell equations

Definition 2.14.6. *The **Maxwell tensor** F_{ab} for the electromagnetic field can also be split into its **electric** and **magnetic** parts relative to u^a*

$$E_a = F_{ab}u^b \qquad \Rightarrow \qquad E_a u^a = 0 \ , \tag{2.64}$$

$$B_a = \frac{1}{2}\eta_{abc}F^{bc} \qquad \Rightarrow \qquad B_a u^a = 0 \ . \tag{2.65}$$

In terms of the electric and magnetic field tensors (2.64), we have:

$$F^{ab} = u^a E^b - E^a u^b + \epsilon^{abc}B_c \ . \tag{2.66}$$

The **Maxwell field equations**

$$\begin{aligned} \nabla_b F^{ab} &= j_e^a \ , & (2.67)\\ \nabla_{[a} F_{bc]} &= 0 \ , & (2.68) \end{aligned}$$

can also be decomposed in the $3+1$ split. The *propagation equations* can be written as

$$\begin{aligned} \dot{E}^{<a>} - \eta^{abc}\tilde{\nabla}_b B_c &= -j_e^{<a>} - \tfrac{2}{3}\Theta E^a + \sigma^a{}_b E^b + \eta^{abc}[\dot{u}_b B_c + \omega_b E_c] \ , \\ \dot{B}^{<a>} + \eta^{abc}\tilde{\nabla}_b E_c &= -\tfrac{2}{3}\Theta B^a + \sigma^a{}_b B^b - \eta^{abc}[\dot{u}_b E_c - \omega_b B_c] \ . \end{aligned} \tag{2.69}$$

Only in the last chapter of this thesis will expansion, shear and vorticity be considered (actually only the expansion will be relevant). In the remainder we simply have

$$\begin{aligned} \dot{E}^{<a>} - \eta^{abc}\tilde{\nabla}_b B_c &= -j_e^{<a>} \ , & (2.70)\\ \dot{B}^{<a>} + \eta^{abc}\tilde{\nabla}_b E_c &= 0 \ , & (2.71) \end{aligned}$$

which looks more familiar from non-relativistic physics if we define $\eta^{abc}\tilde{\nabla}_b X_c = \mathrm{curl} X^a$ for every vector X^a.

The *constraint equations* are decomposed as

$$\begin{aligned} \tilde{\nabla}_a E^a &= \rho_e + 2\omega_a B^a \quad \to \quad \rho_e \ , \\ \tilde{\nabla}_a B^a &= -2\omega_a E^a \quad \to \quad 0 \ , \end{aligned} \tag{2.72}$$

where the rightmost expressions are valid in the absence of vorticity.

Electromagnetic energy-momentum tensor

Definition 2.14.7. *In the irreducible* $3+1$ *decomposition, the* ***electromagnetic energy-momentum tensor*** *takes the same form as the anisotropic imperfect fluid in* (2.62) *(see also Tsagas (2005))*

$$T^{(\mathrm{EM})}_{ab} = \tfrac{1}{2}(E^2+B^2)u_a u_b + \tfrac{1}{6}(E^2+B^2)h_{ab} + \mathcal{P}_{ab} + 2\mathcal{Q}_{(a}u_{b)} \ . \tag{2.73}$$

with energy density $\frac{1}{2}(E^2+B^2)$*, isotropic pressure* $\frac{1}{6}(E^2+B^2)$*, anisotropic stresses given by the symmetric, trace-free tensor*

$$\mathcal{P}_{ab} = \mathcal{P}_{\langle ab\rangle} = \tfrac{1}{3}(E^2+B^2)h_{ab} - E_a E_b - B_a B_b \ , \tag{2.74}$$

and an energy-flux represented by the electromagnetic Poynting vector $\mathcal{Q}_a = \epsilon_{abc}E^b B^c$*.*

The trace-free nature of the radiation stress-energy tensor (2.73) is satisfied by $T^{(\mathrm{EM})\ a}_a = 0$.

2.15 Tedrad formalism

The 1+3 split is the most convenient formalism when a system possesses *one* preferred (time) direction and it allows a transparent geometric interpretation of the covariant physical quantities. When a system has more preferred directions it can be advantageous to use a 2+1+1 split (for instance to study the ring-down of an axi-symmetric Schwarzschild black-hole as in Clarkson et al. (2004)) or even a 1+1+1+1 split, which is essentially the tedrad description. The latter is useful in the description of gravitational waves where the preferred spatial directions are given by the propagation and the perpendicular axes along which matter is deformed by the passing GW (see Figure 2).

This Section closely follows Section 3.1 in Ellis and van Elst (1999b). A different treatment of the tetrad formalism can be found in Weinberg (1972).

Definition 2.15.1. *A **tetrad** is a set of four orthogonal unit basis vector fields $(\boldsymbol{e}_a)$, which can be written in terms of a local coordinate basis by means of the tetrad **components** $e_a{}^i(x^j)$:*

$$\boldsymbol{e}_a = e_a{}^i(x^j)\,\frac{\partial}{\partial x^i} \qquad \Leftrightarrow \qquad \boldsymbol{e}_a(f) = e_a{}^i(x^j)\,\frac{\partial f}{\partial x^i}\,, \qquad e_a{}^i = \boldsymbol{e}_a(x^i)\ , \tag{2.75}$$

The last equality states that the i-th component of the a-th tetrad vector is the directional derivative of the i-th coordinate in the direction $\boldsymbol{e}_a$. Definition 2.15.1 is in fact just a general change of vector basis such that

$$T^{ab}{}_{cd} = e^a{}_i\, e^b{}_j\, e_c{}^k\, e_d{}^l\, T^{ij}{}_{kl}\ , \tag{2.76}$$

where the inverse components $e^a{}_i(x^j)$ are defined by

$$e_a{}^i\, e^a{}_j = \delta^i{}_j \qquad \Leftrightarrow \qquad e_a{}^i\, e^b{}_i = \delta^b{}_a\ . \tag{2.77}$$

It follows from the orthonormality of $(\boldsymbol{e}_a)$ that:

Definition 2.15.2. *The **tetrad components of the metric tensor** are given by*

$$g_{ab} = g_{ij}\, e_a{}^i\, e_b{}^j = \boldsymbol{e}_a \cdot \boldsymbol{e}_b = \eta_{ab}\ . \tag{2.78}$$

Definition 2.15.3. *The **coordinate components of the metric tensor** can be derived from the inverse tetrad components $e^a{}_i(x^j)$ by the inverse of* (2.78)

$$g_{ij}(x^k) = \eta_{ab}\, e^a{}_i(x^k)\, e^b{}_j(x^k)\ . \tag{2.79}$$

Tedrad indices can be raised and lowered using the metric $g_{ab} = \eta_{ab}$ and its inverse $g^{ab} = \eta^{ab}$.

By applying (2.32) to the coordinates x^i we find that in terms of the tetrad components the covariant derivative is related to the commutator coefficients by

$$e_b{}^i\, e_c{}^j\, \nabla_{[i} e^a{}_{j]} = -\tfrac{1}{2}\gamma^a{}_{bc}(x^i)\ . \tag{2.80}$$

The *Ricci rotation coefficients* are the *connection components* $\Gamma^a{}_{bc}$ for the tetrad and were given already in (2.22, 2.45c). Under the assumption of vanishing torsion (2.31), the tetrad relations analogues to the definitions of the usual Christoffel symbols are

$$\Gamma_{abc} = \tfrac{1}{2}\left(g_{ad}\,\gamma^d{}_{cb} - g_{bd}\,\gamma^d{}_{ca} + g_{cd}\,\gamma^d{}_{ab} \right) , \qquad \gamma^a{}_{bc} = -\left(\Gamma^a{}_{bc} - \Gamma^a{}_{cb}\right) , \tag{2.81}$$

with $\Gamma_{(ab)c} = 0$.

The tedrad components of covariant derivatives are completely equivalent to the usual tensor form

$$\nabla_a T_{bc} = \boldsymbol{e}_a(T_{bc}) - \Gamma^d{}_{ba}\,T_{dc} - \Gamma^d{}_{ca}\,T_{bd} , \tag{2.82}$$

where for any function f, $\boldsymbol{e}_a(f) = e_a{}^i\,\partial f/\partial x^i$ is the derivative of f in the direction $\boldsymbol{e}_a$.

Definition 2.15.4. *The components of the* ***Riemann curvature tensor*** *follow from applying the Ricci identities to the tetrad basis vectors* $\boldsymbol{e}_a$

$$R^a{}_{bcd} = \boldsymbol{e}_c(\Gamma^a{}_{bd}) - \boldsymbol{e}_d(\Gamma^a{}_{bc}) + \Gamma^a{}_{ec}\,\Gamma^e{}_{bd} - \Gamma^a{}_{ed}\,\Gamma^e{}_{bc} - \Gamma^a{}_{be}\,\gamma^e{}_{cd} . \tag{2.83}$$

Definition 2.15.5. ***Einstein's Field Equations*** *(*EFE*) in tetrad form are obtained by contracting* (2.83) *on* a *and* c

$$R_{bd} = \boldsymbol{e}_a(\Gamma^a{}_{bd}) - \boldsymbol{e}_d(\Gamma^a{}_{ba}) + \Gamma^a{}_{ea}\,\Gamma^e{}_{bd} - \Gamma^a{}_{de}\,\Gamma^e{}_{ba} = T_{bd} - \tfrac{1}{2}\,T\,g_{bd} . \tag{2.84}$$

More intricacies of the tetrad formalism can be found in Ellis and van Elst (1999b).

Gravitational waves

The metric of a gravitational wave is often given in a transverse-traceless coordinate induced basis which is tuned to the GW as

$$g^{ab}_{\rm TT} = \begin{pmatrix} -1 & 0 & 0 & 0 \\ 0 & 1+h_+(z,t) & h_\times(z,t) & 0 \\ 0 & h_\times(z,t) & 1-h_+(z,t) & 0 \\ 0 & 0 & 0 & 1 \end{pmatrix} . \tag{2.85}$$

A more natural reference frame of an observer, however, is given by the tetrad

$$\begin{aligned} \boldsymbol{e}_0 &= \left(\tfrac{\partial}{\partial_t}, 0, 0, 0\right) , \\ \boldsymbol{e}_1 &= \left(0, \left[1 - \tfrac{h_+}{2}\right]\tfrac{\partial}{\partial_x}, -\tfrac{h_\times}{2}\tfrac{\partial}{\partial_y}, 0\right) , \\ \boldsymbol{e}_2 &= \left(0, -\tfrac{h_\times}{2}\tfrac{\partial}{\partial_x}, \left[1 + \tfrac{h_+}{2}\right]\tfrac{\partial}{\partial_y}\ , 0\right), \\ \boldsymbol{e}_3 &= \left(0, 0, 0, \tfrac{\partial}{\partial_z}\right) . \end{aligned} \tag{2.86}$$

This orthonormal basis will be used in Chapters 3–4.

CHAPTER 3

Gravitational and magnetosonic waves in gamma-ray bursts

J. Moortgat & J. Kuijpers

A&A , **402**, p. 905 (2003)

One of the possible sources of gamma-ray bursts (GRB) are merging, compact neutron star binaries. More than 90% of the binding energy of such a binary is released in the form of gravitational waves (GW) in the last few seconds of the spiral-in phase before the formation of a black hole. In this article we investigate whether a fraction of this GW energy is transferred to magnetohydrodynamic waves in the magnetized plasma wind around the binary. Using the 3+1 orthonormal tetrad formalism, we study the propagation of a monochromatic, plane fronted, linearly polarized GW perpendicular to the ambient magnetic field in an ultra-relativistic wind, first in the comoving and then in the observer frame. A closed set of general relativistic magnetohydrodynamic (GRM) equations is derived in the form of conservation laws for electric charge, matter energy, momentum and magnetic energy densities. We linearize the GRM equations under the action of a monochromatic GW, which acts as a driver and find that fast magneto-acoustic waves grow, with amplitudes proportional to the GW amplitude and frequency and the strength of the background magnetic field.

3.1 Introduction

The coupling between gravitational waves and electromagnetic waves (EMWs) in a magnetized vacuum has been investigated extensively over the past 40 years by a number of authors (Gertsenshtein 1961; Lupanov 1967; Boccaletti et al. 1970; Zel'dovich 1973; Gerlach 1974). These studies demonstrate the coherent excitation of EMWs by a monochromatic GW propagating perpendicularly to a background magnetic field.

The first calculations including the presence of a plasma were done by Macedo and Nelson (1983), who found a coupling of GW to ordinary and extraordinary EMWs, whereas Brodin and Marklund (1999) derived the parametric excitation of Langmuir waves by a GW propagating through unmagnetized plasma. In Marklund et al. (2000); Brodin et al. (2001), the authors adopt the 3+1 tetrad formalism (Thorne et al. 1986; Ellis and van Elst 1998) and show that the dispersion relation in a tenuous plasma differs only from the vacuum solution by a small wavenumber shift. In a plasma, however, subsequent nonlinear conversions such as harmonic generation, might allow the EMW energy to escape as radiation with frequencies high enough to overcome the interstellar plasma frequency (Brodin et al. 2001). A numerical estimate for the case of a merging NS-NS binary shows that the amplitude of the EMWs can be significant. Longitudinal waves are excited by higher-order GW-EMW interactions (Brodin et al. 2000) and magnetosonic waves (MSWs) by GW propagating in a low-β plasma (Papadopoulos et al. 2001).

In this Chapter we consider NS-NS mergers as a source for GRBs and apply the 3+1 formalism to the interaction of the GW emitted by the merger with the *ultra-relativistic wind* of magnetized plasma around the binary. In the last seconds before the collapse to a black hole, a considerable fraction of $M_{\odot}c^2$ is released into this plasma in the form of GW (see Janka et al. 1999, Table 1). We show that these waves distort the extremely strong magnetic field, frozen into the plasma, and excite growing magnetosonic waves in the wind. Already before the merger, the binary is embedded in a relativistically expanding magnetized wind of (mainly) leptons from the orbiting neutron stars, so even a small transfer of GW energy to the wind may provide an interesting *central engine* mechanism to fuel a GRB fireball.

The outline of this Chapter is as follows. In Section 3.2, the covariant expressions for the electromagnetic fields, the energy-momentum densities and the orthonormal tetrad for a linearly polarized GW are recapitulated. A closed set of linearized GRM equations in the metric of a GW is derived in Section 3.3 and solved, first in the comoving frame of the plasma (Section 3.4) and then in the frame of an observer at rest with respect to the merger (Section 3.5). A numerical example and the interpretation of our results are given in Sections 3.6 and 3.7, respectively. Section 3.8 comprises the conclusions of this chapter.

3.2 Covariant fluid equations

Electromagnetic field equations

Maxwell's equations in terms of the electromagnetic field tensors and the 4-current density $j^b_{\rm m} = (\tau, \boldsymbol{j})$ are (2.67, 2.67):

$$\nabla_b F^{ab} = 4\pi j^a_{\rm m} \quad \text{and} \quad \nabla_b \mathcal{F}^{ab} = 0 \ , \tag{3.1}$$

where the covariant Faraday tensor F^{ab} and its dual $\mathcal{F}^{ab}$, can be decomposed into 4-vectors that, in the *rest frame* of an observer with 4-velocity u^a, reduce to the electric and magnetic field strengths, $E^a = (0, \boldsymbol{E})$ and $B^a = (0, \boldsymbol{B})$ ((2.66) or Lichnerowicz (1967)):

$$\begin{aligned} F^{ab} &= u^a E^b - u^b E^a + \epsilon^{abcd} B_c u_d \quad , \quad \mathcal{F}^{ab} \equiv \tfrac{1}{2}\epsilon^{abcd} F_{cd} \ , \\ E^a &\equiv F^{ab} u_b \quad , \quad B^a \equiv \mathcal{F}^{ab} u_b \ . \end{aligned} \tag{3.2}$$

In ideal MHD, the electric field vanishes in the rest frame of the plasma: $\boldsymbol{E} = 0$. Therefore $E^a \equiv F^{ab} u_b = 0$ in any frame and Faraday's tensor reduces to: $F^{ab} = \epsilon^{abcd} B_c u_d$.

Energy and momentum conservation

Energy and momentum conservation follow from the 4-derivative of the energy-momentum tensor. For a magnetized ideal plasma this can be expressed in terms of the proper matter energy density μ, the pressure p and the metric g^{ab} (see Weinberg (1972); Hawking and Ellis (1973) and Sections 2.14, 2.14):

$$\begin{aligned} T^{ab} &= (\mu + p) u^a u^b + p g^{ab} + \frac{1}{4\pi}(F^a{}_c F^{bc} - \frac{1}{4} g^{ab} F^{cd} F_{cd}) \ , \\ \nabla_b T^{ab} &= \nabla_b \left[(\mu + p) u^a u^b + p g^{ab} \right] - F^{ab} j_{{\rm m}b} = 0 \ , \end{aligned} \tag{3.3}$$

where the current density satisfies Eq. (3.1).

Tetrad system for a gravitational wave

In the linearized theory of gravity one usually splits the metric: $g^{ab} = \eta^{ab} + h^{ab}$, where $\eta^{ab} = \mathrm{diag}(-1, 1, 1, 1)$ is the Minkowski metric, and h^{ab} is the space-time perturbation caused by the GW. For a transverse-traceless, linearly (+) polarized, monochromatic GW with frequency $\omega_{\rm g} = k_{\rm g}$ propagating in the z-direction, this field satisfies: $h^{ab} = \mathrm{diag}(0, h, -h, 0)$, with $h(z-t) = h e^{i\omega_{\rm g}(z-t)}$ (Misner et al. 1973).

The *proper* (observer) *reference frame*, however, comoving with freely moving bodies is defined with respect to the natural orthonormal tetrad (see Marklund et al. (2000) and Section 2.15):

$$e_{(0)}{}^a = (\partial_t, 0, 0, 0) \ , \qquad e_{(1)}{}^a = (0, [1 - \tfrac{h}{2}]\partial_x, 0, 0) \ , \tag{3.4a}$$

$$e_{(2)}{}^a = (0, 0, [1 + \tfrac{h}{2}]\partial_y, 0) \ , \qquad e_{(3)}{}^a = (0, 0, 0, \partial_z) \ . \tag{3.4b}$$

Decomposed with respect to this tetrad, the metric reduces to that of flat space: $g^{(ab)} = \eta^{ab}$ and the GRM equations closely resemble their Newtonian equivalents.

3.3 Magnetohydrodynamics in the comoving frame

The physical situation we want to consider is that of a perfectly conducting, ideal plasma in the presence of a background magnetic field along the x-axis, perpendicular to the direction of GW propagation (Fig. 3.1). First we study the plasma rest-frame where: $\boldsymbol{B}^{(0)} = B_0 \boldsymbol{e}_x$, $\mu^{(0)} = \rho$ and $\boldsymbol{v}^{(0)} = \tau^{(0)} = p^{(0)} = \boldsymbol{j}_{\rm m}^{(0)} = \boldsymbol{E}^{(0)} = 0$.

The effect of the GW is to induce small perturbations in all these quantities. Therefore, all equations will be linearized around the unperturbed state.

Maxwell's equations

The relevant, linearized Maxwell equations in the specified tetrad are (Marklund et al. 2000):

$$\nabla \times \boldsymbol{B}^{(1)} - \frac{\partial \boldsymbol{E}}{\partial t}^{(1)} = 4\pi \boldsymbol{j}_{\rm m}^{(1)} + \boldsymbol{j}_E^{(1)} \ , \tag{3.5}$$

$$\nabla \times \boldsymbol{E}^{(1)} + \frac{\partial \boldsymbol{B}}{\partial t}^{(1)} = -\boldsymbol{j}_B^{(1)} \ , \tag{3.6}$$

where the *gravitationally induced current densities* are just the collected Ricci rotation coefficients (2.11.2) or GW-terms:

$$\boldsymbol{j}_{\rm E}^{(1)} \equiv -\frac{B_0}{2}\frac{\partial h}{\partial z}^{(1)} \boldsymbol{e}_y \ , \quad \text{and} \quad \boldsymbol{j}_{\rm B}^{(1)} \equiv -\frac{B_0}{2}\frac{\partial h}{\partial t}^{(1)} \boldsymbol{e}_x \ . \tag{3.7a}$$

The electric field can be eliminated by assuming the ideal MHD approximation of a collisionless plasma (zero resistivity), where the electric field vanishes in the comoving frame and Ohm's law reduces to:

$$\boldsymbol{E}^{(1)} = -\boldsymbol{v}^{(1)} \times \boldsymbol{B}^{(0)} \ . \tag{3.8}$$

Conservation equations

Charge continuity follows readily from the antisymmetry of F^{ab} and Eq. (3.1): $\nabla_a(\nabla_b F^{ab}) = 4\pi\nabla_a j^a_{\rm m} = 0$.

The evolution of the *magnetic energy* W and the *Poynting flux* $\boldsymbol{S}$ are just projections of Eqs. (3.5–3.6) onto $\boldsymbol{B}^{(0)}$:

$$\frac{\partial W}{\partial t}^{(1)} + \nabla\cdot\boldsymbol{S}^{(1)} = -W^{(0)}\frac{\partial h}{\partial t}^{(1)} \quad , \tag{3.9a}$$

$$\frac{\partial \boldsymbol{S}}{\partial t}^{(1)} + \nabla W^{(1)} = W^{(0)}\frac{\partial h}{\partial z}^{(1)}\boldsymbol{e}_z - \boldsymbol{F}^{(1)}_{\rm L} \ , \tag{3.9b}$$

with $\boldsymbol{F}_{\rm L} = \boldsymbol{j}\times\boldsymbol{B}$ the Lorentz force, $W^{(0)} = B_0^2/8\pi$ and:

$$W^{(1)} = \tfrac{\boldsymbol{B}^{(0)}\cdot\boldsymbol{B}^{(1)}}{4\pi}, \quad \boldsymbol{S}^{(1)} = \tfrac{\boldsymbol{E}^{(1)}\times\boldsymbol{B}^{(0)}}{4\pi}, \quad \boldsymbol{F}^{(1)}_{\rm L} = \boldsymbol{j}^{(1)}_{\rm m}\times\boldsymbol{B}^{(0)} \ .$$

Eq. (3.3) results in *particle* and *momentum* conservation in terms of the momentum, $\boldsymbol{\pi}^{(1)} = \mu^{(0)}\boldsymbol{v}^{(1)}$ and the spatial stress tensor $\mathsf{T}^{(1)}$:

$$\frac{\partial\mu}{\partial t}^{(1)} + \nabla\cdot\boldsymbol{\pi}^{(1)} = 0 \quad , \quad \frac{\partial\boldsymbol{\pi}}{\partial t}^{(1)} + \nabla\cdot\mathsf{T}^{(1)} = 0 \ , \tag{3.10}$$

or, equivalently, as a linearized equation of motion (EOM):

$$\mu^{(0)}\frac{\partial\boldsymbol{v}}{\partial t}^{(1)} + c_s^2\nabla\mu^{(1)} = \boldsymbol{F}^{(1)}_{\rm L} \ , \tag{3.11}$$

in terms of the sound velocity $c_s^2 \equiv \Gamma(p^{(1)}/\mu^{(1)})$, where Γ is the polytropic index. To first order, the EOM does not contain any GW terms and the coupling of the GW to the plasma occurs only through the Lorentz force as can be seen from Eqs. (3.9b, 3.11) (or equivalently, through the current density which couples the EOM to Maxwell's equations (3.5–3.6)).

3.4 Wave solutions in the comoving frame

Laplace transforms

The proper way to handle the unstable response of a plasma to a disturbance is to make use of *Laplace transforms* (Landau and Lifshitz 1975; Melrose 1986). By giving the frequency or wavenumber a small positive imaginary part, one allows for damping or growth and a way to deal with singularities due to resonance. In an initial value problem it is customary to Laplace transform with respect to time, whereas in a boundary value problem, as we are considering here, a Laplace transform with respect to space is more suitable. These are defined by:

$$F(s) \equiv \textstyle\int_0^\infty \mathrm{e}^{-sz} f(z)\mathrm{d}z \quad , \quad f(z) \equiv \int_{-i\infty+\eta}^{i\infty+\eta} \mathrm{e}^{sz} F(s)\mathrm{d}s \ , \tag{3.12}$$

where η is an arbitrary positive constant chosen so that the contour of integration lies to the right side of all singularities in $F(s)$. Below, we will transform with respect to $s \equiv ik$, where $\Re[k] \approx k_g = \omega_g$, so the contour of integration follows the real axis except for the poles at $k = \pm\omega_g/u_\mathrm{A}$ and $k = \omega_g$, where it deviates infinitesimally into the *upper* half imaginary plane.

For the time dependence we use Fourier transforms, which implies that the perturbations oscillate at the frequency of the driving GW: $\propto \exp(-i\omega_\mathrm{g} t)$.

Dispersion relations and wave solutions

We will assume that the tenuous, strongly magnetized leptoid surrounding the binary has a low plasma-beta $\beta_\mathrm{pl} = (c_s/v_\mathrm{A})^2 = 4\pi p/B_0^2 \ll 1$, where the gas pressure is negligible with respect to the magnetic pressure. The classical Alfvén speed $v_\mathrm{A}^2 \equiv B_0^2/(4\pi\rho) \gg 1$ so the displacement current is important. Perturbations propagate in the relativistic plasma with the *generalized Alfvén speed*, $1/u_\mathrm{A}^2 \equiv 1 + 1/v_\mathrm{A}^2$.

In Laplace and Fourier space the 13 GRM equations derived in Section 3.3 reduce to an algebraic system with 5 non-trivial solutions:[1]

$$\begin{aligned} v_z(\omega,k) &= \tfrac{\omega}{k}\tfrac{\mu(\omega,k)}{\rho} = \tfrac{B_0 j_y(\omega,k)}{i\omega\rho} = \tfrac{(\omega+k)u_\mathrm{A}^2}{\omega+ku_\mathrm{A}^2}\tfrac{B_x(\omega,k)}{B_0} = \\ -\tfrac{E_y(\omega,k)}{B_0} &= \tfrac{ih\omega}{2}\tfrac{u_\mathrm{A}^2}{\omega^2-k^2u_\mathrm{A}^2}\tfrac{\omega+k}{\omega-k}\delta(\omega-\omega_\mathrm{g})\ . \end{aligned} \tag{3.13}$$

The inverse transformations lead to:

$$\frac{E_y(z,t)}{u_\mathrm{A}B_0} = \zeta\Re\left[\mathrm{e}^{ik(z-u_\mathrm{A}t)}\left\{1-\zeta_1\mathrm{e}^{-i\Delta kz}-\zeta_2\mathrm{e}^{-2ikz}\right\}\right]\ , \tag{3.14a}$$

$$-\frac{v_z(z,t)}{u_\mathrm{A}} = \zeta\Re\left[\mathrm{e}^{ik(z-u_\mathrm{A}t)}\left\{1-\zeta_1\mathrm{e}^{-i\Delta kz}-\zeta_2\mathrm{e}^{-2ikz}\right\}\right]\ , \tag{3.14b}$$

$$\frac{B_0 j_y(z,t)}{u_\mathrm{A}\rho\omega_g} = \zeta\Im\left[\mathrm{e}^{ik(z-u_\mathrm{A}t)}\left\{1-\zeta_1\mathrm{e}^{-i\Delta kz}-\zeta_2\mathrm{e}^{-2ikz}\right\}\right]\ , \tag{3.14c}$$

$$-\frac{B_x(z,t)}{B_0} = \zeta\Re\left[\mathrm{e}^{ik(z-u_\mathrm{A}t)}\left\{1-\zeta_3\mathrm{e}^{-i\Delta kz}+\zeta_2\mathrm{e}^{-2ikz}\right\}\right]\ , \tag{3.14d}$$

$$-\frac{\mu(z,t)}{\rho} = \zeta\Re\left[\mathrm{e}^{ik(z-u_\mathrm{A}t)}\left\{1-\zeta_4\mathrm{e}^{-i\Delta kz}+\zeta_2\mathrm{e}^{-2ikz}\right\}\right]\ , \tag{3.14e}$$

with $ku_\mathrm{A} = \omega_\mathrm{g}$, $\Delta k = k - \omega_\mathrm{g}$, $\xi \equiv u_\mathrm{A}/(1+u_\mathrm{A})^2$ and:

$$\begin{aligned} \zeta = \tfrac{h}{4}\zeta_2^{-\frac{1}{2}} \quad &, \quad \zeta_1 = 4\xi \qquad \gg \qquad \zeta_2 = u_\mathrm{A}\xi\left(\tfrac{\Delta k}{\omega_\mathrm{g}}\right)^2, \\ \zeta_3 = 4u_\mathrm{A}\xi \quad &, \quad \zeta_4 = 2\xi\tfrac{1+u_\mathrm{A}^2}{u_\mathrm{A}} \qquad \gg \qquad \zeta_2\ . \end{aligned} \tag{3.15}$$

[1] Since the only zeroth order quantities are B_0 and ρ, the superscripts indicating the perturbations will be omitted.

Since Δk is very small (see Section 3.6), we can expand the solutions around $\Delta k = 0$, or equivalently $u_{\rm A} = 1$, to find the dominant terms:

$$\frac{B_x(z,t)}{B_0} = \frac{v_z(z,t)}{u_{\rm A}} = \frac{\mu(z,t)}{\rho} = -\frac{E_y(z,t)}{u_{\rm A} B_0} \simeq \frac{h}{2} kz\, \Im\left[\mathrm{e}^{ik(z-u_{\rm A}t)}\right] , \quad (3.16)$$

$$\frac{B_0 j_y(z,t)}{u_{\rm A}\rho\omega_g} \simeq \frac{h}{2} kz\, \Re\left[\mathrm{e}^{ik(z-u_{\rm A}t)}\right] . \quad (3.17)$$

These are *fast magneto-acoustic waves*, propagating at the Alfvén speed in the same direction as the GW and growing linearly with distance.

3.5 Observer frame

For a plasma flowing out relativistically in the z-direction with Lorentz factor $\gamma_{\rm tot} = 1/\sqrt{1-(\beta+v_z)^2} \simeq \gamma + \gamma^3\beta v_z$ ($\gamma \equiv \gamma_\beta$) corresponding to a constant velocity $\beta \approx 1$, the full set of linearized GRM equations is:

$$\left\{\frac{\partial}{\partial t} + \beta\frac{\partial}{\partial z}\right\}\mu = -\gamma^2\rho\left\{\beta\frac{\partial}{\partial t} + \frac{\partial}{\partial z}\right\} v_z \qquad \text{CONTINUITY} \qquad (3.18a)$$

$$\gamma^3\rho\left\{\frac{\partial}{\partial t} + \beta\frac{\partial}{\partial z}\right\} v_z = -j_y B_0 \qquad \text{EOM} \qquad (3.18b)$$

$$\frac{\partial E_y}{\partial t} - \frac{\partial B_z}{\partial z} + 4\pi j_y = \frac{i\omega_{\rm g} h}{2}(B_0 + E_0)\mathrm{e}^{i\omega_{\rm g}(z-t)} \qquad \text{AMPERE} \qquad (3.18c)$$

$$\frac{\partial E_y}{\partial z} - \frac{\partial B_z}{\partial t} = \frac{i\omega_{\rm g} h}{2}(B_0 + E_0)\mathrm{e}^{i\omega_{\rm g}(z-t)} \qquad \text{FARADAY} \qquad (3.18d)$$

$$E_y + v_z B_0 + \beta B_x = 0 \quad , \quad E_0 = -\beta B_0 \qquad \text{OHM} \qquad (3.18e)$$

where all quantities are now defined in the *observer frame* at rest with respect to the binary (primes are used to indicate comoving quantities only where there is the risk of confusion). Explicitly: ρ, β, B_0 and $E_0 = E_y^{(0)}$ are the zeroth order quantities and μ, v_z, B_x, E_y, j_y, h are the perturbations. The most important difference with respect to the comoving frame is the factor $(1-\beta)B_0$ in the GW terms, due to the background electric field seen by the observer.

The solutions to the equilibrium system without the GW-terms, are again $\propto \mathrm{e}^{i\omega_g(z/u_{\rm A}-t)}$ with $u_{\rm A} = \frac{\beta+u'_{\rm A}}{1+\beta u'_{\rm A}}$ the Lorentz boosted, generalized Alfvén speed. The full system can be solved along the same lines as in Section 3.4 by straightforward calculation using Laplace and Fourier transformations. The physical differences between the comoving and the observer frames are clear from Eqs. (3.18).

A different approach – leading to the same result – is to Lorentz transform Eqs. (3.14a). Since Lorentz transformations are linear transformations and furthermore the phase of a plane wave is an invariant, the general solutions have the same form as Eqs. (3.14a), but with different amplitudes.

The MSW components excited by a GW propagating through a relativistically flowing plasma are given in terms of observer quantities by:

$$\frac{E_y(z,t)}{u_{\rm A}B_0} = \Lambda\Re\left[\mathrm{e}^{ik(z-u_{\rm A}t)}\left\{1-\Lambda_1\mathrm{e}^{-i\Delta kz}-\Lambda_2\mathrm{e}^{-2i\kappa z}\right\}\right] , \tag{3.19a}$$

$$-\frac{B_x(z,t)}{B_0} = \Lambda\Re\left[\mathrm{e}^{ik(z-u_{\rm A}t)}\left\{1-\Lambda_3\mathrm{e}^{-i\Delta kz}-\Lambda_4\mathrm{e}^{-2i\kappa z}\right\}\right] , \tag{3.19b}$$

$$-\frac{v_z(z,t)}{u_{\rm A}-\beta} = \Lambda\Re\left[\mathrm{e}^{ik(z-u_{\rm A}t)}\left\{1-\Lambda_5\mathrm{e}^{-i\Delta kz}-\Lambda_6\mathrm{e}^{-2i\kappa z}\right\}\right] , \tag{3.19c}$$

$$\frac{B_0 j_y(z,t)}{u_{\rm A}\rho\omega_g} = \Lambda\Re\left[\mathrm{e}^{ik(z-u_{\rm A}t)}\left\{1-\Lambda_7\mathrm{e}^{-i\Delta kz}-\Lambda_8\mathrm{e}^{-2i\kappa z}\right\}\right] , \tag{3.19d}$$

$$-\frac{\mu(z,t)}{\rho} = \lambda\Re\left[\mathrm{e}^{ik(z-u_{\rm A}t)}\left\{1-\Lambda_9\mathrm{e}^{-i\Delta kz}-\Lambda_6\mathrm{e}^{-2i\kappa z}\right\}\right] , \tag{3.19e}$$

where the constants Λ–Λ_9, λ are defined in Appendix A.1. As in Section 3.4, the dominant terms are found by expanding around $\Delta k = 0$ (justified in Section 3.6):

$$\frac{B_x(z,t)}{B_0} = -\frac{E_y(z,t)}{u_{\rm A}B_0} = \frac{v_z(z,t)}{u_{\rm A}-\beta} = \frac{\mu(z,t)}{\rho} =$$

$$\frac{(1-\beta)h}{2}kz\ \Im\left[\mathrm{e}^{ik(z-u_{\rm A}t)}\right] \simeq \frac{h}{4}\frac{kz}{\gamma^2}\ \Im\left[\mathrm{e}^{ik(z-u_{\rm A}t)}\right] , \tag{3.20a}$$

$$\frac{B_0 j_y(z,t)}{\hat{\rho}\omega_{\rm g}u_{\rm A}} \simeq \frac{h}{4}\frac{kz}{\gamma^2}\ \Re\left[\mathrm{e}^{ik(z-u_{\rm A}t)}\right] , \tag{3.20b}$$

where: $\hat{\rho} \equiv \frac{B_0^2}{4\pi}\frac{1-u_{\rm A}^2}{u_{\rm A}^2}$. Apparently, the interaction is less efficient when the plasma is escaping relativistically, than when it is at rest with respect to the source of GW.

As a final remark: Eq. (3.20a) is equivalent to the result of an initial value approach, where the Laplace transformations are performed with respect to t instead of z. The amplitudes in Eq. (3.20a) become proportional to ωt instead of kz, but the characteristic timescale T is related to the size of the interaction region R by: $\omega T \sim \omega(R/u_{\rm A}) = kR$.

3.6 Numerical estimates

In this section the results obtained in the previous sections are applied to the environs of a NS-NS binary close to merging. Both stars will have an electron-positron wind filling the surrounding space with plasma up to large distances (whether the plasma is $e^{\pm}$ or baryon loaded is not important as long as it satisfies the ideal MHD condition). The extent of the interaction region is determined by the distance $R_{\rm max}$ from the source where either the force-free or the $z \ll 1/\Delta k$ assumption breaks down. Within this scale height, we

Lab/Observer frame					
$\omega_{\rm g}$	$=$	$k_{\rm g}c$	$k_{\rm g}$	$\sim$	$2\cdot 10^{-5}$ m^{-1}
$\omega_{\rm MSW}$	$=$	$\omega_{\rm g}=k_{\rm MSW}u_{\rm A}$	$\omega_{\rm g}$	$\sim$	$2\pi\cdot 10^{3}$ rad s^{-1}
$\rho_\star$	$=$	$\frac{4Mm_{\rm e}}{e}\left(\frac{\Omega_{\rm b}B_\star}{\mu_0 c^2}\right)$	$\rho_{\rm lc}$	$\sim$	10^{-9} kg m^{-3}
$\rho_{\rm lc}$	$=$	$\rho_\star\left(\frac{B_{\rm lc}}{B_\star}\right)$	$\Omega_{\rm e}$	$=$	$\frac{eB_{\rm lc}}{m_{\rm e}}\sim 10^{17}$ rad s^{-1}
$u_{\rm A}$	$=$	$\frac{u'_{\rm A}+\beta c}{1+\beta u'_{\rm A}/c}$			
$\gamma_{u_{\rm A}}$	$\approx$	$2\gamma\gamma_{u'_{\rm A}}$	$\gamma_{u_{\rm A}}$	$\sim$	10^5
Δk	$=$	$\frac{\omega_{\rm g}}{c}\left(\frac{c}{u_{\rm A}}-1\right)$			
	$=$	$\frac{\Delta k'}{2\gamma}$	Δk	$\sim$	$2\cdot 10^{-16}$ m^{-1}
$R\Delta k$	$\ll$	1	$R_{\rm max}$	$\sim$	$\frac{0.075}{\Delta k}\sim 5\cdot 10^{14}$ m

Table 3.1: Formulas and numerical values in the observer frame. In the numerical examples of this table we have taken: $B_\star = 10^9$T, $\gamma=\gamma_{\rm s}=100$, $M=10^5$, $\Omega_{\rm b}/2\pi = 500$Hz.

Plasma/Comoving frame					
$\omega'_{\rm g}\approx\omega_{\rm g}/(2\gamma)$	$=$	$k'_{\rm g}c$	$k'_{\rm g}$	$\sim$	10^{-7} m^{-1}
$\omega'_{\rm MSW}=\omega'_{\rm g}$	$=$	$k'_{\rm MSW}u'_{\rm A}$	$\omega'_{\rm g}$	$\sim$	30 rad s^{-1}
$\frac{v'^2_{\rm A}}{c^2}=\frac{B'^2}{4\pi\rho' c^2}$	$=$	$\frac{B^2_{\rm lc}}{\mu_0\gamma\rho_{\rm lc}c^2}=$			
	$=$	$\frac{\Omega_{\rm e}}{4\gamma_{\rm p}\Omega_{\rm b}}$	$v'_{\rm A}$	$\sim$	$10^3 c$
$\frac{u'^2_{\rm A}}{c^2}$	$=$	$\frac{v'^2_{\rm A}}{c^2+v'^2_{\rm A}}$			
$\gamma^2_{u'_{\rm A}}$	$\approx$	$\frac{\Omega_{\rm e}}{4\gamma_{\rm p}\Omega_{\rm b}}$	$\gamma_{u'_{\rm A}}$	$\sim$	10^3
$\Delta k'\equiv k'-k'_{\rm g}$	$=$	$\frac{\omega'_{\rm g}}{c}\left(\frac{c}{u'_{\rm A}}-1\right)$			
	$\approx$	$Mk_{\rm gw}\frac{\Omega_{\rm b}}{\Omega_{\rm e}}$	$\Delta k'$	$\sim$	$3.6\cdot 10^{-14}$ m^{-1}

Table 3.2: Formulas and numerical values in the frame at rest with respect to the plasma for the same parameters as in Table 3.1.

estimate the magnitude of the excited MSW amplitudes, including the decrease of the GW-amplitude, the density and the magnetic field with distance. A short numerical analysis is made for the magnetic fields, plasma densities, Lorentz factors and Alfvén velocities in the relativistic plasma wind, summarized in Tables 3.1–3.2.

Note: In this section proper dimensions in c are restored and the numerical results are converted to SI units.

Magnetic field configuration

For pulsar-like neutron stars, the magnetic field close to the surface falls off as a dipole: $B(r) = B_\star\,(R_\star/r)^3$. In the MHD approximation the plasma is 'glued' to the field lines and forced to corotate up to the *lightcylinder* where corotation requires superluminal velocities. Here, we consider a NS-NS merger where each NS has its own magnetic field. The key element in the electromagnetic description of rotating magnetized stars is the deviation from inertial motion. In our case this is not the usual stellar rotation but the orbital motion combined with the individual stellar rotations. As the binary coalesces the orbital frequency increases and dominates over any other (rotational) motion. Therefore, we assume that at the end of the spiral-in phase the *orbital* rotation of the binary (with $\Omega_\mathrm{b} \sim 10^3$rad/s) determines the light-cylinder radius: $R_\mathrm{lc} = c/\Omega_\mathrm{b} \simeq 300$km. Here the field lines, anchored on the stellar polar caps, open up and the plasma is free to flow out along the field in a *force-free wind* in which the toroidal component of the field dominates the poloidal component (Kuijpers 2001a):

$$B_\mathrm{t}(r > R_\mathrm{lc}) = B_\mathrm{lc}\left[\frac{R_\mathrm{lc}}{r}\right]\,, \tag{3.21a}$$

$$B_\mathrm{p}(r > R_\mathrm{lc}) = B_\mathrm{lc}\left[\frac{R_\mathrm{lc}}{r}\right]^2\,, \tag{3.21b}$$

$$B_\mathrm{lc} = B_\star\left[\frac{\Omega_\mathrm{b}R_\star}{c}\right]^3 \simeq 4\cdot 10^5\mathrm{T}\left[\frac{B_\star}{10^9\ \mathrm{T}}\right]\left[\frac{\Omega_\mathrm{b}}{10^3\ \mathrm{rad/s}}\right]^3\left[\frac{R_\star}{10^4\ \mathrm{m}}\right]^3\,. \tag{3.21c}$$

Nature of the wind

Above the polar caps of a pulsar the field lines are open, particles flow outwards and a steady charge density cannot be maintained at the *Goldreich-Julian density* everywhere $n_\mathrm{GJ} = \boldsymbol{\Omega}_\mathrm{b}\cdot\boldsymbol{B}/(2\pi ec)$ (Gurevich et al. 1993; Lyubarsky 1995). As a result, a strong electric field develops along the magnetic field above the polar cap and charged 'primary' particles are extracted from the surface with a density $n_\mathrm{p} \simeq n_{\mathrm{GJ}\star}$ and accelerated to high Lorentz factors (a typical number is $\gamma_\mathrm{p} \sim 10^7$). Note that the available potential jump is

proportional to $\Delta\Psi \propto \Omega_\mathrm{b} B_\star$ in our case and can be much larger than for single pulsars.

Processes such as curvature radiation and inverse Compton emission then result in a cascade of 'secondary' $e^\pm$ pairs with a particle number density $n_\mathrm{s} = M n_\mathrm{p}$, where M is called the *multiplicity*. Due to energy conservation $n_\mathrm{p}\gamma_\mathrm{p} = n_\mathrm{s}\gamma_\mathrm{s}$, so the Lorentz factor of the secondary particles is $\gamma_\mathrm{s} = \gamma_\mathrm{p}/M \sim 100$ for $M \sim 10^5$. The secondary plasma flows out as a relativistic wind along the open magnetic field lines which have a dipole-like radial dependence up to R_lc, and develops into a spiral (Eq. 3.21) further out. The charge density in the wind is adjusted to the local Goldreich-Julian density everywhere and the wind remains force-free up to a large distance.

Alfvén speeds & Interaction lengthscale

The classical Alfvén speed v_A is proportional to $B_0/\sqrt{n}$. In the force free wind we have $B_0 \propto 1/r$ and $n \propto 1/r^2$, so $v_\mathrm{A}(r > R_\mathrm{lc}) =$ constant. Therefore, we can evaluate the Alfvén velocities at the light-cylinder in the *comoving frame* (using the expressions in Table 3.2):

$$B'_\mathrm{lc} = \frac{B_\mathrm{lc}}{\gamma_\mathrm{s}} \ , \tag{3.22a}$$

$$n'_\mathrm{lc} = \frac{n_\mathrm{lc}}{\gamma_\mathrm{s}} \ , \tag{3.22b}$$

$$\frac{v'^2_\mathrm{A}}{c^2} = \frac{B'^2_\mathrm{lc}}{\mu_0 n'_\mathrm{lc} m_\mathrm{e} c^2} = \frac{B^2_\mathrm{lc}}{\mu_0 \gamma_\mathrm{s} n_\mathrm{lc} m_\mathrm{e} c^2} = \frac{\Omega_\mathrm{e}}{4\gamma_\mathrm{p}\Omega_\mathrm{b}} \gg 1 \ , \tag{3.22c}$$

in terms of the electron cyclotron frequency $\Omega_\mathrm{e} = \frac{eB_\mathrm{lc}}{m_\mathrm{e}}$. For the *generalized* Alfvén speed and the wavenumber difference $\Delta k'$, one finds (see also Tables 3.1–3.2):

$$\frac{u'^2_\mathrm{A}}{c^2} = \frac{v'^2_\mathrm{A}}{c^2 + v'^2_\mathrm{A}} \simeq 1 \qquad \text{or:} \tag{3.23a}$$

$$\gamma^2_{u'_\mathrm{A}} \approx \frac{\Omega_\mathrm{e}}{4\gamma_\mathrm{p}\Omega_\mathrm{b}} \gg 1 \qquad \text{and:} \tag{3.23b}$$

$$\Delta k' \equiv k' - k'_\mathrm{g} = \frac{\omega'_\mathrm{g}}{c}\left(\frac{c}{u'_\mathrm{A}} - 1\right) \ll 1 \ . \tag{3.23c}$$

The equivalent quantities in the *observer frame* are derived from Lorentz transformations and can be found in Table 3.1. The important conclusion from these estimates is that the maximum distance over which the MSW amplitudes can grow is: $z \ll 1/\Delta k \simeq 10^{16}$ m (see Eq. (3.20a)), which is comparable to the limits on the MHD approximation as calculated by Spruit et al. (2001).

Magnitude of excited magnetosonic waves

The frequency of GW emitted by a merging binary is related to the angular frequency of the last orbits by: $\omega_{\rm g} = 2\Omega_{\rm b} \sim 4\pi \cdot 10^3$ rad/s (Shibata and Uryu 2002), so $R_{\rm lc} \sim 50$km and $B_{\rm lc} \sim 10^7$T. We assume that for $R_{\rm in} \sim 10 R_{\rm lc}$ we are in the far field of the merger and estimate the amplitude of $B_x^{(1)}(z,t)$ in Eq. (3.20a) at the start of the interaction region. Taking into account the (approximate) $1/r$ decrease of h and B_0,

$$h \sim 10^{-3} \left(\frac{R_{\rm in}}{r} \right) , \tag{3.24a}$$

$$B_0 \sim B_{\rm lc} \left(\frac{R_{\rm lc}}{R_{\rm in}} \right) \left(\frac{R_{\rm in}}{r} \right) , \tag{3.24b}$$

we find:

$$B^{(1)}(r > R_{\rm in}) \sim 0.5{\rm T} \left[\frac{R_{\rm in}}{r} \right] \times \left[\frac{h}{10^{-3}} \right] \left[\frac{\gamma}{100} \right]^{-2} \left[\frac{k_{\rm gw}}{10^{-5}\ {\rm m}^{-1}} \right] \left[\frac{B_{\rm lc}}{10^7\ {\rm T}} \right] \left[\frac{R_{\rm in}}{10^5\ {\rm m}} \right] . \tag{3.25}$$

The volume integrated energy of the MSW grows linearly with distance since $B^{(1)} \propto B_0 \propto 1/r$ and $V \propto r^3$. For an interaction region of $R_{\rm max} \sim 0.03$ pc we find for the magnetic component of the excited MHD wave a total energy of:[2]

$$\mathsf{T}_{\rm B}^{(1)} \quad = \quad V \frac{|B^{(1)}|^2}{2\mu_0} \sim 10^{31}{\rm J} . \tag{3.26}$$

3.7 Discussion

It is known that, to first order in h, GW propagating *along* a uniform magnetic field do not couple to the field, neither in vacuum (Boccaletti et al. 1970), nor in a plasma (Brodin et al. 2000; Papadopoulos et al. 2001) so we studied GW-propagation *perpendicular* to the magnetic field frozen into a plasma. An intuitive illustration of the process is given in Fig. 3.1, where a GW traveling in the positive z-direction, deforms (imaginary) rings of plasma-particles in the x–y plane into ellipses with long axes alternating periodically along the magnetic field direction (x-axis) and the y-axis. Consequently, the uniform field is periodically compressed and stretched leading to a *modulated magnetic field strength* even though the GW is divergence-free. The resulting magnetic pressure gradients in the z-direction try to re-establish a uniform field configuration and excite the compressional *matter part* of the MSW. Since the plasma

[2] Note that in the published paper we accidently had $B^0 B^1$ instead of $|B^{(1)}|^2$.

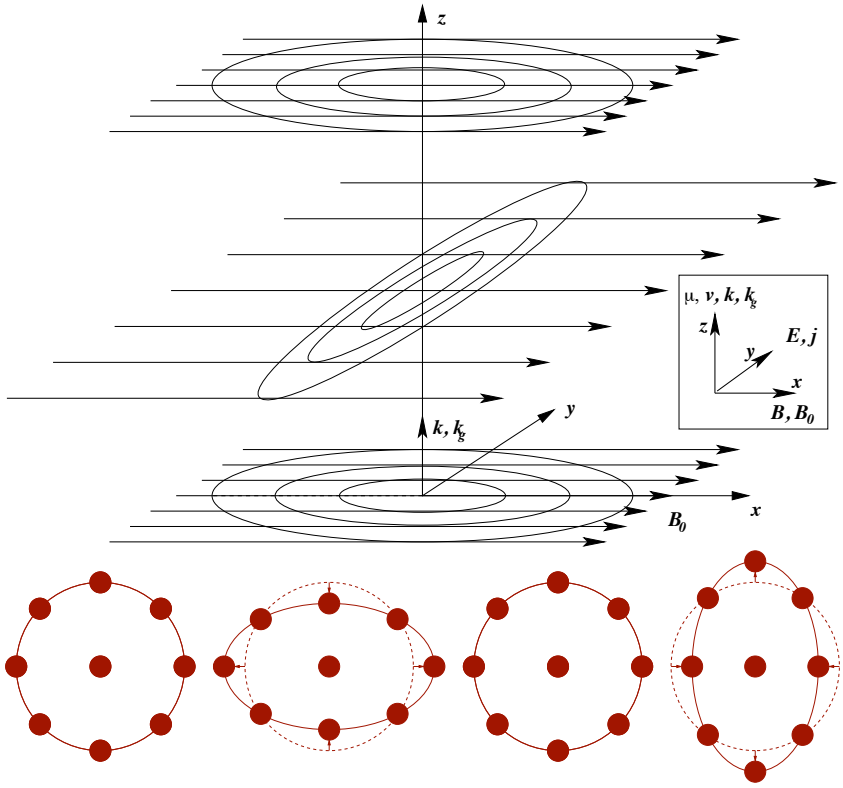

Figure 3.1: A GW propagating in the positive z-direction across an ambient magnetic field (in the x-direction) excites a MSW. The orientations of the MSW components are indicated in the inset.

is glued to the field lines it is dragged along with the field. The velocity in the z-direction generates an *electric field* ($-\boldsymbol{v} \times \boldsymbol{B}$) with a corresponding $\boldsymbol{E} \times \boldsymbol{B}$ *drift-velocity*, whereas the magnetic gradient induces a $\boldsymbol{B} \times \nabla \boldsymbol{B}$ *current density* and *Lorentz force*.

The problem of GW propagation in a plasma at rest was also studied by Papadopoulos et al. (2001) who found that the excitation of MSWs by a GW is only possible when there is a wavenumber mismatch: $B_x^{(1)} \propto \Delta k$. This does not agree with our results (as presented in Section 3.4), nor with those of Marklund et al. (2000) who show that the growth rate in a tenuous plasma

smoothly matches that in a vacuum (Boccaletti et al. 1970). Both from the GRM equations (Eqs. (3.9a–3.11) or (3.18)) and from their solutions (Eqs. (3.16) or (3.20a)) it is clear that in the vacuum limit $\mu^{(1)} \propto j_y^{(1)} \propto \rho \downarrow 0$ vanish as does $v_z^{(1)}$. The GW excite EMWs that propagate with the speed of light ($\Delta k \downarrow 0$) and with amplitudes that can be obtained from Eq. (3.16) or Eq. (3.20a) by taking the limit $u_{\rm A} \rightarrow c$ and $k \rightarrow k_{\rm g}$ (and $\gamma = 1$). This result is not surprising as we have taken into account both the material current and the vacuum displacement current.

3.8 Conclusion

The results presented in this chapter are a first attempt to study the interaction of the relatively strong GW emitted by a GRB with an ultra-relativistic plasma wind. The space surrounding a merging NS-NS binary is already filled with such a wind up to large distances (~ 0.1 pc). Moreover, in the merger almost all of the binding energy is released in the form of GW.

We derive a closed set of GRM equations both in the natural orthonormal measurement frame (the 3+1 split discussed in Section 2.14) of the plasma and for an observer at rest with respect to the binary. These non-coordinate equations strongly resemble their Newtonian equivalents but have extra source terms due to the GW. These gravity terms act as a driver for *fast magnetosonic waves* with amplitudes that grow linearly with distance and are proportional to the GW-frequency and amplitude and to the ambient magnetic field strength. It is the extended force-free wind in which the magnetic field only falls off as $1/r$ that provides the long interaction lengthscale.

The total amount of energy that is transferred from the GW to the plasma, as given in Eq. (3.26), is substantial but for this case still much smaller than the average observed GRB energy. Note that for *magnetars* one can have $B_\star \sim 10^{12}$ T and $\omega_{\rm g} \sim 15$ kHz, so that the magnetic energy density could be as much as a factor 10^7 larger. However, for magnetars it is not obvious what to assume for the surrounding plasma.

In the next Chapter 4 we will extend the results presented here to more general environment, allowing for the gas pressure in the plasma, both GW polarizations and oblique propagation. Chapter 5 turns to the possibility of observing the effects of the GW-MSW interaction by inverse Compton scattering the magneto-acoustic to low-frequency radio waves.

CHAPTER 4

Gravitational waves in magnetized relativistic plasmas

J. Moortgat & J. Kuijpers

Phys. Rev. D **70**, 023001 (2004)

We study the propagation of gravitational waves (GW) in a uniformly magnetized plasma at arbitrary angles to the magnetic field. No a priori assumptions are made about the temperature, and we consider both a plasma at rest and a plasma flowing out at ultra-relativistic velocities. In the 3+1 orthonormal tetrad description, we find that all three fundamental low-frequency plasma wave modes are excited by the GW. Alfvén waves are excited by a $\times$ polarized GW, whereas the slow and fast magneto-acoustic modes couple to the $+$ polarization. The slow mode, however, doesn't interact coherently with the GW. The most relevant wave mode is the fast magneto-acoustic mode which in a strongly magnetized plasma has a vanishingly small phase lag with respect to the GW allowing for coherent interaction over large length scales. When the background magnetic field is almost, but not entirely, parallel to the GW's direction of propagation even the Alfvén waves grow to first order in the GW amplitude. Finally, we calculate the growth of the magneto-acoustic waves and the damping of the GW.

4.1 Introduction

The interaction of gravitational waves (GW) with a magnetized plasma relies on the non-isotropy of the magnetic field and the fact that both GW and electromagnetic waves propagate at the speed of light in vacuum. In vacuum, the GW excites an electromagnetic wave propagating in the same direction as the GW at the speed of light as was first realized by Gertsenshtein (1961). Propagation through a perfect collisionless fluid does not affect a GW (Gayer and Kennel 1979; Thorne 1989), but in an astrophysical plasma the electromagnetic field is coupled to the matter and, indirectly, the GW interacts with both the electromagnetic fields and quantities such as density, pressure and currents (Macedo and Nelson 1983).

For a summary of previous work on the interaction of a GW with plasma waves we refer to the introduction of Moortgat and Kuijpers (2003) presented in Chapter 3, and references therein and Servin (2003) for more recent work.

In this chapter we study the full problem of a plane fronted, monochromatic GW of either $+$ or $\times$ polarization propagating obliquely through a magnetized collisionless plasma. Furthermore, we don't specify whether the plasma is Poynting flux or matter dominated. Also, we allow for relativistic velocities as we want to apply our results to an ultra-relativistic force-free wind or jet.

The outline of this chapter is as follows. We start in Section 4.2 with a discussion of the Einstein field equations (EFE) describing both the background curvature due to the static energy content and the dynamical interaction of space-time with a time dependent energy-momentum density. In the geometric optics limit (Section 4.2) the GW can be treated just like photons traveling on null geodesics. In Sections 4.2 – 4.2 we recapitulate how the proper reference frame of an observer (the $3+1$ orthonormal tetrad frame) is defined by taking snapshots of four-dimensional space-time and using ordinary vector calculus on these spatial hypersurfaces. Also, the covariant derivatives and connection coefficients for such a non-coordinate frame are summarized. A closed set of linearized general relativistic magneto-hydrodynamic (MHD) equations is derived in Section 4.3 and solved algebraically in Section 4.4. We find that all the fundamental plasma waves are excited: a $+$ polarized GW excites fast magneto-acoustic waves, which was expected from previous idealized calculations in Papadopoulos et al. (2001) and Chapter 3. In this chapter we extend this result to a realistic fast mode with both electromagnetic and gas properties and find that also the slow magneto-acoustic mode is excited (Section 4.4). A completely new result is that a $\times$ polarized GW propagating at an angle to an ambient magnetic field excites Alfvén waves in the plasma (Section 4.4). The space-time solutions in the comoving frame are derived in Section 4.5 and boosted to an ultra-relativistic wind in the the observer frame in Section 4.6. In the limit where the phase velocities of the Alfvén and fast mode approach the speed of light the waves can interact coherently, which results in linear growth of the amplitudes. For the Alfvén mode this also requires that the angle with the magnetic field is very small (Section 4.5).

Finally, we investigate the back-reaction on the GW in Section 4.7 and find

that as the plasma waves grow, the GW is damped with a group velocity that decreases linearly with distance. An intuitive interpretation of some of these results is presented in Section 4.8, and we end with conclusions in Section 4.9.

4.2 Einstein-Maxwell equations

In Lorentz gauge, the linearized Einstein field equations (EFE) for weak gravitational waves interacting with a magneto-fluid read (Misner et al. 1973):

$$G^{ab} \simeq -\frac{1}{2}\Box h^{ab} \quad = \quad 8\pi\delta T^{ab} \ , \tag{4.1}$$

where δT^{ab} is the oscillatory part of the energy-momentum tensor. If we further specify to the transverse traceless (TT) gauge and consider a GW propagating in the z direction, the only independent components of h^{ab} are $h^{xx} = -h^{yy} = h_+$ and $h^{xy} = h^{yx} = h_\times$ indicating the + and × GW polarizations respectively. The individual propagation equations for the two polarizations are:

$$\Box h_+ \quad = \quad -8\pi(\delta T^{xx} - \delta T^{yy}) \ , \tag{4.2a}$$

$$\Box h_\times \quad = \quad -8\pi(\delta T^{xy} + \delta T^{yx}) \ . \tag{4.2b}$$

As an example, a GW propagating perpendicularly to a background magnetic field B_x^0 excites perturbations B_x^1 that produce an oscillating cross term in the stress-energy tensor and (4.2) take the form (Gertsenshtein 1961):

$$\Box h_+(z,t) = 4B_x^0 B_x^1(z,t) \ , \qquad \Box h_\times = 0 \ . \tag{4.3}$$

From Maxwell's equations (coupled to the EFE via the twice contracted Bianchi identities and consequently conservation of energy-momentum $\nabla_b T^{ab} = 0$) one finds wave equations for the plasma quantities in which the GW appears as a source term:

$$\hat{\Box} B_x^1(z,t) \quad \propto \quad h_+(z,t) B_x^0 \ , \tag{4.4}$$

where $\hat{\Box}$ is some wave propagator. Eq. (4.2) together with (4.4) self-consistently determine the interaction between the GW and the plasma waves (as we will work out in more detail in Section 4.7).

Background curvature

The exact (non-linear) Einstein field equations describe the curvature of spacetime due to the presence of matter and energy. This curvature is described by the contracted Riemann tensor with an associated characteristic length scale, $\mathcal{R}$, given by the magnitude of it's largest components as:

$$R^{ab} \quad = \quad 8\pi \left(T^{ab} - \frac{1}{2} g^{ab} T \right) \ , \tag{4.5a}$$

$$\frac{1}{\mathcal{R}^2} \quad \sim \quad (B^0)^2 \ . \tag{4.5b}$$

When the interaction with a magnetic field excites electromagnetic waves growing linearly with distance, viz $B^1 \propto B^0 h_+ kz$ we can see from our rough estimate (4.5b) that the fraction of GW energy that is converted into electromagnetic waves is proportional to $B^1/h_+ \propto z/\mathcal{R}$. As an example, a background magnetic field comparable to the surface field of a neutron star ($B^0 \sim 10^8$ T) curves space on a scale of $\sim 10^{10}$ m. If this field would remain constant with distance, all the GW energy would be converted to EM energy on a length scale of order $\mathcal{R}$. In reality, we will be studying a force-free plasma wind in which the magnetic field falls off linearly with distance. In this case the background curvature also decreases and the interaction length scale is much smaller than the radius of curvature.

The opposite limit of a weak primordial magnetic field with an extremely large spatial extent was discussed by Zel'dovich (1973) who argued that it is very difficult to keep the interaction coherent on such a scale in a universe that is not a perfect vacuum.

Geometric optics

The gravitational waves are assumed to be of the form: $h_{+,\times} \sim \mathcal{H}(z)\mathrm{e}^{i\omega(z-t)}$ with a slowly varying amplitude such that $\omega\mathcal{H}(z) \gg \frac{\partial}{\partial z}\mathcal{H}(z)$ and $\frac{\lambda}{\mathcal{R}} \ll 1$. This is the short wavelength, geometric optics limit where GW behave as rays moving on null geodesics $k^a k_a = 0$ that experience dispersion, refraction, lensing etc. The GW move in an essentially flat Minkowski background, η^{ab}, so the full metric is $g^{ab} = \eta^{ab} + h^{ab}$ with $|h^{ab}| \ll 1$ and self-interactions (of order h^2) are negligible.

We will study the propagation of transverse traceless gravitational waves in a magnetized plasma at arbitrary angle θ to a background magnetic field $\boldsymbol{B}_0$. Also we don't specify the temperature (or equivalently the pressure) regime except that the temperature equilibration time between the different particle species is short as compared to other characteristic timescales to comply with a hydrodynamic description. The only other non-vanishing plasma quantities in the equilibrium state are then the energy density μ^0 and pressure p^0. The passing GW will excite small (first-order) perturbations in all plasma quantities, denoted as for instance: $\mu = \mu^0 + \mu^1$.

No coupling to unmagnetized plasma

The stress-energy tensor for a homogeneous perfect fluid in the rest frame of an observer ($u^a = (1, 0, 0, 0)$) is:

$$T^{ab} = (\rho + p)u^a u^b + p g^{ab} \ . \tag{4.6}$$

A linearly polarized GW will produce perturbations in ρ, p and u^i of order $h_{+,\times}$. However, the δT^{ij} components are all higher order except for the trace δT^{ii}, which is purely gauge. Explicitely, in (4.2) $T^{xy} = T^{yx} = 0$ and $T^{xx} - T^{yy} = 0$.

Therefore a gravitational wave cannot couple to an unmagnetized perfect fluid in linearized theory (Thorne 1989). Only relativistically gyrating particles can interact with a × polarized GW through non-linear $(\rho+p)v_iv_j$ terms (Papadopoulos 2002; Servin and Brodin 2003).

Space-time split

To simplify equations, we will use the so-called 3+1 split of space-time (Ellis and van Elst 1999a; Thorne and MacDonald 1982). A time-like observer moving with 4-velocity u^a perceives space as the 3 dimensional hypersurface [1] orthogonal to u^a, and u^a itself as the time axis. We can define $u^a(x^b)$ at each point in space-time as the direction of time, and define space as the *snapshots* of space at constant time. Subsequently, we can split equations into their space and time components by using the parallel and orthogonal projection operators $U^a_{\ b} \equiv -u^a u_b$ and $H_{ab} \equiv g_{ab} + u_a u_b$, respectively, with $U^a_{\ b} + H^a_{\ b} = \delta^a_{\ b}$.

As an example, the covariant electromagnetic Faraday tensor F^{ab} (and it's dual $\mathcal{F}^{ab} \equiv \frac{1}{2}\epsilon^{abcd}F_{cd}$) can be simplified by splitting it into its time and space components:

$$\begin{aligned} F^{ab} &= (U^a_{\ c}U^b_{\ d} + H^a_{\ c}H^b_{\ d})F^{cd} \ , \\ &= u^a E^b - E^a u^b + \epsilon^{abc}B_c = \epsilon^{abc}B_c \ , \end{aligned} \tag{4.7}$$

where we have defined $B_a \equiv \frac{1}{2}\epsilon_{abc}F^{bc}$ and $E^a \equiv F^{ab}u_b$ that reduce to the magnetic and electric field, respectively, in the rest frame of an observer. The last equality in (4.7) is only valid in the ideal MHD approximation $E^a = 0$. Since $E^a = \epsilon^{abc}u_b B_c$ or $\boldsymbol{E} = -\boldsymbol{v} \times \boldsymbol{B}$ the requirement that the comoving electric field vanishes replaces Ohm's law. Similarly, the covariant Maxwell equations can be split into their space and time components. For a derivation we refer to Section 2.14 or Ellis and van Elst (1999a).

Proper reference frame

In describing the interaction of a GW with a plasma, one has two choices for the reference frame (see Section 2.15). One is the transverse-traceless coordinate frame, discussed in the previous sections, which is tuned to a GW with metric:

$$g^{ab}_{\rm TT} = \begin{pmatrix} -1 & 0 & 0 & 0 \\ 0 & 1+h_+(z,t) & h_\times(z,t) & 0 \\ 0 & h_\times(z,t) & 1-h_+(z,t) & 0 \\ 0 & 0 & 0 & 1 \end{pmatrix} \ . \tag{4.8}$$

The natural reference frame of an observer, however, is an orthonormal tetrad frame (ONF). The basis vectors that remain orthogonal in the presence of a TT

[1] The rest-space volume element is related to the 4D element ($\epsilon^{abcd} = \epsilon^{[abcd]}$; $\epsilon^{0123} = \sqrt{|\det g|}$) by $\epsilon^{abc} \equiv \epsilon^{abcd}u_d$.

plane polarized GW are:

$$\begin{aligned} \boldsymbol{e}_0 &= (\tfrac{\partial}{\partial_t}, 0, 0, 0) \ , \\ \boldsymbol{e}_1 &= (0, \left[1 - \tfrac{h_+}{2}\right] \tfrac{\partial}{\partial_x}, -\tfrac{h_\times}{2} \tfrac{\partial}{\partial_y}, 0) \ , \\ \boldsymbol{e}_2 &= (0, -\tfrac{h_\times}{2} \tfrac{\partial}{\partial_x}, \left[1 + \tfrac{h_+}{2}\right] \tfrac{\partial}{\partial_y}, 0) \ , \\ \boldsymbol{e}_3 &= (0, 0, 0, \tfrac{\partial}{\partial_z}) \ , \end{aligned} \tag{4.9}$$

where the partial derivatives reflect the notion that in curved space-time, tangent vectors and partial derivatives are equivalent as discussed extensively in Section 2.2. With respect to the basis vectors in (4.9) the metric is locally Minkowskian η^{ab}.

Covariant derivatives are defined as: $\nabla_a T_{bc} = \boldsymbol{e}_a T_{bc} - \Gamma^d_{\ ba} T_{dc} - \Gamma^d_{\ ca} T_{bd}$, where the connection coefficients are linear combinations of the commutation functions $\gamma^a_{\ bc}$ and not derivatives of the metric as in a coordinate frame (see the definitions in Section 2.10)

$$\Gamma_{abc} = \frac{1}{2}(\eta_{ad}\gamma^d_{\ cb} - \eta_{bd}\gamma^d_{\ ca} + \eta_{cd}\gamma^d_{\ ab}) \ , \tag{4.10}$$

and are skew in the first two indices, $\Gamma_{(ab)c} = 0$.

There seems to be some inconsistency in the literature on the explicit form of the connection coefficients. In a coordinate frame, the connection coefficients are given by the Christoffel symbols. For the metric (4.8) the Christoffel symbols are $\propto \dot{h}/2$ and have 12 non-vanishing components for each polarization. The explicit form of these components are given in Brodin et al. (2001) and Papadopoulos et al. (2001), but it should be noted that in Brodin et al. (2001) one of course also has the symmetric components, and in Papadopoulos et al. (2001) $\Gamma^0_{\ 10}$, $\Gamma^0_{\ 01}$ should be $\Gamma^1_{\ 10}$, $\Gamma^1_{\ 01}$.

In the orthonormal tetrad frame the connection coefficients only have 8 non-vanishing components for each polarization:

$$\Gamma_{[02]2} = -\Gamma_{[01]1} = \frac{1}{2}\frac{\partial h_+}{\partial t} \ , \qquad \Gamma_{[32]2} = -\Gamma_{[31]1} = \frac{1}{2}\frac{\partial h_+}{\partial z} \ ,$$

$$\Gamma_{[20]1} = -\Gamma_{[01]2} = \frac{1}{2}\frac{\partial h_\times}{\partial t} \ , \qquad \Gamma_{[13]2} = -\Gamma_{[32]1} = \frac{1}{2}\frac{\partial h_\times}{\partial z} \ ,$$

where $\Gamma_{[01]1}$ stands for $\Gamma_{011} = -\Gamma_{101}$ etc.

The Einstein field equations and the equations of geodesic deviation are derived from the Riemann curvature tensor, that in the ONF is given to first order in $h_{+,\times}$ by:

$$R^a_{\ bcd} = \boldsymbol{e}_c \Gamma^a_{\ bd} - \boldsymbol{e}_d \Gamma^a_{\ bc} + \mathcal{O}[h^2] \ . \tag{4.11}$$

The Ricci tensor R_{ab} is just a contraction of (4.11) and to first order reduces to the same form as in the TT coordinate frame. This means that the Einstein

field equations in the proper reference frame also have the same form as in (4.1) (we will use this in Section 4.7 when discussing the damping of the GW).

The driving force of a GW on a test particle is also described through the Riemann tensor in the form of the equations of geodesic deviation (see Definition 2.9.10):

$$\frac{\mathrm{d}^2 x^i}{\mathrm{d}t^2} = -R_{i0j0}x^j = \frac{1}{2}\begin{pmatrix} \ddot{h}_+ & \ddot{h}_\times & 0 \\ \ddot{h}_\times & -\ddot{h}_+ & 0 \\ 0 & 0 & 0 \end{pmatrix}\begin{pmatrix} x \\ y \\ z \end{pmatrix} , \tag{4.12}$$

where $\ddot{h}_{+,\times} = \frac{\partial^2}{\partial t^2} h_{+,\times}$. This equation will be important for our interpretation of the interaction with a magnetic field in Section 4.8.

4.3 General relativistic MHD

Throughout this chapter we assume that the MHD approximation is valid, viz that the plasma is a collisionless one-fluid with negligible viscosity, resistivity and heat flow. In contrast to some definitions of the MHD approximation, however, we do allow for relativistic velocities which means that displacement currents cannot be neglected and a generalized definition of the Alfvén velocity is needed (Section 4.4). We don't restrict the angle between the GW propagation and the background magnetic field, but without loss of generality choose it to lie in the x-z plane.

Coupling to the electromagnetic field

A gravitational wave propagating through a uniform magnetic field $\boldsymbol{B}^0$ produces a Lorenz force $\boldsymbol{F}^1_{\mathrm{L}}$ given by the projection of Ampère's law, $\nabla_b F^{ab} = j^a$, perpendicular to $\boldsymbol{B}^0$:

$$\begin{aligned} \boldsymbol{F}^1_{\mathrm{L}} &= \boldsymbol{j}^1 \times \boldsymbol{B}^0 = \frac{(\boldsymbol{B}^0\cdot\nabla)\boldsymbol{B}^1}{4\pi} - \nabla\left(\frac{\boldsymbol{B}^0\cdot\boldsymbol{B}^1}{4\pi}\right) \\ &- \frac{|\boldsymbol{B}^0|^2}{4\pi}\frac{\partial \boldsymbol{v}^1}{\partial t} + \frac{\boldsymbol{B}^0}{4\pi}\frac{\partial}{\partial t}(\boldsymbol{v}^1\cdot\boldsymbol{B}^0) - \frac{\boldsymbol{j}_{\mathrm{E}}\times\boldsymbol{B}^0}{4\pi} . \end{aligned} \tag{4.13}$$

Faraday's law, $\nabla_b \mathcal{F}^{ab} = 0$, is given in the $3+1$ split by:

$$\frac{\partial \boldsymbol{B}^1}{\partial t} = (\boldsymbol{B}^0\cdot\nabla)\boldsymbol{v}^1 - \boldsymbol{B}^0(\nabla\cdot\boldsymbol{v}^1) - \boldsymbol{j}_{\mathrm{B}} . \tag{4.14}$$

The projection of (4.14) onto $\boldsymbol{B}_0$ governs the evolution of the magnetic energy density:

$$\frac{\partial}{\partial t}\frac{\boldsymbol{B}^0\cdot\boldsymbol{B}^1}{4\pi} = \boldsymbol{B}^0\cdot\nabla\frac{\boldsymbol{v}^1\cdot\boldsymbol{B}^0}{4\pi} - \frac{|\boldsymbol{B}^0|^2}{4\pi}\nabla\cdot\boldsymbol{v}^1 - \frac{\boldsymbol{j}_{\mathrm{B}}\cdot\boldsymbol{B}^0}{4\pi} . \tag{4.15}$$

The GW source terms in (4.13–4.15) are given by:

$$\boldsymbol{j}_{\rm E} = \frac{B_x^0}{2}\frac{\partial}{\partial z}\begin{pmatrix} -h_\times \\ h_+ \\ 0 \end{pmatrix} , \qquad \boldsymbol{j}_{\rm B} = -\frac{B_x^0}{2}\frac{\partial}{\partial t}\begin{pmatrix} h_+ \\ h_\times \\ 0 \end{pmatrix} . \tag{4.16}$$

Equation of state & Conservation of number density

From the first law of thermodynamics, $dU = dQ - pdV$, we can find the internal energy per unit mass, U, as a function of the pressure, p, the specific volume per unit mass, $V = 1/\rho$, and the heat flow that, however, vanishes under the MHD condition: $dQ = 0$. We assume an adiabatic *equation of state* $p = K\rho^\gamma$, where γ is the adiabatic index, which lies in $4/3 \leq \gamma \leq 5/3$. The total relativistic matter energy density with respect to the 4-velocity of an ideal fluid (with the velocity of light included explicitly) is given by:

$$\mu = \rho(c^2 + U) = \rho c^2 + \frac{p}{\gamma - 1} , \tag{4.17}$$

and the relativistic enthalpy is defined by $w^0 = \mu^0 + p^0$. From these expressions we can derive the proper relativistic sound velocity by considering the change in pressure with μ at constant entropy:

$$c_{\rm s}^2 = \left.\frac{\partial p}{\partial \mu}\right|_{\rm ad} = \frac{\gamma p^0}{w^0} . \tag{4.18}$$

The matter density ρ can be solved from the covariant conservation of proper number density, $n = \rho/m_e$, which is given by $\nabla_a(nu^a) = 0$. In the orthonormal comoving frame to first order one finds:

$$\frac{\partial \rho^1}{\partial t} + \rho_0 \nabla \cdot \boldsymbol{v}^1 = 0 . \tag{4.19}$$

Energy conservation

The conservation of energy and momentum follows from the divergence of the EFE ((4.1)) as:

$$\nabla_b T^{ab} = \nabla_b \cdot [(\mu + p)u^a u^b + p g^{ab}] - F^{ab} j_b = 0 . \tag{4.20}$$

Contracting (4.20) with $U^c{}_a$ leads to the energy conservation equation:

$$\frac{\partial}{\partial t}[\Gamma^2(\mu + p) - p] + \nabla \cdot [\Gamma^2(\mu + p)\boldsymbol{v}] = 0 , \tag{4.21}$$

In the comoving frame ($\Gamma = 1$) we can eliminate μ in favor of p from (4.17) and (4.19):

$$\frac{\partial p^1}{\partial t} + \gamma p^0 \nabla \cdot \boldsymbol{v}^1 = 0 . \tag{4.22}$$

Note that from hereon, (4.19) is redundant and can be dropped from our set of equations altogether. It can be solved separately to find ρ^1 from $\boldsymbol{v}^1$.

In the cold non-relativistic limit when the internal energy is negligible with respect to the rest-mass energy ($p \ll \mu$), (4.21) reduces to (4.19) as in Chapter 3.

Conservation of momentum

The equation of motion or momentum conservation in a 3 + 1 split (Section 2.14) is projected out by $H^c{}_a$:

$$\frac{\partial}{\partial t}[\Gamma^2(\mu+p)\boldsymbol{v}] + \nabla\cdot[\Gamma^2(\mu+p)\boldsymbol{v}\boldsymbol{v} + p\mathrm{I}] = \boldsymbol{j}\times\boldsymbol{B}\ ,$$

$$(\mu^0+p^0)\frac{\partial \boldsymbol{v}^1}{\partial t} + \nabla p^1 = \boldsymbol{j}^1\times\boldsymbol{B}^0\ . \tag{4.23}$$

The Lorentz force couples the matter to the electromagnetic fields and the GW source terms, which is apparent from combining (4.13) and (4.23):

$$\begin{aligned} w_{\rm tot}\frac{\partial \boldsymbol{v}^1}{\partial t} &= -\nabla p^1 + \frac{(\boldsymbol{B}^0\cdot\nabla)\boldsymbol{B}^1}{4\pi} - \nabla\left(\frac{\boldsymbol{B}^0\cdot\boldsymbol{B}^1}{4\pi}\right) \\ &+ \frac{\boldsymbol{B}^0}{4\pi}\frac{\partial(\boldsymbol{v}^1\cdot\boldsymbol{B}^0)}{\partial t} - \frac{\boldsymbol{j}_{\rm E}\times\boldsymbol{B}^0}{4\pi}\ , \end{aligned} \tag{4.24}$$

where we have defined:

$$w_{\rm tot} = w^0 + \frac{|\boldsymbol{B}^0|^2}{4\pi}\ . \tag{4.25}$$

This form of the equations of motion is also found by explicitly evaluating the divergence of the electromagnetic part of the stress-energy tensor,

$$\nabla_b T^{ab}_{\rm EM} = \frac{1}{4\pi}\nabla_b(F^a{}_c F^{bc} - \frac{1}{4}g^{ab}F^{cd}F_{cd})\ ,$$

instead of using Ampère's law. The time projection, $\nabla_b T^{0b}$, then results in a conservation equation for the total energy density, e.g. (4.15) and (4.22) combined.

To summarize, in this section we have obtained a closed set of partial differential equations of z, t for the 16 variables $\boldsymbol{B}, \boldsymbol{E}, \boldsymbol{j}, \tau, \boldsymbol{v}, \mu, p, \rho$ that constitute the general relativistic MHD description of a GW propagating through a magnetized relativistic plasma. We will first solve these equations algebraically in Fourier and Laplace space in the next section and subsequently derive the space-time solutions in Section 4.5.

4.4 Plasma waves

In a relativistic, magnetized plasma the proper sound velocity of a compressional wave is given in (4.18) and we define the Alfvén velocity of a non-compressional shear wave in the magnetic field, $u_{\rm A}$, and the velocity of a mixed magneto-acoustic wave, $u_{\rm m}$, by:

$$u_{\rm A}^2 = \frac{|\boldsymbol{B}^0|^2}{4\pi w_{\rm tot}} , \tag{4.26a}$$

$$u_{\rm m}^2 = \frac{\gamma p^0}{w_{\rm tot}} + \frac{|\boldsymbol{B}^0|^2}{4\pi w_{\rm tot}} . \tag{4.26b}$$

To construct a wave equation for the plasma perturbations we take a second time derivative of (4.24) and eliminate $\boldsymbol{B}^1$ by (4.14, 4.15) and p^1 by (4.22). In terms of the characteristic velocities (4.26a, 4.26b) we find:

$$\left[\frac{\partial^2}{\partial t^2} - u_{\rm m}^2 \nabla\nabla\cdot\right] \boldsymbol{v}^1 - \left[\boldsymbol{u}_{\rm A}\frac{\partial^2}{\partial t^2} - (\boldsymbol{u}_{\rm A}\cdot\nabla)\nabla\right](\boldsymbol{v}^1\cdot\boldsymbol{u}_{\rm A}) = (\boldsymbol{u}_{\rm A}\cdot\nabla)^2\boldsymbol{v}^1 - \boldsymbol{u}_{\rm A}(\boldsymbol{u}_{\rm A}\cdot\nabla)\nabla\cdot\boldsymbol{v}^1 + \text{GW terms} , \tag{4.27}$$

where the GW source terms are now given by:

$$\sqrt{\frac{w_{\rm tot}}{4\pi}}\left[\nabla(\boldsymbol{j}_{\rm B}\cdot\boldsymbol{u}_{\rm A}) - \frac{\partial}{\partial t}(\boldsymbol{j}_{\rm E}\times\boldsymbol{u}_{\rm A}) - (\boldsymbol{u}_{\rm A}\cdot\nabla)\boldsymbol{j}_{\rm B}\right] .$$

Symmetric matrix representation

We are considering GW-propagation along the z-axis with the wave vector $\boldsymbol{k} = (0,0,k)$ at an arbitrary angle θ to the ambient magnetic field, which is assumed to lie in the $x{-}z$ plane. To solve the system of differential equations algebraically, we Fourier transform with respect to time and Laplace transform the spatial part to allow for growing amplitudes as in Chapter 3. The wave equation (4.27) can be written in a symmetric matrix representation since the non-linear general relativistic MHD equations form a set of symmetric hyperbolic partial differential equations:

$$\mathsf{D}\boldsymbol{v}^1 = \boldsymbol{J}^1_{\rm GW} , \tag{4.28}$$

where

$$\mathsf{D} = \begin{pmatrix} \omega^2(1-u_{\rm A\perp}^2)-k^2u_{\rm A\parallel}^2 & 0 & -(\omega^2-k^2)u_{\rm A\parallel}u_{\rm A\perp} \\ 0 & \omega^2-k^2u_{\rm A\parallel}^2 & 0 \\ -(\omega^2-k^2)u_{\rm A\parallel}u_{\rm A\perp} & 0 & \omega^2(1-u_{\rm A\parallel}^2)-k^2(u_{\rm m}^2-u_{\rm A\parallel}^2) \end{pmatrix} ,$$

and, for $h_{+,\times} \propto \mathrm{e}^{i\omega(z-t)}$ as discussed in Section 4.2 (but see Section 4.7), the GW source terms $\boldsymbol{J}^1_{\rm GW}$ are:

$$\boldsymbol{J}^1_{\rm GW} = -\frac{i\omega^2 u_{\rm A\perp}}{\omega - k} \begin{pmatrix} u_{\rm A\parallel} h_+ \\ u_{\rm A\parallel} h_\times \\ -u_{\rm A\perp} h_+ \end{pmatrix} . \tag{4.29}$$

Dispersion relation

A non-trivial solution for the plasma waves in (4.28) requires the determinant of D to vanish. Solving for $k = k_z(\omega)$, since ω is fixed by the driving GW, we find six solutions:

$$\omega = \pm k_{\rm A} u_{\rm A} \cos\theta = \pm k_{\rm A} u_{\rm A\parallel} , \tag{4.30a}$$

$$\omega = \pm \frac{k_{\rm s,f}}{\sqrt{2}} \sqrt{(u_{\rm m}^2 + c_{\rm s}^2 u_{\rm A\parallel}^2)} \sqrt{1 \pm \sqrt{(1-\sigma)}} , \tag{4.30b}$$

where we have defined the auxiliary parameter:

$$\sigma(\theta) \equiv \frac{4 c_{\rm s}^2 u_{\rm A\parallel}^2}{(u_{\rm m}^2 + c_{\rm s}^2 u_{\rm A\parallel}^2)^2} . \tag{4.31}$$

The negative sign in (4.30b) refers to the the relativistic proper *slow magnetosonic waves* with phase velocity $u_{\rm s} = \omega/k_{\rm s}$, and the positive sign to the *fast magnetosonic waves* with $u_{\rm f} = \omega/k_{\rm f}$. Together with the *Alfvén waves*, we have obtained a 6×6 MHD representation that in the special-relativistic limit reduces to the equations in Achterberg (1983).

In a low plasma-beta ($\beta_{\rm pl} = 4\pi p/B_0^2$), e.g. strongly magnetized, plasma where $u_{\rm A} \gg c_{\rm s}$, the fast mode reduces to the magneto-acoustic mode ((4.26b)) slightly altered by the presence of the gas, whereas for a high plasma-beta ($c_{\rm s} \gg u_{\rm A}$) it reduces to a sound wave with velocity (4.18). For the slow mode, the behavior is essentially the other way around.

The angular dependence is similar: for parallel propagation ($\theta = 0$), $u_{\rm f} \to u_{\rm A}$ and $u_{\rm s} \to c_{\rm s}$, whereas for perpendicular propagation ($\theta = \pi/2$) which we studied in Chapter 3, $u_{\rm f} \to u_{\rm m}$ and $u_{\rm s} \to 0$.

Coupling

In this section we present a formal derivation of the solutions to the inhomogeneous wave equation (4.28) following Melrose (1986). From (4.28) we have:

$$v_i^1 = (\mathsf{D}^{-1} \boldsymbol{J}^1_{\rm GW})_i = \frac{\lambda_{ij} (J^1_{\rm GW})_j}{\Lambda} , \tag{4.32}$$

where $\lambda_{ij}(\omega, k)$ and $\Lambda(\omega, k)$ are the matrix of cofactors of D and its determinant, respectively. These are related by: $D_{ki}\lambda_{kj} = \delta_{ij}\Lambda$.

Each solution of $\Lambda(\omega, k) = 0$ can be identified with a *wave mode* M with $\omega = \omega(k_M)$ and $\omega(-k_M) = -\omega(k_M)$. The determinant can be factored into these wave modes:

$$\begin{aligned} \Lambda(\omega, k) &= (\omega^2 - k^2 u_{\mathrm{A}\parallel}^2)(\omega^2 - k^2 u_{\mathrm{f}}^2)(\omega^2 - k^2 u_{\mathrm{s}}^2) = 0 \ , \\ u_{\mathrm{f,s}}^2 &= c_{\mathrm{s}} u_{\mathrm{A}\parallel} \left(\frac{1 \pm \sqrt{1-\sigma}}{\sqrt{\sigma}} \right) \ . \end{aligned} \tag{4.33}$$

The unit *polarization vector* for a wave in mode M, $\boldsymbol{n}_M(k)$ with $\boldsymbol{n}_M \cdot \boldsymbol{n}_M^* = 1$, can be constructed from λ_{ij}:

$$n_{Mi}(k) n_{Mj}^*(k) = \frac{\lambda_{ij}(\omega, k_M)}{\lambda_{ii}(\omega, k_M)} \ . \tag{4.34}$$

Alfvén waves driven by × polarized GW

The wave solutions can now be evaluated in Laplace space. The λ_{yy} component couples to the ×-polarized source term and excites Alfvén waves, viz perturbations of the magnetic field perpendicular to the background:

$$v_y^1(k, \omega) = -\frac{i}{2} \frac{h_\times \omega u_{\mathrm{A}\parallel} u_{\mathrm{A}\perp}}{\omega^2 - k^2 u_{\mathrm{A}}^2} \frac{\omega + k}{\omega - k} \ , \tag{4.35a}$$

$$B_y^1(k, \omega) = -v_y^1(k, \omega) \frac{B_x^0}{u_{\mathrm{A}\parallel} u_{\mathrm{A}\perp}} \frac{\omega + k u_{\mathrm{A}\parallel}^2}{\omega + k} \ , \tag{4.35b}$$

and similarly for $E_{x,z}^1$ and $j_{x,z}^1$. Note that because the Alfvén wave propagates obliquely with respect to the background magnetic field, the electric field is no longer divergence free and consequently the Alfvén wave is accompanied by perturbations in the charge density: $\nabla \cdot \boldsymbol{E}^1 = ikE_z^1 = 4\pi\tau^1$.

The polarization of the Alfvén wave components is summarized in Fig. 4.1.

Slow and fast MSW driven by + polarized GW

As we expect from our considerations in Chapter 3, a + polarized GW excites slow and fast magneto-acoustic waves in the plasma. The velocity components are:

$$v_z^1(k, \omega) = \frac{i}{2} \frac{h_+ \omega^3 u_{\mathrm{A}\perp}^2}{(\omega^2 - k^2 u_{\mathrm{f}}^2)(\omega^2 - k^2 u_{\mathrm{s}}^2)} \frac{\omega + k}{\omega - k} \ , \tag{4.36a}$$

$$v_x^1(k, \omega) = -\frac{v_z(k, \omega)}{\tan\theta} \left(1 - \frac{k^2 c_{\mathrm{s}}^2}{\omega^2} \right) \ , \tag{4.36b}$$

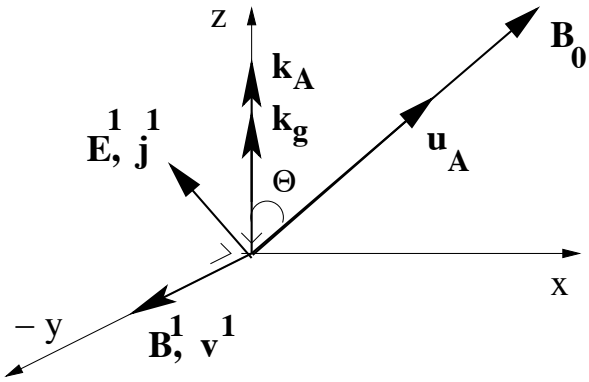

Figure 4.1: Orientation of the perturbations in the Alfvén mode

and from (4.22) one can easily find the pressure: $p^1(k,\omega) = \frac{k}{\omega}\gamma p^0 v_z(k,\omega)$. The magnetic component can be derived from (4.36) as:

$$\frac{B_x^1}{B^0} = v_z^1 \sin\theta - v_x^1 \cos\theta - \frac{\omega}{\omega + k}\frac{1-u_{\rm A}^2}{u_{\rm A}^2}\frac{v_x^1}{\cos\theta} \ . \tag{4.37}$$

The fact that the magnetic field perturbation is orthogonal to the direction of propagation of the GW is dictated by $\nabla \cdot \boldsymbol{B} = 0$.

The polarizations in the magneto-acoustic modes are illustrated in Fig. 4.2.

4.5 Space-time solutions

To find the solutions in space-time we apply the inverse Fourier and Laplace transformations to the results of the previous section. We define the phases of the wave modes as $\phi_{\rm A}^{\pm} = \pm k_{\rm A} z - \omega t$ and similarly for $\phi_{\rm s}^{\pm}$, $\phi_{\rm f}^{\pm}$, and $\phi_{\rm g} = \omega(z-t)$.

Alfvén waves

The most straightforward are the Alfvén waves (4.35) with wavenumber $k_{\rm A} = \omega/u_{\rm A\|}$:

$$\frac{B_y^1}{B_x^0} = \frac{h_\times}{4}\left[\frac{1-u_{\rm A\|}}{1+u_{\rm A\|}}{\rm e}^{i\phi_{\rm A}^-} + \frac{1+u_{\rm A\|}}{1-u_{\rm A\|}}{\rm e}^{i\phi_{\rm A}^+} - \frac{1+u_{\rm A\|}^2}{1-u_{\rm A\|}^2}2{\rm e}^{i\phi_{\rm g}}\right] \ , \tag{4.38}$$

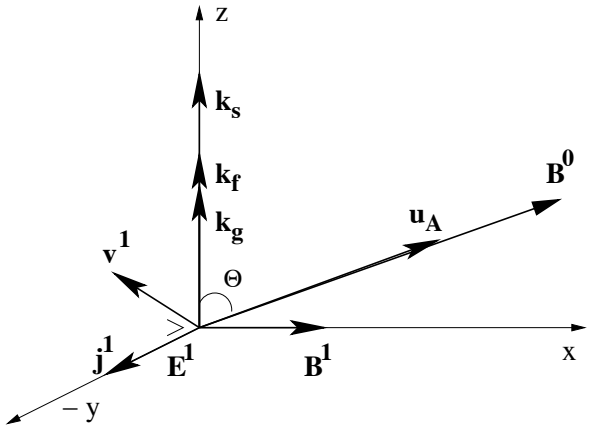

Figure 4.2: Orientation of the perturbations in the MSW modes

and similarly for $v_y^1(z,t)$, $E_{x,z}^1(z,t)$, $j_{x,z}^1(z,t)$, and $\tau^1(z,t)$ (see Appendix A.2). Since the Alfvén waves are non-compressional, we do not find a p^1 or μ^1 contribution.

Magneto-acoustic waves

Slightly more complicated is the coupled superposition of slow and fast wave modes, polarized in the $x-z$ plane:

$$v_z^1 = \frac{h_+}{4}\frac{u_{\mathrm{A}\perp}^2 u_{\mathrm{s}}^2}{u_{\mathrm{f}}^2-u_{\mathrm{s}}^2}\left[\frac{1+u_{\mathrm{s}}}{1-u_{\mathrm{s}}}\frac{\mathrm{e}^{i\phi_{\mathrm{s}}^+}}{u_{\mathrm{s}}}-\frac{1-u_{\mathrm{s}}}{1+u_{\mathrm{s}}}\frac{\mathrm{e}^{i\phi_{\mathrm{s}}^-}}{u_{\mathrm{s}}}-\frac{4\mathrm{e}^{i\phi_{\mathrm{g}}}}{1-u_{\mathrm{s}}^2}\right]$$
$$-\frac{h_+}{4}\frac{u_{\mathrm{A}\perp}^2 u_{\mathrm{f}}^2}{u_{\mathrm{f}}^2-u_{\mathrm{s}}^2}\left[\frac{1+u_{\mathrm{f}}}{1-u_{\mathrm{f}}}\frac{\mathrm{e}^{i\phi_{\mathrm{f}}^+}}{u_{\mathrm{f}}}-\frac{1-u_{\mathrm{f}}}{1+u_{\mathrm{f}}}\frac{\mathrm{e}^{i\phi_{\mathrm{f}}^-}}{u_{\mathrm{f}}}-\frac{4\mathrm{e}^{i\phi_{\mathrm{g}}}}{1-u_{\mathrm{f}}^2}\right], \tag{4.39}$$

and:

$$v_x^1\tan\theta = \frac{h_+}{4}\frac{c_{\mathrm{s}}^2 u_{\mathrm{A}\perp}^2}{u_{\mathrm{f}}^2-u_{\mathrm{s}}^2}\left[\frac{1+u_{\mathrm{f}}}{1-u_{\mathrm{f}}}\frac{\mathrm{e}^{i\phi_{\mathrm{f}}^+}}{u_{\mathrm{f}}}-\frac{1-u_{\mathrm{f}}}{1+u_{\mathrm{f}}}\frac{\mathrm{e}^{i\phi_{\mathrm{f}}^-}}{u_{\mathrm{f}}}\right. \tag{4.40}$$
$$\left.-\frac{4u_{\mathrm{f}}^2\mathrm{e}^{i\phi_{\mathrm{g}}}}{1-u_{\mathrm{f}}^2}-\frac{1+u_{\mathrm{s}}}{1-u_{\mathrm{s}}}\frac{\mathrm{e}^{i\phi_{\mathrm{s}}^+}}{u_{\mathrm{s}}}+\frac{1-u_{\mathrm{s}}}{1+u_{\mathrm{s}}}\frac{\mathrm{e}^{i\phi_{\mathrm{s}}^-}}{u_{\mathrm{s}}}+\frac{4u_{\mathrm{s}}^2\mathrm{e}^{i\phi_{\mathrm{g}}}}{1-u_{\mathrm{s}}^2}\right]-v_z^1\,.$$

Note that for $c_{\mathrm{s}}\downarrow 0$, $\boldsymbol{v}^1\perp\boldsymbol{B}^0$. If also $\theta=\pi/2$ the limiting behavior is: $u_{\mathrm{f}}\to u_{\mathrm{A}}$, $u_{\mathrm{s}}\to 0$ and we retrieve our original idealized solution.

The remaining magneto-acoustic wave components, $B_x^1(z,t)$, $E_y^1(z,t)$, $j_y^1(z,t)$, $p^1(z,t)$, and $\mu^1(z,t)$, are equivalent superpositions of slow and fast waves but with different relative amplitudes, summarized in Appendix A.2.

Growth

In general, for arbitrary $u_\mathrm{A}, c_\mathrm{s}$, and θ, we always find $u_\mathrm{f} > u_\mathrm{s}$. In the limit where the phase velocity of the fast mode approaches the speed of light, $u_\mathrm{f} \uparrow 1$, coherent interaction with the GW is possible. The amplitude of the retreating fast wave $\propto (1+u_\mathrm{f})^{-1}$ is negligible with respect to the forward wave $\propto (1-u_\mathrm{f})^{-1}$. The forward wave grows linearly with distance because with $k_\mathrm{f} = \omega/u_\mathrm{f} = \omega + \Delta k$ to first order in Δk we have:

$$\frac{\mathrm{e}^{ik_\mathrm{f} z} - \mathrm{e}^{i\omega z}}{1-u_\mathrm{f}} = \frac{\omega}{u_\mathrm{f}\Delta k}\mathrm{e}^{i\omega z} i\Delta k\ z\ . \tag{4.41}$$

This limiting behavior is the same for all magneto-acoustic components (see (A.10)).

For the Alfvén waves, the conditions for growing solutions are less favorable because of the angular dependence of the resonance condition. To interact coherently with the GW, the phase speed of the Alfvén wave ($v_\mathrm{ph} = u_\mathrm{A}\cos\theta$) has to approach the speed of light. On the one hand this means that the wave vector of the Alfvén wave should be almost parallel to the background magnetic field, but on the other hand, the magnetic field should also have a transverse component, since the amplitudes are proportional to $B^0\sin\theta \approx B^0\theta$ for small angles. Explicitly:

$$\frac{B_y^1(z,t)}{B^0} = -v_y^1(z,t) \sim \frac{\theta h_\times}{2}\omega z \Im[\mathrm{e}^{i\phi_\mathrm{g}}] + \mathcal{O}[\theta^2]\ . \tag{4.42}$$

The excited slow magnetosonic wave is a purely oscillatory wave propagating both in the forward and the backward directions.

4.6 A warm relativistic plasma wind

We now want to consider a warm relativistic plasma wind flowing out in the z direction with constant (background) velocity β and corresponding Lorentz factor $\gamma_\mathrm{tot} = 1/\sqrt{1-\beta^2}$. We are allowed to use simple Lorentz transformations in this general relativistic treatment, because the whole concept of gravitational waves as small perturbations of the background space-time (linearized theory), relies on the fact that we can treat the GW as a field living in flat space-time as long as the scale of curvature is much larger than the wavelength of the GW: $\mathcal{R} \gg \lambda_\mathrm{GW}$, which was verified in Section 4.2.

From now on, all quantities derived in the previous sections for the comoving frame will be denoted by primes. Since the phase of plane waves, $\phi = k_a x^a$,

is invariant under Lorentz transformations, a boost mostly implies addition of velocities. We then have $u'_f = \frac{u_f - \beta}{1-\beta u_f}$, $u'_s = \frac{u_s - \beta}{1-\beta u_s}$, and $u'_{A\parallel} = \frac{u_{A\parallel} - \beta}{1-\beta u_{A\parallel}}$ for the phase velocities and:

$$v^1_z \approx \frac{(v^1_z)'}{\gamma^2} \quad , \quad v^1_{x,y} \approx \frac{(v^1_{x,y})'}{\gamma} \ . \tag{4.43}$$

The boosted background magnetic field is $\boldsymbol{B}^0 = (\gamma B^{0\prime}_x, 0, B^{0\prime}_z)$ and in the laboratory frame one finds a zeroth order electric field $\boldsymbol{E}^0 = -\beta \times \boldsymbol{B}^0 = (0, -\beta\gamma B^{0\prime}_x, 0)$.

Relativistic Alfvén waves

We define $\gamma^2_{u_A} = 1/(1-u^2_{A\parallel}) + \mathcal{O}[\theta^2]$ as the Lorentz factor associated with the Alfvén speed for small θ and boost (A.1) to the laboratory frame as an example:

$$v^1_y = \frac{h_\times}{4}\frac{u_{A\perp}\gamma^2_{u_A}}{1-u_{A\parallel}\beta}\left\{4\left[u_{A\parallel}(1+\beta^2) - \beta(1+u^2_{A\parallel})\right]\mathrm{e}^{i\phi_g}\right.$$
$$\left.\left[\frac{1+u_{A\parallel}}{1+\beta}\right]^2\frac{\mathrm{e}^{i\phi^+_A}}{\gamma^4} - \left[\frac{1+\beta}{1+u_{A\parallel}}\right]^2\frac{\mathrm{e}^{i\phi^-_A}}{\gamma^4_{u_A}}\right\} \ . \tag{4.44}$$

Or in the ultra-relativistic limit $u_A \uparrow 1$ (and $\beta \simeq 1$):

$$v^1_y(z,t) \approx -\frac{h_\times u_{A\perp}}{4\gamma^2}\ \omega z\ \Im[\mathrm{e}^{i\phi_g}] \ . \tag{4.45}$$

Relativistic MSW

In a Poynting flux dominated force-free plasma wind, where the magnetic energy density strongly dominates the matter density, the plasma flows out at ultra-relativistic velocities. In this regime the phase velocity of the fast mode approaches the Alfvén velocity, $u_f \simeq u_A \uparrow 1$ and the phase velocity of the slow mode becomes negligible, $u_s \downarrow 0$. The solutions are therefore quite similar to those found in Chapter 3, the main difference being the angular dependence. For instance:

$$v_x = \frac{v'_x}{\gamma} \simeq \frac{h_+}{4\gamma^3}\frac{\sin^2\theta}{(1-\beta\cos\theta)^2}\ \omega z\ \Im\left[\mathrm{e}^{i\phi_g}\right] \ , \tag{4.46a}$$

$$v_z = \frac{v'_z}{\gamma^2} \simeq \frac{h_+}{4\gamma^4}\frac{\sin\theta(\cos\theta-\beta)}{(1-\beta\cos\theta)^2}\ \omega z\ \Im\left[\mathrm{e}^{i\phi_g}\right] \ . \tag{4.46b}$$

Appendix A.2 lists the limiting behavior of all the remaining magneto-acoustic wave components in a relativistic wind.

4.7 Damping of the GW

To find an evolution equation for the gravitational waves, we project the transverse traceless part of the stress-energy perturbation as in (4.2) (as we discussed at the end of Section 4.2, (4.1) and (4.2) also hold in the ONF).

The perturbation of the matter part only has $\delta T^{xx}_{\rm TT} = \delta T^{yy}_{\rm TT} = p^1(z,t)$ which is purely gauge (the trace can be removed by a gauge transformation). Only the magnetic field interacts directly with the gravitational waves. All the other perturbations are excited through the MHD processes in the plasma. In the general case where oblique h_+ GW excite slow and fast magneto-acoustic waves and $h_\times$ GW excite Alfvén waves, (4.3) is replaced with:

$$\Box h_+ = 4B^0_x B^1_x \ , \qquad \Box h_\times = 4B^0_x B^1_y \ . \tag{4.47}$$

As we discussed in Section 4.2 we have assumed that the GW have a slowly varying amplitude $\mathcal{H}(z)$. We have neglected this variation in studying the interaction with the plasma since in the short-wavelength approximation all the derivatives have $\frac{\partial}{\partial z}\mathcal{H}(z) \ll \omega\mathcal{H}(z)$. It is however this slowly varying amplitude that describes the damping of the GW. We could find an order of magnitude expression for $\mathcal{H}(z)$ by integrating (4.47) using (A.5) and (4.38), but this wouldn't be entirely self-consistent since in deriving (A.5) and (4.38) we already assumed that $\omega = k$ for the GW.

It is, however, possible to derive a dispersion relation for the damped GW and the excited MHD waves simultaneously in a self-consistent way. If we assume that the GW oscillates at a fixed frequency but leaves the spatial dependence unspecified (e.g. a boundary value problem with $h(z,t) \propto h(z)\mathrm{e}^{-i\omega t}$) we can still solve the full set of MHD equations in Laplace space. For the magnetic field we find:

$$B^1_y(k,\omega) = \frac{B^0_x h_\times(k,\omega)}{2}\frac{\omega^2 + k^2 u^2_{\rm A\parallel}}{\omega^2 - k^2 u^2_{\rm A\parallel}} \ , \tag{4.48a}$$

$$B^1_x(k,\omega) = \frac{B^0_x h_+(k,\omega)}{2}\frac{\omega^2 + k^2 u^2_{\rm A}}{\omega^2 - k^2 u^2_{\rm A}} \ , \tag{4.48b}$$

where the second expression is in the limit of a Poynting flux dominated wind with $u_{\rm A} \gg c_{\rm s} \downarrow 0$ and $h_{+,\times}(k,\omega)$ are the Laplace transforms of $h_{+,\times}(z,t)$ (the reason that (4.48) look different from (4.35b) and (4.37) is that derivatives of $h_{+,\times}$ depend on both ω and k in this more general case).

If we insert (4.48) in the Laplace transform of (4.47), $h_{+,\times}(k,\omega)$ drop out and we find the self-consistent dispersion relation for the coupled fast magnetosonic – gravitational (h_+) mode:

$$\omega^2 - k^2 = 2(B^0_x)^2\frac{\omega^2 + k^2 u^2_{\rm A}}{\omega^2 - k^2 u^2_{\rm A}} \ , \tag{4.49}$$

and the coupled Alfvén - gravitational ($h_\times$) mode which looks the same but with $u_{\rm A}$ replaced with $u_{\rm A\parallel}$.

The two modes allowed by (4.49) are given by:

$$\frac{k_{1,2}^2 u_{\rm A}^2}{1-u_{\rm A}^2} = \frac{\omega^2}{2}\left[\epsilon + \frac{1+u_{\rm A}^2}{1-u_{\rm A}^2} \pm \sqrt{1+2\epsilon\frac{3+u_{\rm A}^2}{1-u_{\rm A}^2}+\epsilon^2}\right] , \tag{4.50}$$

in terms of $\epsilon = \left(\frac{B_x^0}{\omega}\right)^2 \frac{2u_{\rm A}^2}{1-u_{\rm A}^2} = \frac{(B_x^0)^2}{\omega\Delta k}\frac{2u_{\rm A}}{1+u_{\rm A}}$. For small ϵ, (4.50) reduces to:

$$k_1^2 = \omega^2\left(1-\epsilon\frac{1+u_{\rm A}^2}{u_{\rm A}^2}\right)+\mathcal{O}[\epsilon^2] , \tag{4.51a}$$

$$k_2^2 u_{\rm A}^2 = \omega^2(1+2\epsilon)+\mathcal{O}[\epsilon^2] . \tag{4.51b}$$

Mode 1 corresponds to a superluminal mode with phase velocity $\omega/k_1 > 1$:

$$v_{\rm ph,1}^2 = 1+\frac{2(B_x^0)^2}{\omega^2}\frac{1+u_{\rm A}^2}{1-u_{\rm A}^2} , \tag{4.52a}$$

$$v_{\rm gr,1}^2 = 1-\frac{2(B_x^0)^2}{\omega^2}\frac{1+u_{\rm A}^2}{1-u_{\rm A}^2} , \tag{4.52b}$$

whereas mode 2 is subluminal:

$$\frac{v_{\rm ph,2}^2}{u_{\rm A}^2} = 1-\frac{(2B_x^0)^2}{\omega^2}\frac{u_{\rm A}^2}{1-u_{\rm A}^2} , \tag{4.53a}$$

$$\frac{v_{\rm gr,2}^2}{u_{\rm A}^2} = 1+\frac{(2B_x^0)^2}{\omega^2}\frac{u_{\rm A}^2}{1-u_{\rm A}^2} , \tag{4.53b}$$

with $v_{\rm ph,1}\times v_{\rm gr,1}=1$ and $v_{\rm ph,2}\times v_{\rm gr,2}=u_{\rm A}^2$. Both modes have group velocity $\partial\omega/\partial k_{1,2} < 1$ as long as (consistent with Brodin et al. (2001)):

$$\frac{8\pi G}{c^2}\frac{(B_x^0)^2}{\mu_0} < \omega(\Delta k)c . \tag{4.54}$$

In the limit $\epsilon \ll 1$, (4.51b) reduces to a fast magnetosonic wave in flat spacetime (or, equivalently, to the Alfvén mode for $h_\times$). Mode (4.51a) reduces to a vacuum GW, justifying our approximation $h_{+,\times} \propto \exp[i\omega(z-t)]$ in deriving the plasma perturbations in Section 4.4.

4.8 Interpretation

In this section we present an intuitive interpretation of our main results: that a + polarized GW excites magneto-acoustic waves and a × polarized GW excites Alfvén waves in a uniform magnetic field.

The driving force exerted by a GW on test particles is described by (4.12). These equations can be illustrated by force lines in the plane orthogonal to

the propagation of the GW (Misner et al. 1973). Integrating (4.12) twice with respect to time results in the well known equations of spatial deviations of test masses in an interferometer detector such as LIGO:

$$\delta x = \frac{1}{2}(h_+ x_0 + h_\times y_0) \ , \qquad \delta y = \frac{1}{2}(h_\times x_0 - h_+ y_0) \ . \tag{4.55}$$

In the MHD limit these test particles are 'glued' to the magnetic field lines, so the magnetic field will exhibit the same behavior (in fact the presence of the plasma is not required, the magnetic field lines can just be viewed as parametrized by (4.55)). Since the action of the GW is only in the $x-y$ plane, and the magnetic field lies in the $x-z$ plane we expect that a + polarized GW results in:

$$\delta B_x \propto \frac{1}{2} h_+ B_x^0 \ , \qquad \delta B_y \propto \frac{1}{2} h_+ B_y^0 = 0 \ , \tag{4.56a}$$

and a $\times$ polarized GW excites:

$$\delta B_x \propto \frac{1}{2} h_\times B_y^0 = 0 \ , \qquad \delta B_y \propto \frac{1}{2} h_\times B_x^0 \ . \tag{4.56b}$$

This is exactly what we found in the mathematical treatment of the previous section. Perturbations in the other directions are higher order effects.

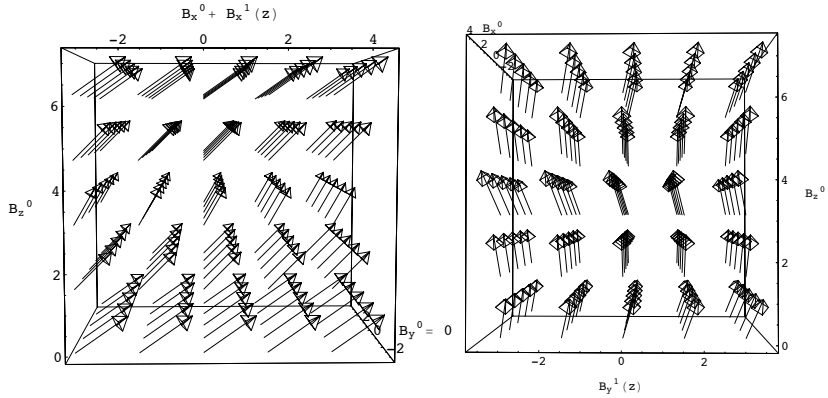

Figure 4.3: The magneto-acoustic (left) and Alfvén mode (right) illustrated as an oscillating vector field. The $x-y$ axes in the right figure are rotated by $\pi/2$ with respect to those in the left figure.

Figure 4.3 gives a schematic illustration of the perturbed magnetic field in the two wave modes. The left figure shows the vector field (in arbitrary units)

for the oblique magneto-acoustic wave propagating in the z-direction. The perturbations are highly exaggerated to emphasize the effect. Amplification of the magnetic field occurs when B_x^0 is amplified and dilution when B_x^0 is suppressed. Since B_z^0 is constant the total magnetic field has an overallwavy pattern.

Alfvén waves are non-compressional and only set up a vibration in the field lines perpendicular to the background field (B_y^1). This is illustrated in the right figure, where the axes are rotated to emphasize the $y-z$ plane.

In a pulsar environment the plasma initially flows out *along* the open field lines but develops into a force-free wind outside the light-cylinder in which the toroidal component of the magnetic field dominates the poloidal one. Here the magnetic field is predominantly perpendicular to the radial propagation of the wind as illustrated in Figure 4.4. Gravitational waves would mainly excite Alfvén waves in the former region, whereas in the latter case the magneto-acoustic waves are favored. In the relativistic wind the GW frequency is red-shifted and the interaction is suppressed by γ^{-2}, but the interaction length scale becomes very large.

4.9 Conclusions

We have studied the propagation properties of a plane polarized gravitational wave in a magnetized astrophysical plasma in the most general case. Both polarizations of the GW have been taken into account. Oblique propagation with respect to the background magnetic field was studied including pressure terms, and relativistic velocities. The only approximations in this treatment are the MHD conditions for the plasma, the linear perturbative approach, the geometric optics or small wavelength limit for the gravitational waves, and our assumed geometry of the interaction region.

The result is a very rich astrophysical problem, where all three fundamental plasma wave modes are excited, two of which can interact coherently with the driving gravitational waves, and as a result grow linearly with distance, dissipating GW energy into the plasma.

Alfvén waves are excited already in linearized theory by $\times$ polarized gravitation waves propagating at an angle with respect to an ambient magnetic field, a result that as far as we know has not been found before (note that both conditions, oblique GW propagation and $\times$ polarization, are required). The Alfvén waves are non-compressional shear waves that have orthogonal electromagnetic components with a corresponding drift velocity in the plasma, a current flowing along the electric field and a deviation from charge neutrality caused by the divergence of the electric field, but no pressure or density components. To interact coherently with a GW one has to find the optimum of longest interaction length scale and significant amplitude as a function of the angle between the Alfvén wave vector and background magnetic field as was discussed in Section 4.5.

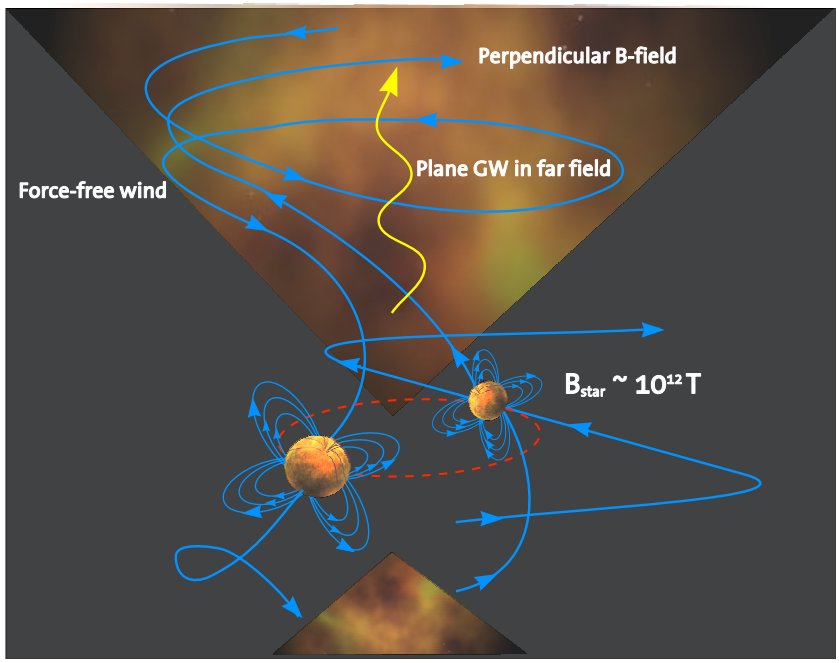

Figure 4.4: Merging neutron star binary

As we already derived in a Chapter 3, + polarized gravitational waves excite magneto-acoustic waves propagating parallel to the gravitational waves. In this Chapter we have generalized our previous treatment to include the oblique magnetic field and a relativistic equation of state with non-vanishing pressure. As a result we find both the slow and the fast magneto-acoustic waves with phase velocities that depend on both the electromagnetic and the matter properties of the plasma.

The magneto-acoustic wave modes are compressional waves, that excite pressure, density, and magnetic field gradients along their wave vector direction, but no perturbation of charge neutrality. The electric and the magnetic field perturbations and the wave vector are mutually orthogonal ($\boldsymbol{E}^1 \perp \boldsymbol{B}^1 \perp \boldsymbol{k}_{\mathrm{s,f}}$), but the drift velocity is no longer exactly perpendicular to the magnetic field due to the pressure. Of course, the plasma motion in a GW is non-compressional but it generates magnetic field compression if it propagates across a magnetic field either in a vacuum or in an ideal frozen-in plasma, and hence couples to the magneto-acoustic wave.

As to the slow magneto-acoustic wave, no coherent interaction can occur

with the GW since the phase velocity of the slow mode is always much smaller than that of the gravitational waves. Therefore the amplitude does not grow in time or with distance and cannot become significant.

The most effective interaction occurs between the GW and the fast magneto-acoustic wave. The phase velocity of those waves can easily approach the speed of light in a strongly magnetized plasma (in the limit $u_\mathrm{A} \gg c_\mathrm{s}$) as we derived in Chapter 3 and therefore the waves will grow linearly with distance. As the plasma waves grow, the amplitude of the gravitational waves decays correspondingly but as long as the total length of the interaction region is smaller than the background curvature produced by the plasma itself, this will only be a small fraction of the total gravitational wave energy.

Astrophysical applications of the above interactions lie in sources of strong gravitational waves embedded in strongly magnetized plasmas. Examples are non-spherical rotating neutron stars, fast rotating neutron stars that are unstable to torsional oscillations, non-spherical supernovae collapses, magnetars, and the progenitors of gamma-ray bursts (non-spherical collapse of a massive star or a merging neutron star binary). Most of these sources are probably accompanied by an extended strongly magnetized and force-free plasma wind, flowing out at ultra-relativistic velocities. Since the coupling constant of gravitational waves is exceedingly small, only in the most extreme sources will the interaction with the plasma be significant.

Figure 4.4 shows as an example a binary neutron star as a gamma-ray burst progenitor. For such a merging binary with a magnetar class surface magnetic field of 10^{12} T (Ibrahim et al. 2003), an angular frequency at the end of the spiral-in phase of the order of 1 kHz and a force-free wind flowing out with a Lorentz factor of $\Gamma \sim 100$ up to a fraction of a light year, a total energy of 10^{35} J can be transferred from the gravitational waves to the wind.

CHAPTER 5

Inverse Compton scattering in anisotropic relativistic plasmas

J. Moortgat & J. Kuijpers

accepted for publication in MNRAS

GRAVITATIONAL WAVES propagating through a magnetized plasma excite low-frequency magnetohydrodynamic (MHD) waves. In this Chapter[1] we investigate whether these waves can produce observable radio emission at higher frequencies by scattering on an an-istropic intrinsically relativistic distribution of electrons and positrons in the force-free wind surrounding a double neutron star binary merger. The relativistic particle distribution is assumed to be strictly along the magnetic field lines, while the magneto-plasma streams out at a relativistic speed from the neutron stars. In the case of Compton scattering of an incident MHD wave transverse to the magnetic field, we find that the probability of scattering to both a transverse x-mode and a quasi-longitudinal Langmuir-o mode is suppressed when the frequency of the incident wave is below the local relativistic gyro-frequency, i.e. when the magnetic field is very strong.

[1]The electronic MNRAS version of this paper should appear in March 2006 and is also available on the pre-print archive: `astro-ph/0602314`.

5.1 Introduction

This decade is expected to witness the historical first direct detection of gravitational waves (GW) with detectors such as the Advanced Laser Interferometer Gravitational Wave Observatory (LIGO[2]) and the Laser Interferometer Space Antenna (LISA[3]). The former is designed to detect gravitational waves from compact sources such as merging neutron star binaries in the kHz regime, whereas the latter will detect the lower frequency (< 1 Hz) gravitational waves from thousands of compact white dwarf binaries (Nelemans et al. 2001) as well as the spiral-in signal of super-massive black holes, throughout the visible universe (see Schutz (1999) or Kokkotas (2004) for a review of likely sources for LIGO and LISA).

Gravitational waves are emitted by highly energetic events but occur at relatively large distances and the signal that reaches Earth is exceedingly weak. To extract the GW from the noisy signal, some theoretical knowledge of the expected waveforms is essential. To confirm the detection of a GW burst, any additional electromagnetic signature of the event would be extremely useful.

It so happens that many of the possible GW sources are embedded in a strong magnetic field. Examples are rapidly spinning neutron stars which have a small oblateness and precess, accrete, or are unstable to the excitation of the r-mode, supernova core collapses and bounces, newly born 'boiling' and oscillating neutron stars, magnetars with crust fracturing (~ 20 Hz), and coalescing compact binaries in which at least one component is a magnetic neutron star.

In the last case, numerical models by Ibrahim et al. (2003) predict that maximum GW luminosities of the order of 10^{48} W are released into a wound-up magnetic field of up to $10^{8} - 10^{12}$ T. We have investigated in Chapters 3–4 and Moortgat and Kuijpers (2005) whether these extreme space-time distortions perturb the ambient magnetic field sufficiently to produce an observable electromagnetic counterpart of the GW burst. We have found that a GW can couple linearly at the same frequency to all three low-frequency plasma eigenmodes. The shear Alfvén mode and the transverse slow and fast magnetosonic waves (MSW) are excited depending on the polarization of the gravitational waves with respect to the ambient magnetic field orientation, but only the fast magneto-acoustic mode can interact coherently with the GW a over longer time (distance) and is therefore the most interesting.

The MSW can not escape directly as observable radiation. In Moortgat and Kuijpers (2005) we pointed out that the MSW encounters relativistic electrons and positrons with Lorentz factors different from the bulk Lorentz factor of the particles carrying the MSW, for instance due to a tail in the distribution function or simply due to inhomogeneities in the plasma such as beams. For typical Lorentz factors of a few hundreds, the MSW would then be inverse Compton scattered to low-frequency radio emission in the LOFAR (the LOw

[2] LIGO website: `http://www.ligo.caltech.edu/`
[3] LISA website: `http://lisa.jpl.nasa.gov/`

Frequency Array [4]) band. In a first estimate, we approximated the scattering cross-section with the Thomson cross-section and predicted a flux that would be easily detectable by LOFAR for a double neutron star merger at a distance of ≤ 1 Gpc. Clearly, the indirect detection of gravitational waves with a radio array would be of extreme interest.

In the present Chapter we study in more detail the scattering process of a fast MSW into escaping electromagnetic waves in a strongly magnetized anisotropic relativistic plasma.

This Chapter is set up as follows. In Section 5.2 we recapitulate the intuitive picture presented in Section 4.8 which underlies the excitation of MHD waves by a gravitational wave propagating through a magnetized pla sma. To investigate the subsequent scattering of these MHD waves we need a covariant relativistic theory for plasma dynamics which was developed largely by Gedalin et al. (1998); Melrose et al. (1999); Melrose and Gedalin (1999); Gedalin et al. (2001); Luo and Melrose (2001); Gedalin et al. (2002) and unpublished work by Melrose (2001) to study emission processes in pulsar magnetospheres. We apply this theory to the force-free wind well outside the effective light cylinder of the merging binary. In particular, we consider a plasma which –in the frame comoving with the wind– has a momentum dispersion along the magnetic field only and construct the covariant equations for the GW excited current, the linear and non-linear response to that current and the scattering emission probability in Sections 5.3–5.5. In Section 5.6 we apply these general results to the geometry of an incident transverse magnetosonic wave that scatters on electrons and positrons with a 1-dimensional relativistic dispersion along the magnetic field and calculate the probability that either transverse or longitudinal waves are emitted in the direction of the observer. A numerical analysis is presented in Section 5.7, where we calculate the energy radiated into scattered radio waves. The conclusions follow in Section 5.9.

5.2 Gravitational wave – magneto-acoustic wave interaction

In a pulsar environment plasma flows out *along* the open field lines and develops into a force-free wind outside the light-cylinder in which the toroidal component of the magnetic field quickly dominates the poloidal one (see Section 5.7 and Fig. 4.4 in the previous chapter). The magnetic field is therefore essentially perpendicular to the radial propagation of the wind as in Fig. 5.1. In this section we discuss what happens when the two neutron stars at the origin of the system merge and release a large amount of GW into the wind.[5]

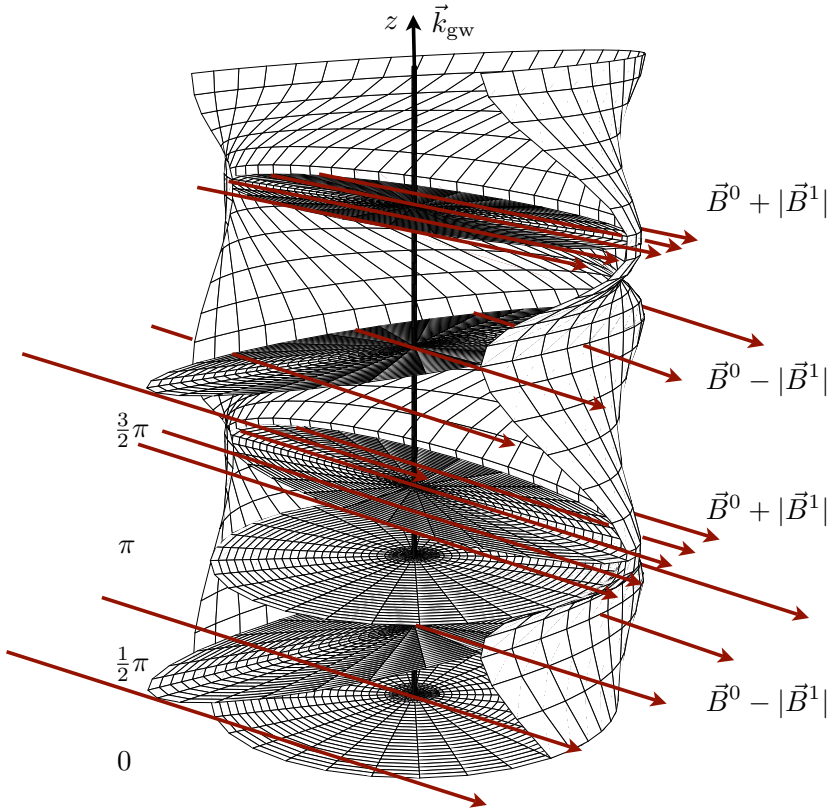

Figure 5.1: Deformation of the world-sheet of a ring of test particles by the tidal force of a passing + polarized GW (with $\boldsymbol{k}_{\rm gw} \perp \boldsymbol{B}^0$). The magnetic field is stretched and compressed and excites a magneto-compressional wave.

Gravitational wave tidal field

The driving force exerted by a GW on test particles is described by Einstein's field equations or alternatively the general relativistic equations for *geodesic deviations* describing tidal accelerations (see for instance Stewart (1990)). Integrating those differential equations twice results in the well-known spatial

[4] LOFAR website: `http://www.lofar.org/`
[5] This Section is basically a recap of Section 4.8.

deviations of test masses in an interferometer detector such as LIGO:

$$\delta x = \frac{1}{2}(h_+ x_0 + h_\times y_0) \ , \qquad \delta y = \frac{1}{2}(h_\times x_0 - h_+ y_0) \ , \tag{5.1}$$

where x_0 and y_0 are the initial separations of test-masses along the x- and y-axis in an L-shaped interferometer, δx and δy are the excursions causes by the passing GW and h_+ and $h_\times$ refer to the two possible polarizations of the GW.

Interaction with magnetic field

In the ideal MHD limit the magnetic field lines are frozen into the plasma, and the magnetic field will exhibit the same excursions as the test particles. The action of a GW propagating in the z direction is only in the $x-y$ plane, and when we choose the orientation of the ambient magnetic field in the $x-z$ plane, a GW which is + polarised with respect to these axes (so $h_\times = 0$) excites a growing magnetic field perturbation with:

$$\delta B_x \propto \frac{1}{2} h_+ B_x^0 \ , \qquad \delta B_y \propto \frac{1}{2} h_+ B_y^0 = 0 \ , \tag{5.2}$$

The resulting interaction is illustrated in Fig. 5.1 where we show the world-sheet of a ring of test particles in the tidal field of a passing GW, which we choose to propagate in the z-direction (and $\boldsymbol{k}_{\rm gw} \perp \boldsymbol{B}^0$). Since the GW amplitude depends only on $z-t$, we can interpret the vertical axis either as the propagation direction z at a certain time t_0 or as the temporal evolution for a ring of particles around the spatial origin $z = z_0$ as in a Minkowski diagram. In the absence of the GW the world-sheet would be a straight cylinder, but due to the GW the circular circumferences are periodically stretched and compressed into ellipses with axes along the x and y axis for this particular + GW polarization. The corresponding behavior of a magnetic field that was spatially uniform in the absence of the GW is a periodic amplification of the magnetic field when B_x^0 is amplified by the GW ($B_x^1 > 0$) and dilution when B_x^0 is suppressed ($B_x^1 < 0$). The result is a magneto-compressional MSW mode.

Magnetosonic wave in Poynting flux wind

When the plasma is tenuous and strongly magnetized such that the magnetic pressure greatly exceeds the gas pressure, the sound velocity is much smaller that the relativistic Alfvén velocity which approaches the speed of light $u_{\rm A} \simeq c$. In this *Poynting flux dominated* limit we can neglect the gas pressure and the MSW and the GW obey almost the same dispersion relation $\omega_{\rm gw} = \omega_{\rm msw} = k_{\rm gw} c = k_{\rm msw} u_{\rm A}$ and can interact coherently over the longest interaction scales.

The orientation of the different components of the fast MSW are shown in Fig. 5.2. The polarization is transverse, such that the electromagnetic field

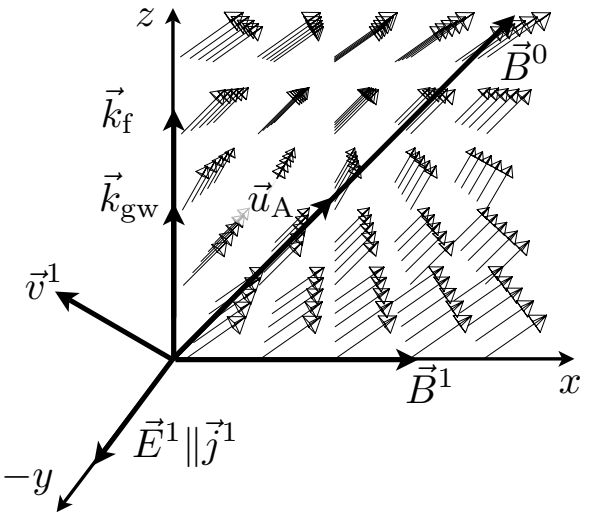

Figure 5.2: The orientation of the MSW components and the perturbed magnetic vector field (inset).

components and the wave vector form a mutually orthogonal triad: $\boldsymbol{E}^1 \perp \boldsymbol{B}^1 \perp \boldsymbol{k}$. Also shown is a schematic illustration of the perturbed magnetic field for an oblique magneto-acoustic wave propagating in the z-direction. The perturbations are exaggerated to emphasize the effect. Since B_z is constant while B_x oscillates, the total magnetic field has an overallwavy pattern.

As was mentioned in the Introduction, the magnetosonic waves excited by a GW have frequencies in the kHz regime and cannot escape the plasma directly. However, upon inverse Compton scattering of the MSW on relativistic particles with a typical Lorentz factor γ of a few hundreds, the photon frequency can be boosted by up to a factor $2\gamma^2$ larger than that of the incident MSW wave and into the LOFAR band (30–240 MHz). The region where scattering into escaping radiation is most likely to occur is far away from the pulsar where the plasma frequency has dropped sufficiently (see also Section 5.7).

In the following sections we will first summarize the covariant description of some fundamental ingredients of relativistic plasma dynamics and then derive the probabilities of scattering a MSW into the higher frequency normal modes of an intrinsically relativistic plasma. Note that while in the context of this section it was most illustrative to choose the GW wave vector along the z axis and the magnetic field at some angle to it, in the remainder of this Chapter it will be more convenient to do the opposite and choose $\boldsymbol{B}^0$ along the z axis and the wave vectors in arbitrary directions.

5.3 Emission

Wave equation and photon propagator

We will study the emission due to the external current generated by a passing MHD wave. The inhomogeneous wave equation for the scattered field of arbitrary wave mode P with vector potential $A^\mu_{\rm P}$ is given by:

$$\Lambda^{\mu\nu}(k)A_{{\rm P}\nu}(k) = -\mu_0 J^\mu_{\rm ext}(k) \ , \tag{5.3}$$

where $\Lambda^{\mu\nu}$ is the wave operator for the homogeneous equation which determines the polarization properties of wave mode P and includes the induced self-consistent field. In the *weak turbulence* regime one can expand the current excited by a field $A^\mu(k)$ in terms of a power series in this field. The first two terms in this expansion define the linear and quadratic non-linear response:

$$\begin{aligned} J^\mu_{\rm ind}(k) &= \alpha^\mu{}_\nu(k)A^\nu(k) + \int \frac{d^4k_1}{(2\pi)^4}\frac{d^4k_2}{(2\pi)^4}\delta^4(k-k_1-k_2) \\ &\times (2\pi)^4\alpha^\mu{}_{\nu\alpha}(-k,k_1,k_2)A^\nu(k_1)A^\alpha(k_2) \ , \end{aligned} \tag{5.4}$$

where k_i stands for the 4-vector $(\omega_i, \boldsymbol{k}_i)$. A plasma theory is different from a vacuum theory in that the linear response of the plasma is included in the wave operator:

$$\Lambda^{\mu\nu}(k) = k^2 g^{\mu\nu} - k^\mu k^\nu + \mu_0\alpha^{\mu\nu}(k) \ , \tag{5.5}$$

which follows from Maxwell's equations $ik_\nu F^{\mu\nu} = \mu_0 J^\mu$ with $F^{\mu\nu} = ik^\mu A^\nu - ik^\nu A^\mu$. The homogeneous wave equation (5.3) with the external current set to zero, and (5.5) for the wave operator then determine the wave eigenmodes of the plasma.

In Section 5.4 we will calculate the external current excited by a (GW induced) magnetosonic wave propagating through a magnetized relativistic plasma and in Section 5.5 we will derive the response of the plasma to this current. To find the associated scattered wave field, (5.3) has to be inverted:

$$A^\mu_{\rm P}(k) = -D^\mu{}_\nu(k)J^\nu_{\rm ext}(k) \ . \tag{5.6}$$

$D^{\mu\nu}$ is the Green's function for the inhomogeneous wave equation or the *photon propagator*. We are interested in the *radiation field* excited by the external current so we only consider the irreversible anti-Hermitian part of the photon propagator which is obtained by imposing the causal condition on it and using the Plemelj formula.

The covariant and gauge independent expressions for the photon propagator and its anti-Hermitian part are [6]:

$$D^{\mu\nu}(k) = \mu_0 \frac{G_\alpha G'_\beta}{(Gk)(G'k)} \frac{\lambda^{\mu\alpha\nu\beta}(k)}{\lambda(k)} , \tag{5.7}$$

$$D^{\mathrm{A}\mu\nu}(k) = -i\pi\mu_0 \frac{G_\alpha G'_\beta}{(Gk)(G'k)} \lambda^{\mu\alpha\nu\beta}(k)\delta[\lambda(k)] , \tag{5.8}$$

where $\lambda^{\mu\alpha\nu\beta}$ and $\lambda(k)$ are the second-order matrix of cofactors and the determinant of $\Lambda^{\mu\nu}$, respectively. G^μ determines the gauge and can be chosen, for instance, as the Lorentz gauge $G_\mu = k_\mu$, Coulomb gauge $G_\mu = [0, \boldsymbol{k}]$ or temporal gauge $G_\mu = [1, \mathbf{0}]$.

We will specify to the temporal gauge as it is the most convenient and the only gauge that allows a unique normalization of the wave polarization 4-vectors: one is free to specify $e^\mu_M(k) e^\star_{M\mu}(k) = -1$ with $e^\mu_M = [0, \boldsymbol{e}_M]$. Furthermore, in the temporal gauge the first-order matrix of cofactors and the determinant of the 3-tensor $\Lambda^i{}_j$ are given by $\lambda^i{}_j = \lambda^{0i}{}_{0j}$ and $\lambda^{(t)}(k) = \omega^2\lambda(k)$, respectively, with $\lambda^i{}_l \Lambda^l{}_j = \lambda^{(t)}\delta^i{}_j$. The polarization vectors can be derived from the spatial matrix of cofactors by

$$e^\star_{Mi}(k) e_{Mj}(k) = \frac{\lambda^i{}_j(k)}{\lambda^i{}_i(k)} . \tag{5.9}$$

The photon propagator only has contributions from the poles at the zeros of $\lambda(k_M)$ corresponding to the dispersion relation $k = k_M$ for a specific wave mode. To make this more explicit we use the identity:

$$\delta[\lambda(k) = \sum_M \frac{\delta[\omega - \omega_M(\boldsymbol{k})] + \delta[\omega + \omega_M(-\boldsymbol{k})]}{|\partial\lambda(k)/\partial\omega|} , \tag{5.10}$$

which can be written in terms of the ratio of electric to total energy

$$R_M(k) = \frac{W^{(E)}_M(k)}{W_M(k)} = \left.\frac{-\omega}{\frac{\partial\lambda(k)}{\partial\omega}}\right|_{\omega=\omega_M} = \left.\frac{\lambda^i{}_i(k)}{\omega\frac{\partial\lambda^{(t)}(k)}{\partial\omega}}\right|_{\omega=\omega_M} . \tag{5.11}$$

Here the wave energy $W_M(k) = P^0_M(k) = T^{00}_M(k)$ is the temporal component of the 4-momentum $P^\mu_M(k)$ and the time-time component of the energy-momentum tensor $T^{\mu\nu}_M(k)$.

Combining (5.8)–(5.11), the radiation field in mode M is found by retaining only the resonant anti-Hermitian part of the photon propagator, given by:

$$\begin{aligned} D^{\mathrm{A}\mu\nu}_M(k) &= -i\pi\mu_0 \frac{R_M(k)}{\omega_M} \{e^\mu_M(k) e^{\star\nu}_M(k)\delta[\omega - \omega_M(\boldsymbol{k})] \\ &+ e^{\star\mu}_M(k) e^\nu_M(k)\delta[\omega + \omega_M(-\boldsymbol{k})]\} , \end{aligned} \tag{5.12}$$

[6] In (5.8) and throughout this Chapter, inner products are denoted as $Gk = g_{\mu\nu}G^\mu k^\nu$.

while $D^{\mathrm{A}\mu\nu}(k) = \sum_M D_M^{\mathrm{A}\mu\nu}(k)$ and since (5.12) is derived using the temporal gauge, only the spatial components $(D_M^{\mathrm{A}})^i{}_j$ are non-zero.

Emission probability and 4-momentum radiated

The 4-*momentum* radiated in an arbitrary wave mode due to an arbitrary source, described by an extraneous current, is identified by the work done by this current on the electromagnetic field. Written covariantly and averaged over a truncation or normalization time T (which we can let go to infinity), using the power theorem, and the charge continuity equation $k^\nu J_\nu = 0$, one has:

$$\begin{aligned} \frac{1}{T}\int d^4x\ J^\nu_{\mathrm{ext}}(x) F_\nu{}^\mu(x) &= \\ \frac{1}{T}\int \frac{d^4k}{(2\pi)^4}\ \Re[-ik^\mu J^\nu_{\mathrm{ext}}(k) A_\nu(k)] &= \int \frac{d^3\boldsymbol{k}}{(2\pi)^3}\ Q^\mu_M(k)\ . \end{aligned} \tag{5.13}$$

$Q^\mu_M(k) \equiv dP^\mu_M(k)/dt$ is the rate at which 4-momentum is radiated into mode M. Using (5.3) with (5.12) and performing the integral over the delta functions we find:

$$\begin{aligned} Q^\mu_M(k) &= \frac{\mu_0 R_M(k)}{T\omega_M} k^\mu_M\, |e^\star_{M\nu}(k) J^\nu_{\mathrm{ext}}(k_M)|^2 \\ &\equiv k^\mu_M w_M(k)\ , \end{aligned} \tag{5.14}$$

Equation (5.14) defines the probability $w_M(k)$ per unit time and unit volume of $\boldsymbol{k}$-space of spontaneous emission of a wave quantum.

The rate of emission Q^μ_M and the ratio of electric to total energy R_M can also be written more conveniently in terms of the eigenvalues of the response tensor

$$\alpha_M(k) = e^\star_{M\mu}(k) e_{M\nu}(k) \alpha^{\mu\nu}(k)\ , \tag{5.15}$$

such that

$$\frac{1}{R_M(k)} = \left[2 - \frac{\mu_0}{\omega}\frac{\partial}{\partial\omega}\alpha_M(k)\right]_{\omega=\omega_M}\ , \tag{5.16a}$$

$$Q^\mu_M(k) = -\frac{2i\mu_0 R_M(k) W_M(k)}{\omega_M^2} k^\mu_M \alpha^A_M(k_M)\ , \tag{5.16b}$$

where the purely imaginary anti-Hermitian part of (5.15), $\alpha^A_M(k_M)$, measures the effect of dissipation in mode M.

5.4 GW induced current

Zeroth order current

The zeroth-order motion of electrons and positrons in a uniform and static magnetic field is a spiraling orbit around the magnetic field given by the covariant equation of motion:

$$\frac{du^\mu(\tau)}{d\tau} = \frac{q}{m} F_0^{\mu\nu} u_\nu(\tau) \ , \tag{5.17}$$

where q is the charge of the particle, m the mass and τ the proper time. One can define a magnetostatic field as having $F^{\mu\nu}F_{\mu\nu} > 0$ in any frame in which case it is possible to choose a particular frame where $\boldsymbol{E} = 0$ and $\boldsymbol{B} \neq 0$. We will orient the axes such that the magnetic field lies along the z-axis and define $B = \frac{1}{2}\sqrt{F_0^{\mu\nu}F_{0\mu\nu}}$. If we specify the initial condition for the 4-velocity as $u_0^\mu = \gamma(1, v_\perp, 0, v_\parallel)$ at $\tau = 0$ we can integrate Eq. 5.17 twice to find the orbit [7]:

$$u^{(0)\mu}(\tau) = i^{\mu\nu}(\tau) u_{0\nu} \ , \tag{5.18a}$$

$$X^{(0)\mu}(\tau) = x_0^\mu + t^{\mu\nu}(\tau) u_{0\nu} \ , \tag{5.18b}$$

where $t^{\mu\nu}(\tau)$ and its Fourier transform $\tau^{\mu\nu}(\omega)$ are given by:

$$t^{\mu\nu}(\tau) = \frac{1}{\Omega_c} \begin{pmatrix} \Omega_c\tau & 0 & 0 & 0 \\ 0 & -\sin\Omega_c\tau & \eta\cos\Omega_c\tau & 0 \\ 0 & -\eta\cos\Omega_c\tau & -\sin\Omega_c\tau & 0 \\ 0 & 0 & 0 & -\Omega_c\tau \end{pmatrix} ,$$

$$\tau^{\mu\nu}(\omega) = \begin{pmatrix} 1 & 0 & 0 & 0 \\ 0 & -\frac{\omega^2}{\omega^2-\Omega_c^2} & -\frac{i\eta\Omega_c\omega}{\omega^2-\Omega_c^2} & 0 \\ 0 & \frac{i\eta\Omega_c\omega}{\omega^2-\Omega_c^2} & -\frac{\omega^2}{\omega^2-\Omega_c^2} & 0 \\ 0 & 0 & 0 & -1 \end{pmatrix} . \tag{5.19}$$

γ, $v_\perp$, $v_\parallel$ and the components of the 4-momentum $p^\mu = mu^\mu$, $p_\perp = \gamma m v_\perp$ and $p_\parallel = \gamma m v_\parallel$ are all constants of the motion. Also, we have defined $\eta \equiv q/|q|$ and the (non-relativistic) gyro-frequency $\Omega_c = |qB/m|$.

Note that in the limit $\Omega_c \to 0$, $\tau^{\mu\nu}(\omega)$ reduces to the Minkowskian metric tensor $g^{\mu\nu} = \eta^{\mu\nu}$ and (5.18) gives rectilinear motion.

The *zeroth-order* single particle current in the absence of any perturbations is now given in Fourier space by:

$$J^\mu_{\rm sp}(k) = q \int d\tau \ u^\mu(\tau) \mathrm{e}^{ikX(\tau)} \ . \tag{5.20}$$

[7] Note that u_0^μ denotes an initial condition, whereas $u^{(0)\mu}$ means the unperturbed 4-velocity and similarly for X.

First-order current

We now study a particle that is orbiting in a static magnetic field when an MHD wave with amplitude $A^\mu(k)$ passes and perturbs the motion, by including the covariant Lorentz acceleration, S^μ, in (5.17):

$$\begin{aligned} \frac{du^\mu(\tau)}{d\tau} &= \frac{q}{m}F_0^{\mu\nu}u_\nu(\tau) + S^\mu(\tau) \ , && \text{(5.21a)} \\ S^\mu(\tau) &= \frac{iq}{m}\int \frac{d^4k_1}{(2\pi)^4}\mathrm{e}^{-ik_1X(\tau)} \\ &\times \quad k_1u(\tau)G^{\mu\nu}(k_1,u(\tau))A_\nu(k_1) \ . && \text{(5.21b)} \end{aligned}$$

where the useful projection tensor $G^{\mu\nu}$ is defined by:

$$G^{\mu\nu}(k,u) = g^{\mu\nu} - \frac{k^\mu u^\nu}{ku} \ . \tag{5.22}$$

The orbits can again be obtained by integrating the first-order equation of motion (5.21):

$$u^{(1)\mu}(\tau) = \int_0^\tau d\tau' \ i^{\mu\nu}(\tau-\tau')S_\nu^{(0)}(\tau') \ , \tag{5.23a}$$

$$X^{(1)\mu}(\tau) = \int_0^\tau d\tau'' \int_0^{\tau''} d\tau' \ i^{\mu\nu}(\tau''-\tau')S_\nu^{(0)}(\tau') \ , \tag{5.23b}$$

where $S_\nu^{(0)}(\tau)$ is given by inserting the zeroth-order orbit Eq. 5.18 in Eq. 5.21b.

The first-order expansion for the current density is:

$$J_{\rm sp}^{(1)\mu}(k) = q\int d\tau \ j^{(1)\mu}(\tau)\mathrm{e}^{ikX^{(0)}(\tau)} \ , \tag{5.24}$$

with:

$$j^{(1)\mu}(\tau) = u^{(1)\mu}(\tau) + ikX^{(1)}(\tau)u^{(0)\mu}(\tau) \ . \tag{5.25}$$

Inserting (5.25) in (5.24), partially integrating with $u^{(1)\mu} = dX^{(1)}/d\tau$ and using (5.23), results in:

$$\begin{aligned} J_{\rm sp}^{(1)\mu}(k) &= iq\int d\tau \ ku^{(0)}(\tau)G^{\alpha\mu}(k,u^{(0)}(\tau))X_\alpha^{(1)}\mathrm{e}^{ikX^{(0)}} \\ &= -\frac{q^2}{m}\int d\tau\int_0^\tau d\tau''\int_0^{\tau''}d\tau'\int\frac{d^4k_1}{(2\pi)^4} \\ &\times \quad \mathrm{e}^{i\left[kX^0(\tau)-k_1X^0(\tau')\right]}\dot{t}_{\alpha\beta}(\tau''-\tau')A_\nu(k_1) \\ &\times \quad ku^0(\tau)G^{\alpha\mu}(k,u^0(\tau))k_1u^0(\tau')G^{\beta\nu}(k_1,u^0(\tau')) \ . \end{aligned} \tag{5.26}$$

Eq. (5.26) is the current associated with a single particle. To calculate the response tensor for the magnetized plasma one can use either the *forward-scattering* method where all the perturbations are included in the orbits of the particles and an average is made over the initial conditions, or the *Vlasov method* in which the perturbations are included in the distribution function. In an *unmagnetized plasma*, the simplest method is to calculate the response tensor for a cold plasma fluid and generalize this result to an arbitrary distribution function by using Lorentz transformations. This method is generally not suitable for a magnetized plasma since there is no inertial frame associated with the gyrating particles. An exception is the case where the particles move strictly along the magnetic field. Since we want to study the effect of a MHD wave propagating through the force-free plasma wind relatively close to the source where the magnetic field is very strong and any transverse momentum is quickly synchrotron radiated, a *strictly parallel particle distribution* should be a reasonable assumption.

One advantage of the small gyro-radius approximation is that while (5.26) generally has to be expanded in Bessel functions ($J_s(k_\perp R)$ with R the gyro-radius) to carry out the integrals, in the strictly parallel case the arguments of all the Bessel functions vanish for $v_\perp \propto R = 0$ which leads to $J_s(0) = 0$ for all integers $s \neq 0$ and $J_0(0) = 1$, and

$$\begin{aligned} J^{(1)\mu}_{\rm sp}(k) &= -\frac{q^2}{m}\int \frac{d^4k_1}{(2\pi)^4} \mathrm{e}^{-i(k-k_1)x_0} 2\pi\delta\left[(k_\parallel - k_{1\parallel})u\right] \\ &\times \quad G^{\alpha\mu}(k,u)\tau_{\alpha\beta}(k_\parallel u) G^{\beta\nu}(k_1,u) A_{\mathrm{M}\nu}(k_1)\ , \end{aligned} \tag{5.27}$$

where A^μ_M denotes the incident fast magneto-acoustic MHD wave and since u is strictly along the magnetic field we implicitly have $ku = (ku)_\parallel = \gamma(\omega - k_\parallel u_\parallel)$, $v_\perp = 0$.

5.5 Linear and non-linear response

To find the linear response tensor for the magnetized plasma, we use the forward-scattering method and average the first-order single-particle current (5.26) over the distribution of particles $F(x_0, p_0)$. The distribution function is defined covariantly in terms of the number $d\mathcal{N}$ of world lines –one per particle– in an 8-dimensional phase space threading a 7-dimensional surface element $d^4x_0d^4p_0/d\tau$ as determined by: $d\mathcal{N}d\tau = F(x_0,p_0)d^4x_0d^4p_0$. With this identification one can replace the integral over $d\tau$ in (5.26) with an integral over $d\mathcal{N}d\tau$ —that is over $d^4x_0d^4p_0$ weighed by $F(x_0,p_0)$— to average over the ensemble of particles.

When the particle distribution is uniform in space and time, $F(p_0)$ does not depend on the initial conditions x_0 and the current (5.26) only depends on x_0 through the unperturbed orbit (5.18b). Explicitly, this results in a factor $\exp[i(k-k_1)x_0]$ as in (5.27) and the integral over x_0 gives a delta function $(2\pi)^4\delta^4(k-k_1)$ over which the k_1 integral is performed.

An alternative and easier procedure is to use (5.27) which is valid in the small gyro-radius approximation, realize that

$$2\pi\delta\left[(k_\parallel - k_{1\parallel})u\right] = \int d\tau \exp\left[i(k_\parallel - k_{1\parallel})u\tau\right] \ ,$$

and replace this integral with the integral over phase space. The result is:

$$\begin{aligned} \alpha^{\mu\nu}(k) &= -\frac{q^2}{m}\int d^4p\ F(p)G^{\alpha\mu}(k,u)\tau_{\alpha\beta}(ku)G^{\beta\nu}(k,u) \\ &= -\frac{q^2}{m}\int \frac{dp_\parallel}{\gamma_\parallel} g(p_\parallel)\alpha^{\mu\nu}(k,u) \ , \end{aligned} \tag{5.28}$$

where the last equality defines $\alpha^{\mu\nu}(k,u)$ and the distribution $F(p)$ is chosen parallel to the magnetic field, so the spatial part can be written as: $f(\boldsymbol{p}) = \delta^2(\boldsymbol{p}_\perp)g(p_\parallel)$. More specifically, a relativistic thermal distribution strictly parallel to the magnetic field is given by the one-dimensional Jüttner distribution:

$$F(p) = 2\pi m\delta(p^2 - m^2)\delta^2(\boldsymbol{p}_\perp)g(p\tilde{u}) \ , \tag{5.29a}$$

$$g(\gamma) = \frac{n\mathrm{e}^{-\frac{m\gamma}{T}}}{2\pi m K_1(m/T)} \ , \tag{5.29b}$$

where K_ν are the modified Bessel or Macdonald functions, T is the temperature in energy units, $\tilde{u}$ is the 4-velocity of the rest frame in which $\tilde{u} = [1, \mathbf{0}]$ such that $p\tilde{u} = m\gamma$.

The Jüttner distribution (5.29) is normalized by the (non invariant) number density n evaluated in the rest frame:

$$n = \int d^4p\ u^0 F(p) = \int_{-\infty}^{\infty} dp_\parallel\ g(\gamma) \ ,$$

rather than the invariant proper number density

$$n_{\rm pr} = \int d^4p\ F(p) = \int_{-\infty}^{\infty} dp_\parallel\ \frac{g(\gamma)}{\gamma} \ , \tag{5.30a}$$

which does not correspond to the actual number density in any frame (when the plasma is not cold).

In this special case of a strictly parallel distribution (5.28) can also be obtained from a fluid description as in the unmagnetized case, as was mentioned in the previous section. The covariant linear response tensor for a cold magnetized plasma (fluid) with rest frame 4-velocity $\tilde{u}$ and proper number density $n_{\rm pr}$ is:

$$\alpha^{\mu\nu}_{\rm cold}(k) = -\frac{q^2 n_{\rm pr}}{m} G^{\alpha\mu}(k,\tilde{u})\tau_{\alpha\beta}(k\tilde{u})G^{\beta\nu}(k,\tilde{u}) \ , \tag{5.31}$$

and the response tensor (5.28) for an arbitrary but strictly parallel distribution is found by interpreting $n_{\rm pr}$ as the proper number density $d^4pF(p)$, which implies implicitly that for each particle with 4-velocity u the response is calculated in its rest frame using (5.31) and subsequently Lorentz boosted *along the magnetic field* to the frame of interest and then the contributions of all particles are summed by integrating over d^4p.

The cold plasma response (5.31) can be recovered from (5.28) in the limit $F(p) = n\delta^4(pu - m\tilde{u})$ where $n = n_{\rm pr}$.

Linear response of cold magnetized plasma

The explicit spatial components of (5.31) will be useful later on. In terms of the total plasma frequency $\omega_p^2 = \omega_{\rm p+}^2 + \omega_{\rm p-}^2$, the positron plasma frequency $\omega_{\rm p+}^2 = e^2 n_+/(\epsilon_0 m)$ (and similarly for the electron plasma frequency) and the average charge number $\xi = (n_+ - n_-)/(n_+ + n_-)$ measuring the excess of positrons (with density n_+) to electrons, one has (Melrose 1986):

$$\alpha_{\rm cold}^{ij} = -\frac{\omega_{\rm p}^2}{\mu_0}\begin{pmatrix} \frac{\omega^2}{\omega^2-\Omega_c^2} & \frac{i\xi\omega\Omega_c}{\omega^2-\Omega_c^2} & 0 \\ -\frac{i\xi\omega\Omega_c}{\omega^2-\Omega_c^2} & \frac{\omega^2}{\omega^2-\Omega_c^2} & 0 \\ 0 & 0 & 1 \end{pmatrix} . \tag{5.32}$$

We are interested in a pure pair plasma with $\xi = 0$ in which case the linear cold plasma response tensor (5.32) becomes diagonal and the contributions of the electrons and positrons add in the (linear) Thomson scattering process, in contrast to for instance an electron gas which has $\xi = -1$.

More generally, the plasma might have some charge excess, for instance related to the Goldreich-Julian charge density $n_{\rm GJ}$ such that $\xi \simeq n_{\rm GJ}/n_{\rm tot} = 1/M$. M is the *multiplicity* of secondary particles created by a primary particle that emits curvature radiation while it flows out along a open field line anchored to the polar cap. The curvature photons then produce a cascade of pair creation (Gurevich et al. 1993). The multiplicity is largely unknown but varies from 10^2–10^6. The gyrotropic terms only contribute quadratically in the dispersion relation for the plasma, i.e. of order $1/M^2$, which is the motivation to neglect those terms in Gedalin et al. (1998), Section V A. For very low-frequency waves and low multiplicity the gyrotropic terms become important when $1/M \simeq \xi \sim \omega/\Omega_c$ as can be seen by comparing the components of (5.32). Although this might lead to interesting behavior, we will assume for simplicity that the plasma is sufficiently neutral that ξ can be neglected.

Linear response of relativistic magnetized pair plasma

In evaluating (5.28) for more complicated response tensors it is convenient to define the average, $\langle V\rangle$, of any variable V by:

$$\langle V\rangle \equiv \frac{1}{n}\int \frac{dp_\parallel}{\gamma} V g(p_\parallel) \ . \tag{5.33}$$

The frame in which the bulk momentum vanishes, $\langle \gamma v \rangle = 0$, is defined as the rest frame and the non-gyrotropic components can be written in terms of the Alfvén speed, $v_{\rm A}$, a mean square speed, Δv^2,

$$v_{\rm A} = \frac{\Omega_c}{\sqrt{\langle\gamma\rangle}\omega_{\rm p}} \ , \quad \Delta v^2 = \frac{\langle \gamma v^2 \rangle}{\langle \gamma \rangle} \ , \tag{5.34}$$

and the *relativistic plasma dispersion function* for the phase velocity $z = \omega/k_\parallel$ parallel to the magnetic field:

$$W(z) = \left\langle \frac{1}{\gamma^3 (z-v)^2} \right\rangle = \int_{-\infty}^{\infty} \frac{dp}{v-z} \frac{dg(p)}{dp} \ . \tag{5.35}$$

Since we are interested in scattering of kHz waves to $\sim$ 100 MHz waves that both have $ku \ll \Omega_c$, we can expand in ku/Ω_c and only keep terms up to second order. Under these approximations, the linear response tensor is given in terms of the refractive index $n = k/\omega$ (and $n_\perp = n \sin\theta$, $n_\parallel = n\cos\theta$) by:

$$\alpha^{ij}_{\rm rel} = \frac{-\omega^2}{v_{\rm A}^2 \mu_0} \begin{pmatrix} 1 + n_\parallel^2 \Delta v^2 & 0 & -n_\perp n_\parallel \Delta v^2 \\ 0 & 1 + n_\parallel^2 \Delta v^2 & 0 \\ -n_\perp n_\parallel \Delta v^2 & 0 & n_\perp^2 \Delta v^2 - f(n) \end{pmatrix} \ , \tag{5.36}$$

with $f(n) = \frac{\omega_p^2}{\omega^2} v_{\rm A}^2 z^2 W(z)$.

Note that for $\xi = 0$, $\Delta v^2 \downarrow 0$, $\gamma = \langle\gamma\rangle \downarrow 1$, $v_{\rm A}^2 \to \Omega_c/\omega_{\rm p}$ and consequently $W(z) \to z^{-2}$, (5.36) reduces to the low-frequency limit of the cold plasma response tensor (5.32) with $\xi = 0$.

In the remainder of this Chapter, we will investigate whether the fast MSW eigenmode of (5.32) —induced by the GW— can scatter into an eigenmode of (5.36) when it propagates through a relativistic plasma region.

Non-linear response tensor

The quadratic response tensor for a relativistic magnetized pair plasma is obtained in the forward-scattering approach by averaging the second order (in the field) current over an arbitrary distribution function (Melrose 2001). We

take the small gyro-radius limit to find:

$$\alpha^{\mu\nu\rho}(k_0,k_1,k_2) = \sum_{\pm}\frac{\pm e^3}{4m^2}\int d^4p\; F_{\pm}(p)\times \tag{5.37}$$
$$\times\, G^{\star\alpha\mu}(k_0,u)G^{\star\beta\nu}(k_1,u)G^{\star\gamma\rho}(k_2,u)\times$$
$$\left\{\frac{k_1^\sigma}{k_{0\parallel}u}\tau_{\sigma\alpha}(k_{0\parallel}u)\tau_{\beta\gamma}(k_{2\parallel}u) + \frac{k_2^\sigma}{k_{0\parallel}u}\tau_{\sigma\alpha}(k_{0\parallel}u)\tau_{\beta\gamma}(k_{1\parallel}u)+\right.$$
$$\frac{k_0^\sigma}{k_{1\parallel}u}\tau_{\sigma\beta}(k_{1\parallel}u)\tau_{\alpha\gamma}(k_{2\parallel}u) + \frac{k_0^\sigma}{k_{2\parallel}u}\tau_{\sigma\beta}(k_{2\parallel}u)\tau_{\alpha\gamma}(k_{1\parallel}u)+$$
$$\left.\frac{k_1^\sigma}{k_{2\parallel}u}\tau_{\sigma\gamma}(k_{2\parallel}u)\tau_{\beta\alpha}(k_{0\parallel}u) + \frac{k_1^\sigma}{k_{1\parallel}u}\tau_{\sigma\beta}(k_{1\parallel}u)\tau_{\gamma\alpha}(k_{0\parallel}u)\right\}\ .$$

The cold plasma limit can be derived from (5.37) by choosing $F_\pm(p) = n_\pm\delta^4(p - m\tilde{u})$ (where again $\tilde{u} = [1,\mathbf{0}]$ in the plasma rest frame). The only components in (5.37) that depend on the sign of the charge are the gyrotropic terms which are proportional to $\eta = q/|q|$. In a pure pair plasma with equal distributions for the electrons and positrons the non-gyrotropic terms are therefore the only ones that do not vanish in the sum over the species (see also the next section 5.6).

5.6 Scattering

As mentioned previously, the emission probability (5.13) is very general and applies to any emission process due to an arbitrary source expressed as an external current density. The specific probability of scattering of a specific mode M, say a MHD wave, off an electron into a different mode P can now be calculated by inserting the extraneous single particle current (5.26) into (5.13) and interpreting the resulting emission as the scattered wave:

$$w_{MP}(k,k_1,u) = \frac{3\sigma_{\rm T}(4\pi)^2}{\gamma}\frac{R_M(k)R_P(k_1)}{\omega_M(k)\omega_P(k_1)} \tag{5.38a}$$
$$\times\,|a_{MP}(k,k_1,u)|^2\delta\left[(k_{M\parallel}-k_{1P\parallel})u\right]\ ,$$
$$a_{MP}(k,k_1,u) = e^\star_{M\mu}(k)e_{P\nu}(k_1)\,\{ \tag{5.38b}$$
$$G^{\alpha\mu}(k_M,u)\tau_{\alpha\beta}(k_{M\parallel}u)G^{\star\beta\nu}(k_{1P},u)$$
$$-\ \frac{2m}{q}\alpha^{\mu\nu\rho}(k_M,k_{1P},k_M-k_{1P})u_\rho\Big\}\ ,$$

where we have used $[\delta((k-k_1)u)]^2 = T\delta((k-k_1)u)/(2\pi\gamma)$. We have included the non-linear scattering probability $\alpha^{\mu\nu\rho}(k_M,k_{1P},k_M-k_{1P})$ due to the scattering of the MHD wave on the self-consistent field associated with the zeroth-order current related to the beat between the MHD wave and the scattered

wave. As can be seen from (5.38) the total scattering probability is proportional to $\sigma_{\rm T} \propto q^4/m^2$. The non-linear scattering probability has an additional (small) factor $2m/q$ as can be seen from (5.38b) and consequently the gyrotropic terms are the *only* terms that *do not* vanish when the contributions of the two species are added up for a pure pair plasma. The components of the quadratic response, however, are proportional to $(\omega/\Omega_c)^4$ and are negligible in our long-wavelength approximation (Melrose 1997; Gedalin and Machabeli 1983; Mikhailovskii 1980).

Polarization vectors

The polarization properties of the incident MHD wave and the scattered modes are determined by the eigenvectors of the wave operator $\Lambda^{\mu\nu}(k)$ as defined by (5.5) and (5.9) with the linear response tensors derived in (5.32) and (5.36). When the z-axis is chosen along the magnetic field and the wave vectors in the $x-z$ plane, then the spatial parts of both the wave operator for the cold plasma and that for the relativistic anisotropic plasma are of the form:

$$\Lambda_{ij}(k) = \begin{pmatrix} \Lambda_{11} & 0 & \Lambda_{13} \\ 0 & \Lambda_{22} & 0 \\ \Lambda_{13} & 0 & \Lambda_{33} \end{pmatrix} . \tag{5.39}$$

So the dispersion relations for the different wave modes, used in (5.10), follow from:

$$|\Lambda_{ij}(k)| = \Lambda_{22}(\Lambda_{11}\Lambda_{33} - \Lambda_{13}^2) = 0 , \tag{5.40}$$

and the polarization vectors are given by:

$$\boldsymbol{e}_{\rm t} = \{0, 1, 0\} , \tag{5.41a}$$

$$\boldsymbol{e}_{-} = \frac{1}{\sqrt{(\Lambda_{13})^2 + (\Lambda_{11})^2}} \{-\Lambda_{13}, 0, \Lambda_{11}\} , \tag{5.41b}$$

$$\boldsymbol{e}_{+} = \frac{1}{\sqrt{(\Lambda_{13})^2 + (\Lambda_{11})^2}} \{\Lambda_{11}, 0, \Lambda_{13}\} . \tag{5.41c}$$

Obviously, $\boldsymbol{e}_{\rm t}$ always corresponds to a mode where the electric field is purely transverse to the magnetic field with dispersion relation $\Lambda_{22} = 0$, such as the magneto-acoustic waves excited by a gravitational wave.

The modes $\boldsymbol{e}_{\pm}$ that have an electric field component along the magnetic field correspond to the eigenfrequency solutions of

$$(\Lambda_{11} - \Lambda_{33}) \mp \sqrt{(2\Lambda_{13})^2 + (\Lambda_{11} - \Lambda_{33})^2} = 0 . \tag{5.42}$$

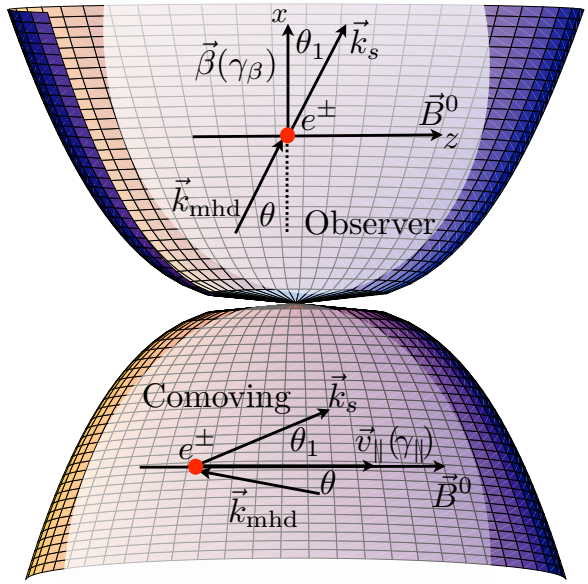

Figure 5.3: Scattering geometry in observer (top) and comoving (bottom) frames.

Response to an incident magneto-acoustic wave

To evaluate the scattering probability (5.38) explicitly, it is most convenient to orient our coordinate axes such that the background magnetic field is aligned with the z-axis and the wave vector of the *scattered* wave ($\boldsymbol{k}_P$) lies in the x-z plane. The direction of the *incident* magnetosonic wave is then completely arbitrary, but we know from (5.39) and (5.41a) that it is polarized perpendicular to both the magnetic field and the wave vector. Hence, we have

$$k_M = \{\omega, k\sin\theta\cos\psi, k\sin\theta\sin\psi, k\cos\theta\}\ , \tag{5.43a}$$
$$e_M = \{0, -\sin\psi, \cos\psi, 0\}\ , \tag{5.43b}$$
$$k_P = \{\omega_1, k_1\sin\theta_1, 0, k_1\cos\theta_1\}\ , \tag{5.43c}$$

where θ (θ_1) is angle of the incident (scattered) wave vector with respect to the magnetic field and ψ (ψ_1) the angle with the x-axis.

Similarly, the polarization of the scattered modes is found from the eigenvectors of the wave operator (5.5) with the relativistic linear response tensor

given by (5.36) using (5.41):

$$\boldsymbol{e}_t(k_1) = \{0,1,0\} \ , \tag{5.44a}$$

$$\boldsymbol{e}_-(k_1) = \frac{1}{\sqrt{1+\Xi^2}}\{-\Xi,0,1\} \ , \tag{5.44b}$$

$$\boldsymbol{e}_+(k_1) = \frac{1}{\sqrt{1+\Xi^2}}\{1,0,\Xi\} \ , \tag{5.44c}$$

with

$$\Xi = \frac{k_1^2 u_A^2 \sin\theta_1 \cos\theta_1}{\omega_1^2 - k_1^2 u_A^2 \cos^2\theta_1} \ . \tag{5.45}$$

With this choice of geometry, the explicit expression for the linear scattering response summed over the two species such that the gyrotropic terms vanish, is:

$$a^{\mu\nu}(k,k_1,u) = G^{\alpha\mu}(k_M,u)\tau_{\alpha\beta}(k_{M\parallel}u)G^{\star\beta\nu}(k_{1P},u) \ ,$$

with the spatial components written explicitly as:

$$a_{ij}(k,k_1,u) = -\frac{(ku)^2}{(ku)^2-\Omega_c^2}\times \begin{pmatrix} 1 & 0 & -\frac{\gamma\beta k_1 \sin\theta_1}{ku} \\ 0 & 1 & 0 \\ \frac{\gamma\beta k \sin\theta\cos\psi}{ku} & \frac{\gamma\beta k\sin\theta\sin\psi}{ku} & \Psi \end{pmatrix} \ , \tag{5.46}$$

and $\Psi = \frac{1}{\gamma^2}\frac{\omega}{ku}\frac{\omega_1}{k_1 u}\frac{(ku)^2-\Omega_c^2}{(ku)^2} + (1-\gamma^2)\frac{k\sin\theta\cos\psi}{ku}\frac{k_1\sin\theta_1}{k_1 u}$.

Probability of transverse-transverse scattering

The probability that the incident (transverse) magneto-acoustic wave scatters into a transversely polarized electromagnetic wave, as in (5.44a), is proportional to (the square of):

$$\begin{aligned} a_{Mt}(k,k_1,u) &= e^\star_{M\mu}(k)e_{t\nu}(k_1)a^{\mu\nu}(k,k_1,u) \\ &= -\frac{(ku)^2}{(ku)^2-\Omega_c^2} = \frac{1}{\frac{\Omega_c^2}{\gamma^2(\omega-k\beta\cos\theta)^2}-1} \ . \end{aligned} \tag{5.47}$$

In the two limits of nearly parallel and perpendicular propagation and assuming that $\gamma\omega \ll \Omega_c$, this is approximately $\sim (\omega/\gamma\Omega_c)^2$ and $\sim (\gamma\omega/\Omega_c)^2$, respectively.

Furthermore, it can be easily seen from the linear response tensors in (5.32) and (5.36), with the polarization vectors of the corresponding transverse eigenmodes given in (5.43b) and (5.44a), respectively, that the amplitudes

$$a_{M,t}(k) = e^\star_{M,t\mu}(k)e_{M,t\nu}(k)\alpha^{\mu\nu}(k_{M,t}) \mid_{\omega=\omega_{M,t}} \ , \tag{5.48}$$

are independent of ω for the transverse magneto-acoustic and electromagnetic wave modes. Hence, the ratio of electric to total energy given by (5.16a) is $R_M = R_t = \frac{1}{2}$ just like for transverse modes in an isotropic non-dispersive plasma.

Compared to the probability of scattering of a fast magneto-acoustic mode to a transverse electromagnetic mode in unmagnetized vacuum, this probability is suppressed in a strongly magnetized plasma by the factor in (5.47) squared.

Probability of transverse-LO scattering

The probability that the transverse magneto-acoustic mode is scattered into a quasi-transverse Langmuir-ordinary mode is obtained by contracting (5.46) with the polarization vectors (5.43b) and either (5.44b) or (5.44c).

The only component of (5.46), however, that is of lower order in $1/\Omega_c$ is the purely longitudinal zz component, which has a term independent of Ω_c. This component drops out, though, as soon as (5.46) is contracted with the polarization vector of the purely transverse incident magnetosonic wave. We find that the probability for scattering into a LO mode is equal or less than (5.47) depending on the relevant angles, the maximum being when the incident wave is perpendicular to the magnetic wave and the electric field of the scattered wave lies in the plane spanned by the electric field of the magnetoacoustic wave and the magnetic field.

Emitted power

In the previous section we derived the probability (5.38) that one quantum in the MSW mode scatters into one quantum in another mode. To calculate the actual *rate* at which scattered waves are emitted we have to average (5.38) over the distribution of particles. One subtlety is that the scattering probability per unit time is clearly a frame-dependent quantity. We should therefore integrate either the scattering probability $\gamma w_{MP}(k, k_1, u)$ per unit *proper time* along the particles motion, multiplied by the *proper number density* $d^4pF(p)$ or equivalently the probability per unit time over the physical number density $\gamma d^4pF(p)$, similar to the averaging of the response tensor of the distribution function performed in (5.28).

Appealing to the semiclassical formalism of detailed balance, we find a kinetic equation for the increase of wave energy in the scattered modes:

$$\begin{aligned} \frac{DW_P(k_1)}{Dt} &= \int \frac{d^3\boldsymbol{k}}{(2\pi)^3} \int dp_\parallel w_{MP}(k, k_1, u) g(p_\parallel) \\ &\times \left(\frac{\omega_{1P}}{\omega_M} W_M(k) - W_P(k_1) \right) , \end{aligned} \tag{5.49}$$

where we only consider spontaneous scattering of $M \rightarrow P$ and $P \rightarrow M$ and neglect induced scattering [8].

The total power in (5.49) is calculated for the scattering on the relativistic distribution of particles along the magnetic field in the frame that is comoving with the average bulk flow carrying the magnetic field. Because the power is Lorentz invariant (when the scattered radiation has front-back symmetry in the comoving frame) it is the same in the observer frame.

However, because of propagation and angular effects there is a difference between the *emitted* power $P_{\rm e}$ and the *received* power $P_{\rm r}$ in the observer frame (Rybicki and Lightman 1979). The scattered radiation is *emitted* during the time it takes the GW and MSW to cross a scale-height, i.e. $\mathcal{H}/c$, but because this shell propagates at a relativistic velocity β, the radiation is *received* in an interval $\mathcal{H}/(2\gamma_\beta^2 c)$ with a power

$$P_{\rm r} \simeq 2\gamma_\beta^2 P_{\rm e} \ . \tag{5.50}$$

These relativistic effects also play an important role in the physics of gamma-ray bursts as reviewed in Zhang and Mészáros (2004); Paradijs et al. (2000). Hence the time-integrated emitted and received energies are the same but (with sufficient time resolution) the observed flux is much higher.

5.7 Application to neutron star binary merger

We consider the specific environment of a highly relativistic electron-positron wind surrounding the merger of two neutron stars as illustrated in Fig. 4.4 in the previous Chapter, and apply the general results for the scattering of low-frequency fast MSWs into escaping electromagnetic waves as derived in the previous sections from the framework in Gedalin et al. (1998); Melrose et al. (1999); Melrose and Gedalin (1999); Gedalin et al. (2001); Luo and Melrose (2001); Gedalin et al. (2002).

We assume that the in the last phase of coalescence, the *orbital* motion dominates the spin of the individual neutron stars. The orbital angular frequency Ω_b then determines the radius of the light-cylinder $R_{\rm lc} = c/\Omega_b$ where the magnetic field lines that are anchored on the stellar polar caps break open because co-rotation of the plasma which is frozen onto the field lines would result in an unlimited increase in inertia if the field lines were closed at this distance. For a more extensive treatment of how the spinning magnetic dipole of a neutron star sets up a voltage jump and an electric field at the stellar polar caps and extracts charges from the neutron star filling the magnetosphere, see for instance Gurevich et al. (1993). Suffice to say that during the last stage of spiral-in, the double neutron star is assumed to behave essentially as a single millisecond pulsar with a charge separated closed magnetosphere and an ultra-relativistic force-free electron-positron plasma wind.

[8] D/Dt is a time-derivative operator that allows for a possible slow variation of the medium itself as $D/Dt = (\partial\omega_M/\partial k_\mu)\partial_\mu + (\partial\omega_M/\partial x_\mu)\partial/\partial k^\mu$ as in Melrose (2001).

An important observation is that the relativistic leptonic wind is already present before the actual merger. It doesn't have to be generated by the merger event, which is a problematic issue in collapsar models for gamma-ray bursts, where inside a collapsing massive star a region has to be evacuated of baryons and an almost mass-less jet has to form and then pierce through the entire star without slowing down much or losing its collimation.

As the neutron stars finally merge, a large fraction of the binding energy of the entire system is released in the form of gravitational waves that propagate through the pre-exisiting strongly magnetized plasma wind. Since a *magnetized* perfect fluid possesses an anisotropic pressure due to the magnetic stress, the GW couples to the plasma and excites magnetohydrodynamic waves. In Chapter 4 we found that GW can excite both Alfvén and (slow and fast) magneto-acoustic waves but that coupling to the fast mode is the most efficient because the dispersion relations are nearly the same in a tenuous, relativistic magnetoplasma and coherent interaction is always possible.

Even though we proved that the energy transfer from GW to MSW in the plasma can be substantial, we still have to find an efficient radiation process to release this energy. The MSW cannot escape the plasma directly, so we will now investigate whether the MSW are likely to inverse Compton scatter into electromagnetic radiation in the radio regime.

Magnetosonic wave amplitude and energy

The excitation of fast magneto-acoustic waves by a GW propagating through a uniform magnetic field was discussed in Section 5.2. The orientation of the ambient magnetic field is now chosen in the z-direction such that the wind flows out in the x-direction with average bulk velocity β and corresponding Lorentz factor γ_β. The wave vector of the gravitational waves, $\boldsymbol{k}_{\rm gw}$, is allowed to have an arbitrary angle θ with respect to the magnetic field (and the wave vector of the excited MSW will have the same orientation). In reality, the GW are emitted more or less radially and $\boldsymbol{k}_{\rm gw}$ will be almost perpendicular to the toroidal magnetic field in the wind in the observer frame (i.e. as in the top Figure 5.3).

In the approximation of a uniform background magnetic field, the amplitude and energy of the excited MSW are given in the observer frame by

$$B_z^{(1)}(x) \simeq \frac{h_+|B^{(0)}|}{2\gamma_\beta^2}\sin\theta\; k_{\rm gw}x\; \mathrm{e}^{ik_{\rm gw}(x-ct)}\;, \tag{5.51a}$$

$$W^{(B)} = \int_V d^3x\; \frac{|B^{(1)}|^2}{2\mu_0}\;, \tag{5.51b}$$

$$W_M = T^{00} \simeq W^{(E)} + W^{(B)} \simeq 2W^{(B)}\;. \tag{5.51c}$$

This result will be generalized to a non-uniform background in the following sections.

Eikonal approximation

We generalized (5.51a) to a non-uniform magnetoplasma wind by appealing to the *eikonal* or *geometric optics* two-length-scale expansion (also known as the WKB approximation). When the wavelength of the modes under consideration is small compared to the scale of spatial variation in the background [9], the waves can still be considered locally planar and monochromatic. Furthermore, in the Poynting flux dominated regime where the gaspressure is negligible (Section 5.7), the classical Alfvén velocity $v_{\rm A} \propto B/\sqrt{n}$ is constant since $B \simeq B_\phi \propto 1/R$ well outside the light-cylinder and $n \propto B_z \propto 1/R^2$ (which will be derived in ((5.53)). Consequently, the relativistic Alfvén phase velocity $1/u_{\rm A}^2 = 1 + 1/v_{\rm A}^2$ is also constant and the dispersion relation $\omega \simeq k u_{\rm A}$ is spatially non-dispersive even in the inhomogeneous background.

The important space-dependent background quantities are the ambient magnetic field $B^{(0)}(r)$ and plasma density $n(r)$, and the corresponding gyrofrequency $\Omega_c(r) \propto B^{(0)}(r)$ and plasma frequency $\omega_{\rm pl}(r) \propto \sqrt{n(r)}$. Note that the gravitational waves $h_+(r)\exp ik_{\rm gw}(r-t)$ are also treated in the geometric optics approximation as a field living on a flat space-time background, neglecting the curvature due to the neutron star and the (largely magnetic) energy density in the wind. The GW amplitude is estimated from the total energy released by the merger in GW at a distance from the source where we are in the far field approximation, such that the GW can be treated as linear, plane wave space-time perturbations. The GW amplitude then falls off as $1/r$ and we can scale it such that $h_+(r) = h_{\rm lc} R_{\rm lc}/r$.

Finally, the linear growth of the excited MSW perturbation in (5.51a) can be generalized to the inhomogeneous jet by considering growth over single *scale heights* $\mathcal{H}$ (see (5.55)). Putting all of this together, we find

$$\frac{B_\phi^{(1)}(r)}{B_\phi^{(0)}(r)} \simeq \frac{h_{\rm lc} k_{\rm gw} R_{\rm lc}}{\gamma_\beta^2} {\rm e}^{ik_{\rm gw}(r-t)} \tag{5.52a}$$

$$= \Psi_I {\rm e}^{ik_{\rm gw}(r-t)} , \tag{5.52b}$$

where the interaction factor Ψ_I is now a constant determined by (5.52a) and the dependence of $B_\phi^{(1)}$, $B_\phi^{(0)}$ on r will be determined in the next sections.

Note that because the GW and the MSW both have essentially the same dispersion relation, and the energy flux, $S_1 c B_{\rm mhd}^2/(4\pi)$, through each surface S_1 (as in Fig. 5.4) is a constant because of (5.52b), both waves can propagate in phase and interact coherently over a long distance even in the non-uniform background.

[9] We assume a time-independent background, but one can obviously also use the eikonal approximation on a time-dependent background when the period of the waves is small compared to the time scale of variations in the background.

Magnetic field configuration

The morphology of the 'pulsar' wind in which the GW–MSW interaction and the subsequent inverse Compton scattering take place, is fully determined by the magnetic field geometry since the particles are 'frozen' to the field lines. We assume that the wind is steady and has a constant bulk velocity v_x, the magnetic field is axially symmetric and force-free, and we use the fact that the field is solenoidal.

For such a field, the *toroidal* component follows from the torque free condition as $RB_\phi = \text{const.}$ along each field line (Lüst and Schlüter 1954), where (R, ϕ, x) denote cylindrical coordinates. Note that because of (5.52), the discussion in this section is valid for both B^0_ϕ and $B^1_\phi \propto B^0_\phi$ and we will omit the superscripts to avoid clutter.

The *poloidal* magnetic field B_p through any flux tube cross-section ΔS must be proportional to the particle flux through ΔS because of flux conservation and the constant flow velocity v: $B_p \Delta S = \text{const.}$, $nv\Delta S = \text{const.}$, and thus $B_p \propto n$. In particular, we will assume that the particle and (poloidal) magnetic flux through an azimuthal cross-section of the *entire jet* will approximately be conserved (as illustrated in the right Figure 5.4): $B_x S_1 = B_x(\pi R_\mathrm{j}^2) \simeq \text{const.}$

Summarizing, we have

$$B_\phi(R) \propto \frac{1}{R} \ , \quad B_x(R_\mathrm{j}(x)) \propto n(R_\mathrm{j}(x)) \propto \frac{1}{R_\mathrm{j}^2} \ , \tag{5.53}$$

where $R_\mathrm{j}(x)$ is the radius of the jet which is related to the opening angle by $\theta_\mathrm{o}(x) = 2 \arctan R_\mathrm{j}(x)/x$.

Parametrized wind collimation

In Chapters 3–4 and Moortgat and Kuijpers (2005) we have discussed different degrees of collimation of the wind. We can generalize these results by parametrizing the collimation as in Fig. 5.4, such that the radius R_j of the wind as a function of the vertical distance x is given by $R_\mathrm{j} = x^\kappa$. From (5.53) then follow the more useful expressions for the vertical dependence

$$B_\phi \propto x^{-\kappa} \ , \qquad B_x \propto x^{-2\kappa} \ , \tag{5.54a}$$

$$n \propto x^{-2\kappa} \ , \qquad V = \int \pi R^2 dx \propto x^{2\kappa+1} \ . \tag{5.54b}$$

We can define a scale-height $\mathcal{H}$ (as in Section 5.7) by the distance over which the toroidal magnetic field falls off to half its strength:

$$\frac{B_\phi(x+\mathcal{H})}{B_\phi(x)} = \tfrac{1}{2} \quad \Rightarrow \quad \mathcal{H} \equiv (2^{\frac{1}{\kappa}} - 1)x \ . \tag{5.55}$$

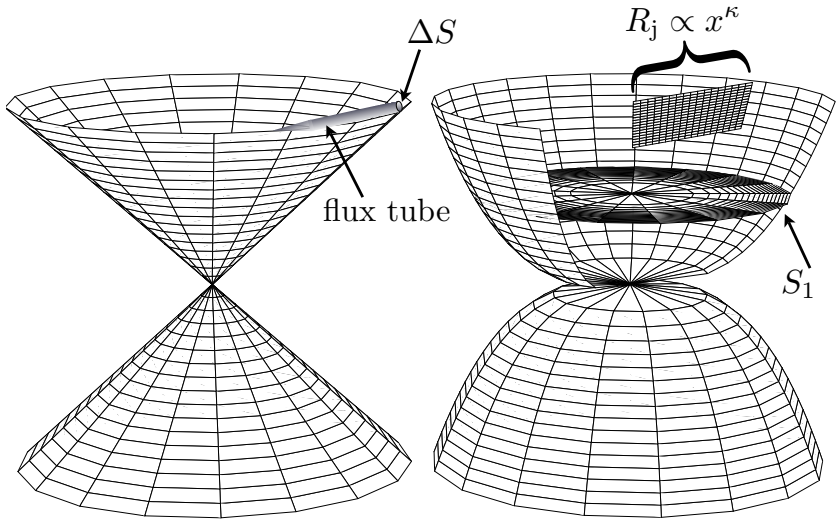

Figure 5.4: Wind collimation by the magnetic field for $\kappa = 1$ (left) and $\kappa = \frac{1}{3}$ (right).

$\kappa = 1$

In Chapter 3 we assumed a wide conical wind with $\kappa = 1$ (see also Kuijpers (2001b)) as depicted in Figure 5.4 (left) which has

$$B_\phi \propto \frac{1}{r} \ , \quad B_x \propto \frac{1}{r^2} \ , \tag{5.56a}$$

$$W_M \propto \frac{1}{r^2} \ , \quad V \propto r^3 \ , \tag{5.56b}$$

with the radial distance $r = \sqrt{R^2 + x^2} \simeq x$. The volume integrated energy increases linearly with the interaction length-scale set by the scale-height $\mathcal{H} = r$ from (5.55). We will only consider the energy deposited in the last scale-height of the force-free wind, as the radiation will escape most easily there.

For a magnetar strength surface magnetic field of $B_\star \sim 10^{12}$ T, a millisecond orbit, a Lorentz factor of $\gamma_\beta \sim 100$, a GW amplitude $h_{\rm lc} = 10^{-3} R_{\rm lc}/r$ and $R_{\rm max} \sim 10^{14}$ m we find that the total energy transferred from the GW to the MSW in the plasma is

$$W_{\rm tot}(\kappa = 1) = \int_{R_{\rm max}-\mathcal{H}}^{R_{\rm max}} W_M(r) \pi r^2 \ dr \sim 10^{35} \text{ J} \ . \tag{5.57}$$

$\kappa = \frac{1}{2}$

In Moortgat and Kuijpers (2005) we made a numerical estimate of the power density in inverse Compton scattered radiation by neglecting the magnetic field in the scattering process and using Rybicki and Lightman (1979) and (5.50)

$$P_{\rm ic}(r) \simeq c\gamma_\beta^4\beta^2\ \sigma_{\rm T} n(r) W_M(r)\ , \tag{5.58}$$

with γ_β and n the Lorentz factor and particle density of the scattering particles, respectively, and as before, W_M the energy density in incident MSW.

The power in scattered radiation not only depends on the energy density in the MHD waves $W_M(r)$ but also on the density of scattering particles $n(r)$, and the parametrized distance dependence of the inverse Compton power density follows from (5.54) as

$$P_{\rm ic} \propto x^{-4\kappa}\ . \tag{5.59}$$

To obtain a volume integrated power we assumed in Moortgat and Kuijpers (2005) a collimation parameter of $\kappa = 1/2$ in which case the spatial dependence in (5.59) is the same $1/r^2$ decay as for the MSW energy density for the $\kappa = 1$ collimation in (5.56b). However, we overestimated the total scattered power by integrating over a spherical shell $\propto r^3$. From (5.54b) and (5.59) we find that for $\kappa = 1/2$ the volume integrated power is a constant and that it increases with distance only for $2\kappa < 1$. Hence, we will next consider a collimation of $\kappa = 1/3$.

$\kappa = \frac{1}{3}$

Clearly, for $\kappa = 1/3$ the magnetic field and hence the MSW energy density remain much higher throughout the wind, but the decrease in integration volume is also significant as can be seen from (5.54b) and (5.59). The total energy deposited in MSW by the GW for the same parameters as in Section 5.7 and over the last scale-height, which is now $\mathcal{H} = 7r$ from (5.55) and with $r = \sqrt{x^2 + R^2} \simeq r$ is

$$W_{\rm tot}(\kappa = \tfrac{1}{3}) = \int_{R_{\rm max}/8}^{R_{\rm max}} W_M(r)\pi r^{\frac{2}{3}}\ dr \sim 10^{28}\ {\rm J}\ . \tag{5.60}$$

Note that from (5.54) and (5.52) it is clear that the volume integrated energy in the MSW *always* increases linearly with distance, which is a consequence of flux conservation and the discussion leading to (5.52) (such that $h\mathcal{H} = {\rm const.}$). If we repeat the estimate in Moortgat and Kuijpers (2005) and integrate (5.58) but now for $\kappa = 1/3$ such that

$$n(r) = \frac{4M\epsilon_0\Omega_b B_{\rm lc}}{e}\left(\frac{R_{\rm lc}}{r}\right)^{\frac{2}{3}}\ , \tag{5.61}$$

derived from the Goldreich-Julian density in terms of the multiplicity $M \sim 10^3$ and orbital frequency Ω_b, and

$$P_{\rm ic,tot} = c\gamma_\beta^4 \, \sigma_{\rm T} \int_{R_{\rm max}/8}^{R_{\rm max}} W_M(r) n(r) \pi r^{\frac{2}{3}} \, dr \sim 10^{36} \text{ W} \, , \tag{5.62}$$

which for a binary merger close enough for a LIGO detection, e.g. in the Virgo cluster at a distance of ~ 1 Gpc, would yield a flux on earth observable by LOFAR. The duration of this kind of transient signal is relatively short: $\Delta t = \mathcal{H}/(2\gamma_\beta^2 c) \approx 15$ sec, but still much longer than the cosmic ray events that LOFAR will also detect.

Unfortunately, we have learned in this Chapter that a more careful analysis including the polarization of the incident and scattered wave modes with respect to the strong ambient magnetic field leads to a strong suppression of the emitted power in the scattered radio waves. We can find a relation similar to (5.62) from (5.49) by considering mono-energetic particles with, say, a Lorentz factor $\gamma_\beta(\beta) \sim 10^2$ and distribution function $g(p_\parallel) = \delta(p_\parallel - m\beta)n/(2\pi m)$. To evaluate the integral over wavelengths in (5.49) we assume that the incident GW and MHD waves are mono-chromatic with $k = k_{\rm gw}$. In comparing (5.62) with (5.49), however, the latter has an additional factor w, the scattering probability, which depends on the small value of (5.47).

In Fig. 5.5 we plot the (non-relativistic) gyro-frequency Ω_c for a pulsar strength magnetic field ($B_\star = 10^8$ T) as a function of the distance in the wind, together with the plasma frequency (middle line) and for comparison a characteristic LOFAR frequency of 100 MHz (bottom line). Although the relativistic gyro- and plasma-frequencies are suppressed by the Lorentz factor, it is clear from Fig. 5.5 that even for $\gamma \sim 10^2$–10^7, the gyro-frequency greatly exceeds the MSW frequency and even the frequency of the scattered waves everywhere in the wind.

Synchrotron radiation

In the discussion so far we have assumed that the ambient magnetic field in the wind is sufficiently strong that any transverse momentum is radiated on a time-scale short to that of the other processes considered. This allowed us to treat the particle distribution function as strictly one-dimensional. However, if the magnetic energy density drops sufficiently, the small gyro-radius approximation in Section 5.4 is not valid anymore. Particles acquire a pitch-angle and synchrotron radiation can become important.

We calculate whether, as the magnetic field drops to its minimum strength, either the radius of curvature of the magnetic field or the MSW wavelength could become comparable to the maximum gyro-radius $r_c(R_{\rm max})$ of particles that acquire some transverse momentum. In the former case, the adiabatic invariant of the particle motion, the magnetic flux through the particles orbit $\pi r_c^2 B^0 = $ const. could be violated.

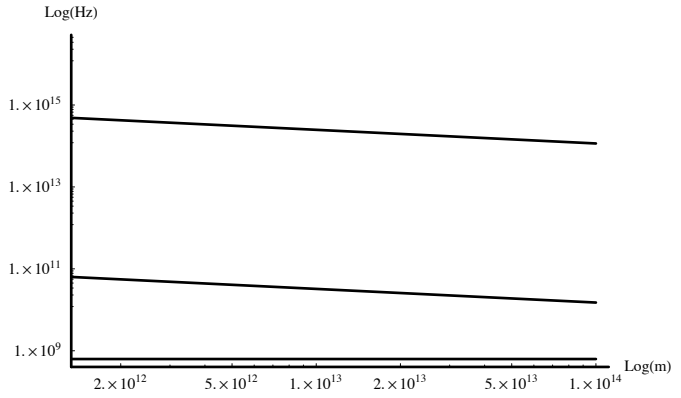

Figure 5.5: Relevant frequencies as a function of distance. Top: (non-relativistic) gyro-frequency; Middle: (non-relativistic) plasma frequency; Bottom: characteristic LOFAR frequency of 100 MHz.

However, we find that even when the particles orbit the magnetic field with relativistic velocity $v_\perp \sim v_\parallel \simeq c$ and corresponding Lorentz factor $\gamma_c \sim 100$, we find

$$r_c(R_{\rm max}) = \frac{\gamma_c c}{\Omega_c} \simeq 0.3\ 10^{-3}{\rm m}\left[\frac{\gamma_c}{100}\right]\left[\frac{B_\star}{10^8\ {\rm T}}\right]^{-1}\ , \tag{5.63}$$

which is clearly much smaller than the curvature radius of the magnetic field (which is proportional to $\mathcal{H}^{1/3}$) and the MSW wavelength $\lambda_{\rm msw} = 2\pi c/\omega_{\rm gw} =$ 150 km.

The smallness of r_c is partly due to the rapid rotation of the source, causing the magnetic dipole field to drop only by a factor ~ 125 from the surface to the light-cylinder. In the wind, the field remains strong because of the force-free condition combined with the collimation. For $\kappa = 1/3$, it only decreases by another factor $\sim 10^3$ in the entire wind and at $R_{\rm max} = 10^{14}$ m the field is still $B_\phi^{(0)}(R_{\rm max}) \sim 0.7\ 10^3$ T. Even for $\kappa = 1$, though, we still have $B_\phi^{(0)}(R_{\rm max}) \sim 0.4\ 10^{-3}$ T and $r_c(R_{\rm max}) \sim 0.4$ km (and now the radius of curvature of the magnetic field is $\propto \mathcal{H} \propto R_{\rm max}$).

The comparison of r_c to the wavelength of the magnetosonic waves is related to the factor (5.47) suppressing the inverse-Compton scattering

$$\frac{r_c(r)}{\lambda_s} = \frac{1}{2\pi}\frac{\gamma_c\omega_s}{\Omega_c}\ . \tag{5.64}$$

Consequently, if the electrons and positrons are initially confined to the

magnetic field lines, it is unlikely that they will acquire transverse momentum and emit synchrotron radiation anywhere in the wind.

5.8 Discussion

Since a strong magnetic field is essential to have efficient interaction between GW and MSW, and millisecond rotation (with a correspondingly tight light-cylinder at $R_{\rm lc} \sim 50$ km) is necessary to have sufficiently large frequencies for the MSW and the scattered waves, $\gamma\omega/\Omega$ will be small throughout the wind. For the range of parameters studied here, frequencies in the LOFAR band never exceed the local relativistic gyrofrequency within the entire extent of the wind.

Furthermore, we know from Chapters 3–4 that GW most efficiently excite purely transverse magneto-acoustic waves, so the scattering channel from a (quasi-)longitudinal to another (quasi-)longitudinal mode, which doesn't suffer from cyclotron suppression, is not a viable alternative. The reason that scattering is suppressed is that the incident MSW does not have an electric field component along the magnetic field, and since the electrons and positrons are assumed to be constrained along the field lines they are unable to oscillate in the applied electric field perturbation.

Given the large amount of energy transferred from the GW to the MSW in the plasma (5.57) it is very likely that some radiation mechanism will produce observable radiation in a higher frequency band. The analysis presented here proves that the simplest possibilities, synchrotron radiation, and inverse Compton scattering of the GW induced MSW into low-frequency radio waves are ineffective. We have yet to find a more viable alternative.

5.9 Conclusions

In this Chapter we have studied the scattering processes in an essentially one-dimensional, intrinsically relativistic, magnetized plasma in some detail with the aim of investigating whether very low-frequency magnetosonic waves excited by a passing GW can scatter off the relativistic electrons and positrons in the wind to produce radio emission in the frequency regime observable with LOFAR. To treat the highly relativistic system properly, we used the covariant and gauge independent theory of plasma dynamics developed by Gedalin et al. (1998); Melrose et al. (1999); Melrose and Gedalin (1999); Gedalin et al. (2001); Luo and Melrose (2001); Gedalin et al. (2002). This approach also allows clear comparison with our general relativistic MHD wave treatment in Chapters 3–4 of the propagation of gravitational waves through a magnetized plasma. By specifying to the temporal gauge, our results are translated to more familiar vector expressions. To our knowledge, the explicit expressions for the scattering probabilities for inverse Compton scattering in a strongly magnetized, force-free and intrinsically relativistic plasma jet have not been

derived before in the literature. These results are useful as well in the theory of ordinary pulsar winds and the jets of X-ray binaries and active galactic nuclei.

We assumed that the magnetoacoustic waves are excited in a cold, essentially mono-energetic plasma that satisfies the ideal MHD wave condition. As they propagate outwards these waves are assumed to encounter either high energy tails of the particle distribution or, in general, a region with an intrinsically relativistic particle distribution on which they scatter. Since the plasma is strongly magnetized, all momentum transverse to the magnetic field is synchrotron radiated on a short time-scale, and as a result the charged particles are strictly confined to the magnetic field lines. In evaluating the response of the plasma, we therefore average over the relativistic one-dimensional Jüttner-Synge distribution function.

To simplify our results we restrict ourselves to the long wavelength regime with $\omega \ll \Omega_c$, which is justified in Section 5.7. Since the incident magnetosonic waves excited by the GW are strictly transverse to the magnetic field, the scattering probability for all possible scattered modes is found to be suppressed by a factor $(\gamma\omega/\Omega_c)^4$. Thus, inverse Compton scattering of the kHz MSW to ~ 100 MHz radio waves does not seem to be a preferred radiation mechanism for the energy dumped in the plasma by the GW.

The covariant formalism for relativistic plasma dynamics that we have used was developed primarily to study emission mechanisms in pulsar magnetospheres where the dipolar field lines point out almost radially from the polar caps, the charged particles flow out along these field lines and the most interesting scattering processes usually have both the incident and scattered wave vectors almost parallel to the magnetic field. The situation that we have studied is the opposite: in the force-free wind well outside the light cylinder, the magnetic field is dominated by the toroidal component and is essentially perpendicular to the incident and scattered modes of interest (for the observer). For a millisecond pulsar and a slightly collimated wind, the magnetic field is very strong throughout the wind and the particles move along the field lines. Note, however, that the particles have relativistic velocities both in the radial direction and along the magnetic field lines and in the laboratory frame appear to be moving outwards like 'beads on a spiraling wire' predominantly in the radial direction. Consequently, the angle between both the incident and scattered wave vectors and the velocity of the particles along the magnetic field can be quite small in the lab frame (due to relativistic beaming), while they are almost at right angles in the (average) rest frame.

CHAPTER 6

Scalar perturbations in two-temperature cosmological plasmas

J. Moortgat & M. Marklund

submitted to MNRAS

We study the properties of density perturbations of a two-component plasma with a temperature difference on a homogeneous and isotropic background.[1] For this purpose we extend the general relativistic gauge invariant covariant (GIC) perturbation theory to include a multi-fluid with a particular equations of state (ideal gas) and imperfect fluid terms due to the relative energy flux between the two species. We derive closed sets of GIC *vector* and subsequently *scalar* evolution equations. We then investigate solutions in different regimes of interest. In particular, we study long wavelength and arbitrary wavelength Langmuir and ion-acoustic perturbations. The harmonic oscillations are superposed on a Jeans type instability. We find a generalized Jeans criterion for collapse in a two-temperature plasma, which states that the species with the largest sound velocity determines the Jeans wavelength. Furthermore, we find that within the limit for gravitational collapse, initial perturbations in either the total density or charge density lead to a growth in the initial temperature difference. These results are relevant for the basic understanding of the evolution of inhomogeneities in cosmological models.

[1] This paper has been recommended for publication by the referee after implementing some minor changes.

6.1 Introduction

Plasmas and electromagnetic fields are common in our Universe. They play an important role in a diverse setting of astrophysical and cosmological processes. Plasmas may be found, e.g. in stars, accretion disks of rotating black holes, the Earth's ionosphere, and also constitute the intergalactic, interstellar as well as the intrasolar medium. There also are occasions when general relativistic gravity has to be taken into account in conjunction with plasma physics, such as in the close vicinity of the aforementioned rotating black holes. Another prominent example is our Universe, in which the plasma state has over time been more or less prominent. Obviously, in such situations gravitational effects due to general relativity, such as gravitational waves, can not be neglected, and may lead to interesting results.

Moreover, perturbation theory within gravitational physics has always held a special place within physics, due to, e.g. the pioneering work of Jeans, and its relation to the basic question of structure formation. The issue of structure formation is now a mature science and cosmological observations have been taken into the high precision regime by observational tools such as COBE, WMAP, Chandra, and the planned LISA mission The development of new observational instruments also calls for new theoretical models and concepts to be tested, in order to refine the current standard model of cosmology. Thus, there is ample interest in extending the existing models by including other physical effects.

In perturbation theory there are two main distinct schools of thought. The first could be described as *metric based* and follows from a seminal paper by Bardeen (1980) which was extended to multi-fluids by Kodama and Sasaki (1984) and developer further in a more recent paper by Malik and Wands (2005). The second paradigm is a *covariant and gauge-invariant perturbation theory* due to Hawking (1966) and Ellis and Bruni (1989) (for reviews see Ellis (1995) or Ellis and van Elst (1999b)), which was extended to multifluids in Dunsby et al. (1992); Marklund et al. (2000, 2003); Betschart et al. (2004) and applied to the cosmic microwave background (CMB) by Challinor and Lasenby (1998). The equivalence of the two theories has been shown in Dunsby et al. (1992).

We will adopt the second approach because the physical quantities defined as gauge invariant and covariant (GIC) variables are not only convenient mathematically, because they avoid spurious non-physical gauge modes, but also clearly reflect the physical quantities that an observer would measure and these variables allow a clear geometrical interpretation. In this paper we will apply the theory to a two-component, two-temperature plasma in a cosmological setting. In particular, we assume that the two plasmas each satisfy the perfect gas law, but with different temperatures. We formulate the set of governing equations for the plasma dynamics on a general relativistic background. These equations are analysed by perturbing the two-fluid model around an isotropic and homogeneous background using the covariant gauge invariant approach. Applications of the results are discussed.

6.2 Gauge invariant covariant theory

To make this Chapter more self-consistent we will recapitulate some of the results in the literature that we use here and make the appropriate approximations to linear perturbations.

$3+1$ split

To start with, we will consider two perfect fluid species that flow in a curved space-time. Both in an astrophysical and a cosmological context it is often possible to identify a preferred family (congruence) of *fundamental world lines* associated with the motion of typical observers. In the former case, one could for example choose the world lines of observers that move with the bulk velocity of the matter in a (relativistic) plasma wind or jet associated with a pulsar or active galactic nucleus. In cosmology it is customary to treat the Universe as consisting of a perfect fluid whose world lines are determined by the motion of distance clusters of galaxies with respect to an observer.

When such fundamental word lines can be identified, it is possible and convenient to split 4-dimensional space-time into 'time' and 'space' again with respect to 4-velocity vector field tangent to the world lines

$$u^a = \frac{dx^a}{d\tau} \quad \Rightarrow \quad u^a u_a = -1 \ , \tag{6.1}$$

where τ is the proper time along the world lines. The tensors that project onto u^a and into the tangent 3-spaces orthogonal to u^a are given, respectively, by

$$U^a_{\ b} \equiv -u^a u_b \quad \text{and} \quad h_{ab} \equiv g_{ab} + u_a u_b \ . \tag{6.2}$$

Associated with the 3+1 split are two derivatives. The 'time derivative' is the covariant derivative along the fundamental world-lines and the 'spatial derivative' is the covariant derivative of any tensor, where all the indices are projected on the hypersurface orthogonal to u^a. For an arbitrary tensor $T^{ab}_{\ \ cd}$ these are defined by

$$\dot{T}^{ab}_{\ \ cd} = u^e \nabla_e T^{ab}_{\ \ cd} \ , \tag{6.3a}$$

$$\tilde{\nabla}_e T^{ab}_{\ \ cd} = h^a_{\ f} h^b_{\ g} h^p_{\ c} h^q_{\ d} h^r_{\ e} \nabla_r T^{fg}_{\ \ pq} \ . \tag{6.3b}$$

The derivative $\tilde{\nabla}$ is a proper 3-dimensional derivative if and only if the vorticity of u^a is zero, for instance in a Friedman-Lemaître-Robertson-Walker (FLRW) Universe (or a FRW Universe when we neglect the cosmological constant).

Multi-fluid stress-energy tensor

We assume a congruence u^a corresponding to fundamental observers as defined in Section 6.2 and a Universe filled with a plasma made up of two species that

are allowed to move in arbitrary directions with respect to the observer with individual (non-relativistic) 4-velocities satisfying

$$u^a_{(i)} = u^a + v^a_{(i)} \ . \tag{6.4}$$

The index $i = 1, 2$ or $i = +, -$ labels the two fluids. Each species is assumed to be a *perfect fluid* in its own rest frame. Then $u^a_{(i)}$ is the *unique* hydrodynamical 4-velocity that is time-like and allows a split of the energy-momentum tensor in the perfect fluid form[2]

$$T^{ab}_{(i)} = \mu_{(i)} u^a_{(i)} u^b_{(i)} + p_{(i)} h^{ab} \ . \tag{6.5}$$

Here $p_{(i)}$ is the pressure and $\mu_{(i)}$ the energy density and for a perfect fluid $u^a_{(i)}$ is also parallel to the particle and entropy flux, such that

$$N^a_{(i)} = n_{(i)} u^a_{(i)} \ , \quad S^a_{(i)} = s_{(i)} u^a_{(i)} \ , \tag{6.6}$$

and there is neither a particle drift nor an energy flux ($J^a_{(i)} = q^a_{(i)} = 0$, $n_{(i)}$ the number density and $s_{(i)}$ the entropy).

In the frame of the fundamental observers u^a, which in general will move relative to the rest frame of the individual fluids, the energy-momentum tensor is clearly different from (6.5). In particular it can be written in the general form of an imperfect fluid. Eq. (6.4) defines the *velocity* $v^a_{(i)}$ of the fluid i with respect to the observer u^a. If we assume that in the background all species share the same hydrodynamical 4-velocity u^a then $v^a_{(i)} = 0$ in the background and is therefore gauge invariant by the lemma of Stewart and Walker (1974).

We linearize the stress-energy tensor for non-relativistic deviations from the average flow such that $v^a_{(i)} \ll 1$ and the anisotropic pressure is negligible, but to linear order there is a contribution to the energy flux, or heat, given by $q^a_{(i)} \equiv (\mu_{(i)} + p_{(i)}) v^a_{(i)}$ such that

$$T^{ab}_{(i)} = \mu_{(i)} u^a u^b + p_{(i)} h^{ab} + 2 u^{(a} q^{b)}_{(i)} \ , \tag{6.7}$$

which are the linearized equivalents of Eqs. (3-4) in Marklund et al. (2003).

Equation of state

In this Chapter we will use a particular equation of state to study temperature effects in a two-component plasma by a first order perturbation analysis on a FRW background. We assume a ideal gas equation of state for each species and corresponding energy density and enthalpy $h_{(i)}$:

$$p_{(i)} = k_B n_{(i)} T_{(i)} \ , \tag{6.8a}$$

$$\mu_{(i)} = \left(m_{(i)} + \tfrac{3}{2} k_B T_{(i)} \right) n_{(i)} \ , \tag{6.8b}$$

$$h_{(i)} = \mu_{(i)} + p_{(i)} = \left(m_{(i)} + \tfrac{5}{2} k_B T_{(i)} \right) n_{(i)} \ , \tag{6.8c}$$

[2] This is the u^a_E 4-velocity in Dunsby et al. (1992).

where $T_{(i)}$ is the temperature, $m_{(i)}$ the rest mass, and k_B Boltzmann's constant. We will allow for different temperatures between the species, and note that $T_{(i)}$ is time-dependent in the background FRW space-time. Moreover, we will re-scale $k_B T_{(i)} \to T_{(i)}$ for the sake of brevity.

Conservation of particles, energy and momentum

Conservation of energy and momentum is guaranteed automatically by the twice-contracted Bianchi identities and Einstein's field equations and is given for each fluid by

$$\nabla_b T^{ab}_{(i)} = \mu_0 F^a{}_b j^b_{(i)} \ , \tag{6.9}$$

where $T^{ab}_{(i)}$ is the stress-energy tensor for the matter and the right-hand-side follows from the electromagnetic part by $\nabla_b T^{ab}_{\mathrm{em},(i)} = -\mu_0 F^a{}_b j^b_{(i)}$ with $j^b_{(i)}$ the 4-current density. Similarly, conservation of number density of particles is given by $\nabla_a N^a_{(i)} = 0$.

The time-like and space-like projections (6.2) of (6.9) provide separate linearized equations for energy and momentum conservation, respectively (Marklund et al. 2000)

$$\dot{\mu}_{(i)} = -h_{(i)}(\Theta + \tilde{\nabla}_a v^a_{(i)}) \ , \tag{6.10a}$$

$$h_{(i)}(\dot{u}^a + \dot{v}^{\langle a\rangle}_{(i)}) = -\tilde{\nabla}^a p_{(i)} - (\tfrac{\Theta}{3} h_{(i)} + \dot{p}_{(i)}) v^a_{(i)} + \rho_{(i)} E^a \ , \tag{6.10b}$$

where Θ is the expansion, $\rho_{(i)} = q_{(i)} n_{(i)}$ is the charge density and E^a the electric field strength.

A separate evolution equation for the temperature can be found from combining (6.8b) and (6.10a) with the linearized equation of particle conservation:

$$\dot{n}_{(i)} = -(\Theta + \tilde{\nabla}_a v^a_{(i)}) n_{(i)} \ , \tag{6.11a}$$

$$\dot{T}_{(i)} = -\tfrac{2}{3}(\Theta + \tilde{\nabla}_a v^a_{(i)}) T_{(i)} \ . \tag{6.11b}$$

Expansion

The basic equation for gravitational attraction is the *Raychaudhuri* equation that in a FRW Universe with vanishing acceleration, shear, vorticity and cosmological constant[3] reduces to

$$\dot{\Theta} = -\frac{\Theta^2}{3} - \frac{\kappa}{2}(\mu + 3p) \ , \tag{6.12}$$

illustrating that $\mu + 3p$ is the active gravitational mass density of the plasma (with $\kappa = 8\pi G/c^4$). The volume rate of expansion $\Theta = \tilde{\nabla}_a u^a$ is the trace of

[3] All equations can easily be generalised to include a cosmological constant, but for simplicity we will specify to a FRW Universe.

the covariant derivative of u^a and is related to the Hubble parameter H and the scale-factor S by

$$\frac{\dot{S}(t)}{S(t)} = \frac{\Theta}{3} = H \ . \tag{6.13}$$

Electromagnetic field equations

The electromagnetic field is determined by the linearized Maxwell evolution and constraint equations:

$$\dot{E}^{\langle a\rangle} = -\tfrac{2}{3}\Theta E^a + \operatorname{curl} B^a - \mu_0 j^a \ , \tag{6.14a}$$

$$\dot{B}^{\langle a\rangle} = -\tfrac{2}{3}\Theta B^a - \operatorname{curl} E^a \ , \tag{6.14b}$$

$$\tilde{\nabla}_a E^a = \frac{\rho}{\epsilon_0} \ , \tag{6.14c}$$

$$\tilde{\nabla}_a B^a = 0 \ , \tag{6.14d}$$

where $\rho = q_{(1)}n_{(1)} + q_{(2)}n_{(2)}$ and $j^a = q_{(1)}n_{(1)}v^a_{(1)} + q_{(2)}n_{(2)}v^a_{(2)}$ are the total charge density and total 3-current density, respectively, and $q_{(i)}$ is the particle charge.

To be more specific, we will choose species 1 to correspond to protons or positrons with $q_{(1)} = e$ and species 2 to electrons $q_{(2)} = -e$.

Definition of gauge invariant quantities

Since the background space-time is *homogeneous and isotropic*, we require that the electromagnetic fields vanish to zeroth order. This implies that the charge density and current density should vanish and thus $\rho = 0 \Rightarrow n_{(1)} = n_{(2)}$, and $j^a = en(v^a_{(1)} - v^a_{(2)}) = 0 \Rightarrow v^a_{(1)} = v^a_{(2)}$. Because the energy flux should also vanish in the background $q^a = \sum_{(i)}(\mu_{(i)} + p_{(i)})v^a_{(i)} = 0 \Rightarrow v^a_{(1)} = v^a_{(2)} = 0$.

Thus, the only nonzero variables in the background are the expansion Θ, the energy density $\mu_{(i)}$, the number density $N_{(i)}$, and the pressure $p_{(i)}$, or equivalently the temperature $T_{(i)}$. The background evolution of these quantities follows from the zeroth order terms in (6.8a), (6.10a) and (6.11)

$$\dot{\mu}_{(i)} = -\Theta(\mu_{(i)} + p_{(i)}) \ , \tag{6.15a}$$

$$\dot{T}_{(i)} = -\tfrac{2}{3}\Theta T_{(i)} \ , \tag{6.15b}$$

$$\dot{p}_{(i)} = -\tfrac{5}{3}\Theta p_{(i)} \ . \tag{6.15c}$$

The remaining variables are gauge invariant covariant (GIC) first order perturbations on the FRW background by the lemma in Stewart and Walker (1974). For an extensive physical motivation of using gauge invariant variables that vanish in the (fictitious) background see Bardeen (1980); Ellis and Bruni (1989); Ellis and van Elst (1999b). In the next section we will define GIC variables for all the physical quantities that govern the two fluids separately,

Table 6.1: Variables for the summed and subtracted quantities for the two fluid species.

Total	Differential
$\mu = \mu_{(1)} + \mu_{(2)}$	$\delta\mu = \mu_{(1)} - \mu_{(2)}$
$p = p_{(1)} + p_{(2)}$	$\delta p = p_{(1)} - p_{(2)}$
$h = h_{(1)} + h_{(2)}$	$\delta h = h_{(1)} - h_{(2)}$
$T = T_{(1)} + T_{(2)}$	$\delta T = T_{(1)} - T_{(2)}$
$N = N_{(1)} + N_{(2)}$	$\delta n = n_{(1)} - n_{(2)}$
$V = \frac{1}{2}(v_{(1)} + v_{(2)})$	$\delta v = \frac{1}{2}(v_{(1)} - v_{(2)})$
$M = m_{(1)} + m_{(2)}$	$\delta m = m_{(1)} - m_{(2)}$

and their mutual interactions and derive covariant evolution equations for all these variables.

6.3 Evolution of GIC vector perturbations

We now proceed to find evolution equations for the combined two-fluid as determined by the observers u^a (note that until now this frame is still left arbitrary). To facilitate this we define the variables in Table 6.1.

In terms of the variables in Table 6.1 we can write the first order charge and current densities as:

$$\rho = e\delta n \ , \qquad\qquad j^a = eN\delta v^a \ . \tag{6.16}$$

Or alternatively, the velocity difference can be interpreted as a normalised current density $\delta v^a = j^a/(eN)$ and similarly, the number density difference δn is clearly equivalent to the charge density $\delta n = \rho/e$.

The evolution equations for the density and temperature variables (with $\delta T \neq 0$ in the background) follow from (6.11) and (6.15b):

$$\frac{\dot{\delta n}}{N} = -\Theta\frac{\delta n}{N} - \tilde{\nabla}_a\delta v^a, \tag{6.17a}$$

$$\frac{\dot{N}}{N} = -\Theta - \tilde{\nabla}_a V^a, \tag{6.17b}$$

$$\frac{\dot{\delta T}}{T} = -\tfrac{2}{3}(\Theta + \tilde{\nabla}_a V^a)\frac{\delta T}{T} - \tfrac{2}{3}\tilde{\nabla}_a\delta v^a \ , \tag{6.17c}$$

$$\frac{\dot{T}}{T} = -\tfrac{2}{3}(\Theta + \tilde{\nabla}_a V^a) - \tfrac{2}{3}(\tilde{\nabla}_a\delta v^a)\frac{\delta T}{T} \ . \tag{6.17d}$$

Similarly, we find the total momentum conservation equation by summing (6.10b) over the two species

$$h\dot{u}^a = -\tilde{\nabla}^a p - \tfrac{4}{3}\Theta q^a - \dot{q}^{\langle a\rangle} \ , \tag{6.18}$$

while subtracting (6.10b) yields

$$\begin{aligned} \delta h\dot{V}^{\langle a\rangle} + h\dot{\delta v}^{\langle a\rangle} &= -(\tfrac{\Theta}{3}\delta h + \delta\dot{p})V^a - (\tfrac{\Theta}{3}h + \dot{p})\delta v^a \\ &\quad - \delta h\ \dot{u}^a - \tilde{\nabla}^a\delta p - \delta\rho E^a \ . \end{aligned} \tag{6.19}$$

Frame choice

From hereon it will be convenient to specify to a particular observer frame u^a. Customary choices are either the *particle frame* in which to linear order $\sum n_{(i)}v_{(i)} = NV^a = 0$ such that the total velocity perturbation with respect to the observer always vanishes, or the *energy frame* in which $q^a = \sum h_{(i)}v_{(i)} = hV^a + \delta h\delta v^a = 0$.

Both are useful in eliminating either V^a or δv^a. In the particle frame, this relation is particularly simple with $V^a = 0$ and $\delta v = v_{(1)} = v_{(2)}$. However, requiring the total velocity perturbation to vanish when studying wavelength dependent perturbations in the total density, for instance, doesn't seem like an obvious frame choice. Choosing the energy frame means that the acceleration is driven only by pressure gradients: $h\dot{u}^a = -\tilde{\nabla}^a p$ from the total momentum equation (6.18). The relation $V^a = \delta v^a(\delta h/h)$ is convenient in a cold plasma when $h_{(i)} = m_{(i)}n_{(i)}$ and $\delta h/h$ is time independent. In our case, however, when the pressure contributes to the energy density, this coefficient has a complicated temporal dependence and doesn't really simplify the calculations.

In this Chapter we therefore prefer to choose the *geodesic frame* of freely-falling observers such that $\dot{u}^a = 0$ (and $q^a \neq 0$). The corresponding 4-velocity is covariantly defined and reduces to the perfect fluid flow velocity of the fundamental observers in the background. Therefore the GI variables defined by gradients orthogonal to the fluid flow are properly defined and the geodesic frame is a valid choice.

One could interpret (6.18) as defining δv^a as a function of V^a and eliminate V^a in favour of δv^a in (6.19) to get an equation similar to those in the energy frame. Rather, we treat (6.18) and (6.19) on equal footing as two coupled differential equation for the total velocity and the normalised current density. By eliminating $\dot{p}$ and $\delta\dot{p}$ using (6.15c), we find from (6.18) and (6.19) the (almost) symmetrical relations

$$\begin{aligned} h\dot{V}^{\langle a\rangle} + \delta h\dot{\delta v}^{\langle a\rangle} &= -\tfrac{\Theta}{3}(\mu - 4p)V^a - \tfrac{\Theta}{3}(\delta\mu - 4\delta p)\delta v^a \\ &\quad - \tilde{\nabla}^a p \ . \end{aligned} \tag{6.20a}$$

$$\begin{aligned} \delta h\dot{V}^{\langle a\rangle} + h\dot{\delta v}^{\langle a\rangle} &= -\tfrac{\Theta}{3}(\delta\mu - 4\delta p)V^a - \tfrac{\Theta}{3}(\mu - 4p)\delta v^a \\ &\quad - \tilde{\nabla}^a\delta p - \delta\rho E^a \ . \end{aligned} \tag{6.20b}$$

Table 6.2: GIC dimensionless comoving scalar variables.

Total	Differential
$X^a = S\frac{\tilde{\nabla}^a N}{N}$	$x^a = S\frac{\tilde{\nabla}^a \delta n}{N}$
$Y^a = S\frac{\tilde{\nabla}^a T}{T}$	$y^a = S\frac{\tilde{\nabla}^a \delta T}{T}$
$W^a = S\tilde{\nabla}^a\tilde{\nabla}_b V^b$	$w^a = S\tilde{\nabla}^a\tilde{\nabla}_b \delta v^b$
$Z^a = S\tilde{\nabla}^a\Theta$	

The above equations are clearly GIC since $V^a, \delta v^a, \tilde{\nabla}^a p, \tilde{\nabla}^a \delta p$ and E^a all vanish in the background (implying that all the coefficients in (6.20) should be evaluated in the background).

Definition of GIC vector quantities

It is argued in Ellis and Bruni (1989) that the physically relevant variables characterizing the spatial variation of scalar quantities that do not vanish in the background (such as the energy density) are the *dimensionless comoving fractional spatial gradients* of those quantities. In particular, we define GIC variables for the density, temperature, expansion and velocity perturbations in Table 6.2.

The variables such as X^a are the quantities that a typical observer would measure. For instance, at a particular time one can measure the comoving gradient in the number density (with respect to the length-scale given by the background scale-factor S) by simply counting the number of distant galaxies or clusters of galaxies at each distance (obviously, sources closer to us like those in our own galaxy do not follow the 'cosmic fluid' and are neither homogeneous nor isotropic). Other choices like $\delta\mu/\mu$ comparing the perturbed energy density with its background value depend on the fictitious background and are gauge dependent to the extent that some perturbations can be eliminated by a choice of gauge and the distinction between physical modes and spurious gauge modes can be obscured.

The velocity variables such as $\tilde{\nabla}^a(\tilde{\nabla}_b V^b)$ might be interpreted as the gradient of some kind of fluid compression, but in this Chapter will be treated simply as auxiliary variables needed to couple (6.20) to (6.17).

Evolution of GIC vector perturbations

To obtain GIC evolution equations for vector perturbations in the total and relative densities and temperatures and the expansion we take the comoving gradients of (6.17) which conveniently commute with the time derivative (this follows from the commutation relations (A.14) and the definition (6.13)). The

expansion terms proportional to Θ in (6.17) are absorbed by choosing dimensionless variables. For example from (6.17a) and (6.17b) we find (to linear order):

$$\left(\frac{\delta n}{N}\right)^{\cdot} = \frac{\delta \dot{n}}{N} + \Theta \frac{\delta n}{N} \ .$$

The resulting GIC evolution equations for the vector quantities in Table 6.2 are

$$\begin{aligned}
\dot{X}^{\langle a\rangle} &= -[W^a + Z^a] \ , && (6.21a)\\
\dot{x}^{\langle a\rangle} &= -w^a \ , && (6.21b)\\
\dot{Y}^{\langle a\rangle} &= -\tfrac{2}{3}[W^a + \alpha w^a + Z^a] \ , && (6.21c)\\
\dot{y}^{\langle a\rangle} &= -\tfrac{2}{3}[\alpha W^a + w^a + \alpha Z^a] \ , && (6.21d)\\
\dot{Z}^{\langle a\rangle} &= -\tfrac{2}{3}\Theta Z^a - \tfrac{\kappa MN}{4}\left[\tfrac{9}{2}\bar{T}Y^a\right. \\
&+ \left.\left(1+\tfrac{9}{2}\bar{T}\right)X^a + \left(\bar{m}+\tfrac{9}{2}\alpha\bar{T}\right)x^a\right] \ , && (6.21e)
\end{aligned}$$

where $\bar{m} = \delta m/M$, $\bar{T} = T/M$ and $\alpha = \delta T/T$. Note that (6.21) are still valid in any observer frame u^a and also that α is constant in the background.

We define $\Omega^a = \mathrm{curl}V^a$, $\omega^a = \mathrm{curl}\delta v^a$, and $\mathcal{C}^a = \mathrm{curl}E^a$ and take the curl of (6.20). The pressure gradients vanish and using (A.14) we find

$$\begin{aligned}
h\dot{\Omega}^a + \delta h\dot{\omega}^a &= \Theta\left[(p-\tfrac{2}{3}\mu)\Omega^a + (\delta p - \tfrac{2}{3}\delta\mu)\omega^a\right] \ , && (6.22)\\
h\dot{\omega}^a + \delta h\dot{\Omega}^a &= \Theta\left[(p-\tfrac{2}{3}\mu)\omega^a + (\delta p - \tfrac{2}{3}\delta\mu)\Omega^a\right] + eN\mathcal{C}^a \ .
\end{aligned}$$

The curl-free part of the velocity perturbations follows from taking the divergence of (6.20) and eliminating $\tilde{\nabla}_a E^a$ in favor of a charge density perturbation and the background plasma frequency

$$\omega_p^2 = \sum_{(i)} \omega_{p,(i)}^2 = \frac{e^2}{\epsilon_0}\left(\frac{n_{(1)}}{m_{(1)}} + \frac{n_{(2)}}{m_{(2)}}\right) = \frac{e^2 N}{\epsilon_0 M}\frac{2}{1-\bar{m}^2} \ . \qquad (6.23)$$

More important though is the gradient of the resulting equations, which yields the equations for W^a and w^a that couple back to the density and temperature perturbations (6.21). These GIC auxiliary velocity variables evolve as:

$$\begin{aligned}
&h\dot{W}^{\langle a\rangle} + \delta h\dot{w}^{\langle a\rangle} = \\
&-\tfrac{NT}{2}\left[\tilde{\nabla}^2 + \tfrac{2}{9}(\Theta^2 - 3\mu)\right][X^a + Y^a + \alpha x^a] \qquad (6.24a)\\
&-\Theta\left[\left(\tfrac{2}{3}\mu - p\right)W^a + \left(\tfrac{2}{3}\delta\mu - \delta p\right)w^a\right] \ ,
\end{aligned}$$

and

$$h\dot{w}^{\langle a\rangle} + \delta h\dot{W}^{\langle a\rangle} = (1-\bar{m}^2)\tfrac{NM\omega_p^2}{2}x^a$$
$$-\frac{NT}{2}\left[\tilde{\nabla}^2 + \tfrac{2}{9}(\Theta^2 - 3\mu)\right][\alpha X^a + y^a + x^a]$$
$$-\Theta\left[\left(\tfrac{2}{3}\mu - p\right)w^a + \left(\tfrac{2}{3}\delta\mu - \delta p\right)W^a\right] \ , \tag{6.24b}$$

where we have used (6.14c), the commutation relations (A.14) and

$$\tilde{\nabla}^a p = \frac{NT}{2}(X^a + \alpha x^a + Y^a) \ , \tag{6.25a}$$
$$\tilde{\nabla}^a \delta p = \frac{NT}{2}(\alpha X^a + x^a + y^a) \ . \tag{6.25b}$$

GIC electromagnetic equations

To investigate how the velocity perturbations couple to the electromagnetic field we need the solenoidal part of (6.20b), which couples to $\dot{B}^a$ through (6.14b) and the curl-free scalar part which through (6.14c) couples to the plasma frequency (6.23).

From the constraint (6.14c) and (6.21b) we trivially find an evolution equation related to the curl free part of the electric field in terms of $S\tilde{\nabla}^a(\tilde{\nabla}_b E^b) \equiv \mathcal{E}^a = eNx^a/\epsilon_0$

$$\dot{\mathcal{E}}^{\langle a\rangle} = -\frac{eN}{\epsilon_0}w^a \ . \tag{6.26}$$

From Maxwell's equations, we find (in agreement with Tsagas (2005)) the wave equations to linear order

$$\ddot{E}^{\langle a\rangle} - \tilde{\nabla}^2 E^a = \tfrac{1}{3}(\mu + 3p)E^a - \tfrac{5}{3}\Theta\dot{E}^{\langle a\rangle} - \tfrac{4}{9}\Theta^2 E^a$$
$$-\frac{e}{\epsilon_0}\tilde{\nabla}^a\delta n - \mu_0 eN\dot{\delta v}^{\langle a\rangle} \ , \tag{6.27a}$$
$$\ddot{B}^{\langle a\rangle} - \tilde{\nabla}^2 B^a = \tfrac{1}{3}(\mu + 3p)B^a - \tfrac{5}{3}\Theta\dot{B}^{\langle a\rangle} - \tfrac{4}{9}\Theta^2 B^a$$
$$+\mu_0 eN\omega^a \ . \tag{6.27b}$$

The expansion normalised curl of the electric field $\mathcal{C}^a = S\,\mathrm{curl}\,E^a$ satisfies the wave equation

$$\ddot{\mathcal{C}}^{\langle a\rangle} - \tilde{\nabla}^2\mathcal{C}^a + \tfrac{5}{3}\Theta\dot{\mathcal{C}}^{\langle a\rangle} = \tfrac{1}{3}(\mu + 3p - \tfrac{4}{3}\Theta^2)\mathcal{C}^a$$
$$-\mu_0 eN\left[\dot{\omega}^{\langle a\rangle} + \tfrac{\Theta}{3}\omega^a\right], \tag{6.28}$$

from (6.27a) and (A.14).

The evolution equation derived in this section together with the constraints completely determine the behaviour of GIC vector perturbations of the two-temperature plasma. Here we will focus on scalar perturbations. In the next section we will derive the corresponding evolution equations.

Table 6.3: Gauge invariant scalar expansion normalized variables.

Total	Differential
$\Delta = S^2\frac{\tilde{\nabla}^2 N}{N}$	$\delta = S^2\frac{\tilde{\nabla}^2\delta n}{N}$
$\Gamma = S^2\frac{\tilde{\nabla}^2 T}{T}$	$\gamma = S^2\frac{\tilde{\nabla}^2\delta T}{T}$
$\mathcal{W} = S^2\tilde{\nabla}^2\tilde{\nabla}_b V^b$	$\mathcal{V} = S^2\tilde{\nabla}^2\tilde{\nabla}_b\delta v^b$
$\zeta = S^2\tilde{\nabla}^2\Theta$	

6.4 GIC scalar perturbations

The easiest way to obtain a closed set of differential equations for scalar perturbations of the two-temperature plasma is to take the divergence of the vector equations derived in the previous section. The resulting GIC expansion normalised dimensionless variables are summarised in Table 6.3.

Since the comoving divergence again commutes with the time derivative, the scalar equations look very similar to (6.21). All the coefficients have to be zeroth order and it is more illustrative to re-write those in terms of the background quantities N, T, $\rho_m = MN/2$ etc. The resulting evolution equations are

$$\dot{\Delta} = -[\mathcal{W}+\zeta]\ , \tag{6.29a}$$

$$\dot{\delta} = -\mathcal{V}\ , \tag{6.29b}$$

$$\dot{\Gamma} = -\tfrac{2}{3}[\mathcal{W}+\alpha\mathcal{V}+\zeta] = \tfrac{2}{3}[\alpha\dot{\delta}+\dot{\Delta}]\ , \tag{6.29c}$$

$$\dot{\gamma} = -\tfrac{2}{3}[\alpha\mathcal{W}+\mathcal{V}+\alpha\zeta] = \tfrac{2}{3}[\alpha\dot{\Delta}+\dot{\delta}]\ , \tag{6.29d}$$

$$\dot{\zeta} = -\tfrac{2}{3}\Theta\zeta - \tfrac{1}{2}\kappa\rho_m\left[\tfrac{9}{2}\bar{T}\Gamma + \left(1+\tfrac{9}{2}\bar{T}\right)\Delta + \left(\bar{m}+\tfrac{9}{2}\alpha\bar{T}\right)\delta\right]\ . \tag{6.29e}$$

In comparing with the non-thermal dust results in Betschart et al. (2004) we find that (6.29b, 6.29a) agree with their (24a,d). For the latter identification one should transform back from the energy frame where $V^a = -\delta v^a\delta\mu/\mu$ was used to eliminate V^a, and instead leave the equation in terms of δv^a. Clearly the equations for the thermal perturbations are new and the evolution equations for the velocity and expansion perturbations are more complicated when including temperature effects.

Harmonic decomposition

In terms of the variables in Table 6.3, the evolution of the scalar velocity variables is found by taking the divergence of (6.24a, 6.24b) using (A.14).[4]

[4]The commutation rule for $\tilde{\nabla}_a\tilde{\nabla}^2$ cancels the factor proportional to the expansion in the previous $\tilde{\nabla}^a\tilde{\nabla}^2$ commutator.

Furthermore, we harmonically decompose the Laplacians in terms of the scalar harmonic functions $Q^{(\ell)}$ that satisfy the Helmholtz equation

$$\tilde{\nabla}^2 Q^{(\ell)} = -\frac{\ell^2}{S^2} Q^{(\ell)} \ , \quad \dot{Q^{(\ell)}} = 0 \ , \quad f = \sum_\ell f_{(\ell)} Q^{(\ell)} \ , \tag{6.30}$$

where f is any perturbation scalar and $f_{(\ell)}$ the corresponding harmonic (Harrison 1967). For the sake of clarity we will drop the index ℓ, as we will not encounter harmonic mixing due to the linearity of the equations. Each evolution equation is understood to represent the temporal behaviour in one harmonic mode ℓ. The *comoving wavelength* of a perturbation is given in terms of the wave-number ℓ by $\lambda(\tau) = 2\pi S(t)/\ell$ where time dependencies are given in terms of $\tau = t/t_0$, the proper time along a world-line normalised to some initial time t_0. The velocity variables then evolve as

$$\left(1 + \tfrac{5}{2}\bar{T}\right)\dot{\mathcal{W}} + \left(\bar{m} + \tfrac{5}{2}\alpha\bar{T}\right)\dot{\mathcal{V}} = \tag{6.31a}$$
$$\frac{\ell^2\bar{T}}{S^2}(\Delta + \alpha\delta + \Gamma) - \tfrac{2}{3}\Theta(\mathcal{W} + \bar{m}\mathcal{V}) \ ,$$
$$\left(1 + \tfrac{5}{2}\bar{T}\right)\dot{\mathcal{V}} + \left(\bar{m} + \tfrac{5}{2}\alpha\bar{T}\right)\dot{\mathcal{W}} = \tag{6.31b}$$
$$\frac{\ell^2\bar{T}}{S^2}(\alpha\Delta + \delta + \gamma) - \tfrac{2\Theta}{3}(\mathcal{V} + \bar{m}\mathcal{W}) + (1 - \bar{m}^2)\omega_p^2\delta \ .$$

Sound velocities

We assume that the background plasma is non-relativistic such that the total thermal energy is small compared to the total rest-mass energy. Consequently, $\bar{T} = T/M \ll 1$ and we will neglect $\bar{T}$ in the gravitational interactions and use $\mu \simeq \mu + p \simeq \rho_m$ in the background.

We define the sound velocity for each species as:

$$c^2_{s,(i)} = \frac{\dot{p}_{(i)}}{\dot{\mu}_{(i)}} \simeq \frac{\dot{n}_{(i)}T_{(i)} + n_{(i)}\dot{T}_{(i)}}{m_{(i)}\dot{n}_{(i)}} = \frac{5}{3}\frac{T_{(i)}}{m_{(i)}} \ , \tag{6.32}$$

using (6.15). We define total and differential sound speeds similar to V^a and δv^a as

$$C_s^2 = \tfrac{1}{2}(c^2_{s,1} + c^2_{s,2}) = \tfrac{5}{3}\bar{T}\left(\frac{1 - \bar{m}\alpha}{1 - \bar{m}^2}\right), \tag{6.33a}$$

$$\delta c_s^2 = \tfrac{1}{2}(c^2_{s,1} - c^2_{s,2}) = \pm\tfrac{5}{3}\bar{T}\left(\frac{\alpha - \bar{m}}{1 - \bar{m}^2}\right), \tag{6.33b}$$

where the sign of (6.33b) is positive when $c^2_{s,1} > c^2_{s,2}$ and negative when $c^2_{s,1} < c^2_{s,2}$. The variable C_s^2 is related to the mass-weighted total sound velocity

$c_s^2 = \sum_{(i)} c_{(i)}^2 \dot{\mu}_{(i)}/\dot{\mu} = 5p/3\mu$ (for our particular equation of state) by

$$C_s^2 = c_s^2 \left(\frac{1 - (\delta\mu/\mu)(\delta p/p)}{1 - (\delta\mu/\mu)^2} \right) = c_s^2 \left(\frac{1 - \bar{m}\alpha}{1 - \bar{m}^2} \right) \ , \tag{6.34}$$

where the second expression follows from the fact that the number densities are the same in the background. In the remainder of this paper it will be apparent that C_s^2 in (6.33a) is a more convenient variable than c_s^2 in (6.34) because the former only depends only on the temperature whereas the latter depends on both the temperature (pressure) and number density. The results will only depend on the (physical) sound speed of one of the two species.

Wave equations

In the non-relativistic limit and using the definitions in the previous section, the evolution equations for the expansion and the auxiliary variables $\mathcal{W}$ and $\mathcal{V}$ are given by

$$\dot{\zeta} + \tfrac{2}{3}\Theta\zeta = -\tfrac{1}{2}\kappa\rho_m \left[\Delta + \bar{m}\delta\right] \ , \tag{6.35a}$$

$$\dot{\mathcal{W}} + \tfrac{2}{3}\Theta\mathcal{W} = \frac{3\ell^2 c_s^2}{5S^2}\left[\Delta + \frac{\delta c_s^2}{c_s^2}\delta + \frac{\Gamma - \bar{m}\gamma}{1 - \bar{m}\alpha}\right] - \bar{m}\omega_p^2\delta \ , \tag{6.35b}$$

$$\dot{\mathcal{V}} + \tfrac{2}{3}\Theta\mathcal{V} = \frac{3\ell^2 c_s^2}{5S^2}\left[\delta + \frac{\delta c_s^2}{c_s^2}\Delta + \frac{\gamma - \bar{m}\Gamma}{1 - \bar{m}\alpha}\right] + \omega_p^2\delta \ , \tag{6.35c}$$

where in this limit the expansion evolution (6.35a) does reduce to equation (24b) in Betschart et al. (2004) for the gravitational attraction of pressure-less dust.

Since we want to study wave-like harmonic perturbations of the density and temperature we take the second time derivative of (6.29a–6.29d) and use the evolution equations (6.35) to eliminate ζ, $\mathcal{V}$ and $\mathcal{W}$ from the second order differential equations for δ, Δ, γ and Γ

$$\ddot{\Delta}(\tau) = -[\dot{\mathcal{W}}(\tau) + \dot{\zeta}(\tau)] \ , \tag{6.36a}$$

$$\ddot{\delta}(\tau) = -\dot{\mathcal{V}}(\tau) \ , \tag{6.36b}$$

$$\ddot{\Gamma}(\tau) = -\tfrac{2}{3}[\dot{\mathcal{W}}(\tau) + \alpha\dot{\mathcal{V}}(\tau) + \dot{\zeta}(\tau)] \ , \tag{6.36c}$$

$$\ddot{\gamma}(\tau) = -\tfrac{2}{3}[\alpha\dot{\mathcal{W}}(\tau) + \dot{\mathcal{V}}(\tau) + \alpha\dot{\zeta}(\tau)] \ . \tag{6.36d}$$

Equivalently, we can simultaneously solve the combined set of first order ordinary differential equations (6.29) and (6.35). The solutions for initial conditions and limiting cases of interest are studied in the next section.

6.5 Solutions

In studying inhomogeneities as perturbations on a FRW Universe filled with an unmagnetized cold dusty plasma we expect the perturbations to behave as eigenmodes of such a plasma altered by the background curvature. We will therefore study the longitudinal Langmuir mode, ion-acoustic oscillations and the gravitational Jeans instability.

General discussion

By examining (6.35) we can make the following observations:

- From (6.35a) we find that an initial perturbation in either the total density *or* the charge density causes a (gravitational) perturbation of the expansion, unless the plasma consists of electrons and positrons with $\bar{m} = 0$ (in which case only a total density perturbation couples to the expansion);
- A perturbation in the charge density corresponds to a longitudinal electric field perturbation (such that $\tilde{\nabla}_a E^a \neq 0$) which enters the equations of motion as a Lorentz force term and excites perturbations in the current density and (unless the plasma is $e^{\pm}$) the total velocity variables. This is expressed in (6.35b–6.35c) in terms of the plasma frequency;
- When the electric field perturbation is unimportant, only the wavelength dependent pressure gradient terms contribute in (6.35b–6.35c). When the sound velocities of the two species are equal in the background, a perturbation in the total density only drives a perturbation in the total velocity, while a perturbation in the charge density only excites a current density perturbation. If the plasma also were $e^{\pm} \Rightarrow \bar{m} = 0$ then (6.35b–6.35c) completely de-couple and we have $\mathcal{W} = \mathcal{W}(\Delta, \Gamma)$ and $\mathcal{V} = \mathcal{V}(\delta, \gamma)$. However, in the general case that we want to investigate in this Chapter where the sound velocities in the background are allowed to differ, a perturbation in the charge density will excite a total velocity perturbation and more interestingly *a total density perturbation will excite a current density* from (6.35c).

The excited modes in ζ, $\mathcal{W}$ and $\mathcal{V}$ derived from (6.35) feed into (6.36), or equivalently (6.29) and we can make some remarks on how they drive perturbations, particularly in the temperature variables.

- The behavior of the temperature variables can be found most readily by integrating the second expressions in (6.29c–6.29d) and setting the integration constants to match the appropriate initial conditions. For a one-temperature background we find that the total temperature is simply proportional to the total density, whereas a temperature difference only couples to a perturbation in the charge density.

- It again is clear from (6.36c–6.36d) that a temperature difference in the background allows for additional coupling between the equations. In particular, a perturbation in the total velocity or the expansion excites perturbations in the temperature difference. For instance, a growing mode in the expansion such as gravitational collapse can lead to a *growing temperature difference*.

This concludes our general discussion of the allowed excitations and couplings of the scalar perturbation variables in a non-trivial background. We now proceed to study some analytical solutions of these differential equations in more detail.

Evolution of the background

In solving the evolution equations for the perturbations we also have to include the evolutions of the coefficients in the background. In the approximation that we introduced in Section 6.4 where the pressure is included in the sound velocity but not in the gravitational mass we can just use the well known evolution of a dust dominated Universe.

The scale factor then evolves as $S(\tau) \propto \tau^{2/3}$ and the dimensionless expansion and gravitational mass as $\Theta = 2/\tau$ from (6.13) and $\kappa MN/4 = \kappa\mu/2 = 2/(3\tau^2)$ from (6.12). The number density, which is hidden in the plasma frequency, evolves as $N/N_0 = \omega_p^2/\omega_{p0}^2 = \tau^{-2}$ from (6.17b, 6.23).

Long wavelength Langmuir modes

The differential equations in the previous section are most readily solved in the long wavelength limit or alternatively the dust limit where $\bar{T} = 0$ everywhere. In both cases the terms proportional to $\bar{T}\ell^2/S^2$ vanish. The exact solutions derived in this section for Δ and δ agree with those in Betschart et al. (2004) (where δ is expressed in $Y = \delta n/N$) but we can now extend these results to include the possible thermal effects.

In this limit the wave equations for the charge density and total number density are

$$\ddot{\delta}(\tau) + \frac{4}{3}\frac{\dot{\delta}(\tau)}{\tau} + \omega_p^2\frac{\delta(\tau)}{\tau^2} = 0 \ , \tag{6.37a}$$

$$\ddot{\Delta}(\tau) + \frac{4}{3}\frac{\dot{\Delta}(\tau)}{\tau} - \frac{2}{3}\frac{\Delta(\tau)}{\tau^2} = \bar{m}[\omega_p^2 + \tfrac{2}{3}]\frac{\delta(\tau)}{\tau^2} \ . \tag{6.37b}$$

The first mode we consider is excited by an initial perturbation in the charge density $\delta(1) = \delta_0$ when all the other perturbations are zero initially. From (6.29) we then find that

$$\dot{\Delta}(1) = \dot{\delta}(1) = \dot{\Gamma}(1) = \dot{\gamma}(1) = 0 \ .$$

The solution of (6.37a) subject to these initial conditions is

$$\delta(\tau) = \delta_0 \tau^{-\frac{1}{6}} \left[\cos(\omega \ln \tau) + \tfrac{1}{6\omega} \sin(\omega \ln \tau)\right] \ , \tag{6.38}$$

where $\omega^2 = \omega_p^2 - 1/36 \simeq \omega_p^2$. This oscillatory solution agrees with Betschart et al. (2004). It is a non-propagating oscillation at the plasma frequency and is similar to the longitudinal Langmuir mode. The solutions are not simple plane waves but a more complicated harmonic oscillation with a decaying ($\tau^{-1/6}$) envelope due to the background expansion and corresponding evolution of the plasma frequency.

On inserting the solution (6.37a) in (6.37b) we can solve for $\Delta(\tau)$ to find

$$\Delta(\tau) = \bar{m}\delta_0 \left(g(\tau) - \frac{\delta(\tau)}{\delta_0} \right) \ , \tag{6.39a}$$

with

$$g(\tau) = \frac{2}{5}\tau^{-1} + \frac{3}{5}\tau^{\frac{2}{3}} \ . \tag{6.39b}$$

The solution (6.39) for the total density perturbation is a superposition of the oscillatory Langmuir mode and the usual growing and decaying (power-law) modes of the standard gravitational instability picture. The growing mode always dominates (since $\tau > 1$) leading to gravitational collapse on all length-scales. This is a well known result for dust since there is no pressure to act as a restoring force.

The temperature perturbations can be found by solving the wave equations (6.36c–6.36d), but even simpler is to integrate the right-most expressions in (6.29c–6.29d) taking care of the initial conditions, i.e.

$$\Gamma(\tau) = \tfrac{2}{3}\delta_0 \left[(\alpha - \bar{m}) \frac{\delta(\tau)}{\delta_0} - (\alpha - \bar{m} g(\tau)) \right] \ , \tag{6.40a}$$

$$\gamma(\tau) = \tfrac{2}{3}\delta_0 \left[(1 - \bar{m}\alpha) \frac{\delta(\tau)}{\delta_0} - (1 - \bar{m}\alpha g(\tau)) \right] \ . \tag{6.40b}$$

From (6.40) we find that in an equal temperature plasma the relative temperature perturbation only fluctuates with the oscillation in the charge density, but by allowing for a temperature difference in the background ($|\alpha| > 0$) the *temperature difference grows as a power-law* during gravitational collapse. Note that from (6.33) $(\alpha - \bar{m}) \propto \delta c_s^2$, so the total temperature perturbation only couples to the charge density oscillation when the two fluids have unequal sound velocities in the background (by comparison $(1 - \bar{m}\alpha) \propto c_s^2$ in (6.40b)).

Gravitationally driven temperature difference

We now study (6.37) in the same long wavelength or dust regime but start with the more common initial condition where the total density rather than

the charge density is perturbed (so $\Delta(1) = \Delta_0$ and all the other perturbations vanish at $t = t_0$). With these initial conditions no perturbation of the charge density is excited and the total density only experiences the continuous gravitational collapse which couples to the temperature variables through the expansion (6.35). The solutions are given in terms of the gravitational mode (6.39b) by

$$\delta(\tau) = 0 , \tag{6.41a}$$
$$\Delta(\tau) = \Delta_0 g(\tau) , \tag{6.41b}$$
$$\gamma(\tau) = \tfrac{2}{3}\alpha\Delta_0(g(\tau) - 1) , \tag{6.41c}$$
$$\Gamma(\tau) = \tfrac{2}{3}\Delta_0(g(\tau) - 1) , \tag{6.41d}$$

and we find from (6.41c) that even in this case *gravitational collapse increases an initial temperature difference* when we start with a perturbation in the total density such as those that are observed in the cosmic microwave background (CMB).

Wavelength dependent perturbations

In treating perturbations of all wavelengths, the system of differential equations becomes substantially more complicated. We therefore specify to perturbations on time-scales that are small compared to the Hubble time such that the scale-factor is approximately constant $S(\tau) \sim S_0 \Rightarrow \Theta = 0$ (or equivalently, the wavelengths are small with respect to the Hubble scale). Consequently, the $\kappa\rho_m/2$ terms vanish because of (6.12) and we can neglect the evolution of the coefficients (N, ω_p and $\bar{T}$) in the background. In this limit, the perturbations locally behave as plane waves and we can solve the system of equations algebraically and derive a dispersion relation.

For the wave equations we find in terms of $k_0 = \ell/S(1)$

$$\omega_f^2\delta = \frac{3k_0^2c_s^2}{5}\left[\delta + \frac{\delta c_s^2}{c_s^2}\Delta + \frac{\gamma - \bar{m}\Gamma}{1 - \bar{m}\alpha}\right] + \omega_p^2\delta , \tag{6.42a}$$
$$\omega_f^2\Delta = \frac{3k_0^2c_s^2}{5}\left[\Delta + \frac{\delta c_s^2}{c_s^2}\delta + \frac{\Gamma - \bar{m}\gamma}{1 - \bar{m}\alpha}\right] - \omega_p^2\bar{m}\delta , \tag{6.42b}$$

and from (6.29) we simply have

$$\Gamma = \tfrac{2}{3}\left[\alpha\delta + \Delta\right] , \tag{6.43a}$$
$$\gamma = \tfrac{2}{3}\left[\alpha\Delta + \delta\right] . \tag{6.43b}$$

A dispersion relation follows readily with solutions:

$$\omega_\pm^2 = k_0^2c_s^2 + \tfrac{1}{2}\omega_p^2\left[1 \pm \sqrt{1 - \frac{4k_0^2|\delta c_s^2|}{\omega_p^2}\left(\bar{m} - \frac{k_0^2|\delta c_s^2|}{\omega_p^2}\right)}\right] .$$

If the ion-acoustic frequency is small compared to the total plasma frequency, we can expand the square-root term in $k_0^2\delta c_s^2/\omega_p^2 \ll 1$ to find

$$\begin{aligned} \omega_-^2 &\simeq k_0^2[c_s^2 + |\delta c_s^2|] = k_0^2 \max(c_{s,1}, c_{s,2})^2 \ , && \text{(6.44a)} \\ \omega_+^2 &\simeq k_0^2[c_s^2 - |\delta c_s^2|] + \omega_p^2 \\ &= k_0^2 \min(c_{s,1}, c_{s,2})^2 + \omega_p^2 \ , && \text{(6.44b)} \end{aligned}$$

which are the *ion-acoustic* and *Langmuir* modes, respectively.

Jeans criterion

To obtain a Jeans length-scale for collapse, the gravitational interaction is clearly essential. Therefore we cannot neglect $\kappa\rho_m$ which means we cannot neglect Θ and $\dot{\Theta}$ so we have to treat the full system of equations. The goal is to study the properties of the wave equation for the total density perturbations and find the critical length-scale distinguishing collapse from oscillatory behavior. From the non-relativistic limit of the expansion equation (6.35a) and (6.36) one realizes that rather than to study perturbations in the total number density Δ, a more physical choice is to study perturbations of the GI normalised density variable

$$\mathcal{D} = \Delta + \bar{m}\delta = S^2 \frac{\tilde{\nabla}^2 \rho_m}{\rho_m} \ , \qquad \text{(6.45)}$$

where $\rho_m = \frac{1}{2}(MN + \delta m \delta n)$ to first order. Furthermore, we have to eliminate the temperature variables Γ and γ from (6.35, 6.36) which is achieved by integrating (6.29) to find

$$\begin{aligned} \Gamma - \bar{m}\gamma &= \tfrac{2}{3}\left[(\alpha - \bar{m})\delta + (1 - \bar{m}\alpha)\Delta\right] \ , && \text{(6.46a)} \\ \gamma - \bar{m}\Gamma &= \tfrac{2}{3}\left[(\alpha - \bar{m})\Delta + (1 - \bar{m}\alpha)\delta\right] \ . && \text{(6.46b)} \end{aligned}$$

Putting all of this together, we find

$$\ddot{\mathcal{D}} + \tfrac{2}{3}\Theta\dot{\mathcal{D}} + \left[\frac{\ell^2}{S^2}(c_s^2 + \bar{m}|\delta c_s^2|) - \tfrac{1}{2}\kappa\rho_m\right]\mathcal{D} = \frac{\ell^2}{S^2}(1 - \bar{m}^2)|\delta c_s^2|\delta \ . \qquad \text{(6.47)}$$

We assume that the term on the right-hand-side of the equation is negligible for $\bar{m} \sim 1$. Note also that the plasma frequency dependent terms have dropped out in the equation for $\mathcal{D}$ which can be seen from (6.35, 6.36) or (6.42).

Finding an exact solution of (6.47) is complicated by the fact that all the coefficients are themselves time dependent: $\Theta(\tau)$, $c_s(\tau)$, $\delta c_s(\tau)$, $S(\tau)$ and $\rho_m(\tau)$. However, a general result from differential calculus which in this particular

case is called the *Jeans criterion* states that the solution for $\mathcal{D}$ changes from oscillatory to growing or decaying solutions when the term in square brackets changes sign (which corresponds to the perturbation frequency changing from real to imaginary).

The limiting case is generally expressed as a Jeans wavelength $\lambda_J(\tau) = 2\pi S(\tau)/\ell$ which corresponds to the length-scale at which the plasma becomes unstable to gravitational collapse. For length-scales smaller than λ_J the pressure prevents collapse. For an electron-ion plasma with $\bar{m} \simeq 1$ we find

$$\lambda_J^2 = \frac{\pi}{G\rho_m}(c_s^2 + |\delta c_s^2|) \ , \tag{6.48}$$

which corresponds to a well known result when $\delta c_s = 0$ (see for instance equation (220) in Ellis and van Elst (1999b)). In our more general treatment we find, given (6.33), that in a two-temperature plasma, the Jeans wavelength is determined by the species with the largest sound velocity. Note that, as in Ellis and van Elst (1999b) the Jeans length λ_J is time-dependent.

The corresponding *Jeans mass* is given by

$$M_J = \frac{4\pi\lambda_J^3}{3}\rho_m = \left[\frac{\pi}{G}\right]^{\frac{3}{2}} \frac{4\pi \max(c_{s,1}, c_{s,2})^3}{3}\sqrt{\rho_m} \ . \tag{6.49}$$

The limiting cases discussed in Sections 6.5–6.5 are valid for wavelengths much longer that the Jeans wavelength (6.48).

6.6 Conclusions

In this Chapter we have extended the gauge invariant covariant perturbation theory on curved manifolds to include temperature effects in a multi-fluid that is not in complete thermal equilibrium. We have derived two closed sets of differential equations: one for gauge invariant covariant *vector* quantities in Section 6.3 and one for corresponding *scalar* variables in Section 6.4. The system in Section 6.3 could be the subject of further investigations, but in this Chapter we have focused on studying the behavior of the scalar perturbations.

In the long wavelength limit for a pressure-less plasma we recover the results in Betschart et al. (2004) but we have generalized the treatment to a two-fluid where both species are perfect fluids with an ideal gas equation of state and find that the total temperature and relative temperature perturbations follow the total and charge densities, respectively. If the two fluids furthermore have slightly different temperatures in the background, we find that they also couple to each other. Most interestingly, the temperature difference grows during gravitational collapse. This result applies both to initial perturbations in the charge density and in the total density. We expect that the process of structure formation will be affected by this thermal evolution.

To find propagating oscillatory modes we have included the wavelength dependent behavior but neglected the evolution of the background which allows

us to treat the perturbations as locally plane waves. In this approximation we have algebraically obtained a dispersion relation with eigen-frequency solutions corresponding to Langmuir and ion-acoustic modes.

Finally, in Section 6.5 we have derived a modified Jeans wavelength that includes thermal effects and depends on the sound velocities of the two plasma species. In particular, the length-scale and mass for gravitational collapse are set by the species with the largest sound velocity.

The theoretical framework presented in this Chapter could be used for a more detailed numerical analysis of the perturbations observed in the CMB incorporating thermal effects in a gauge invariant and covariant fashion.

CHAPTER 7

Summary & Conclusions

In this thesis we have contemplated several areas in astrophysics and cosmology where a Newtonian approach to plasma physics is insufficient. Matter in the plasma state makes up most of the (visible) Universe and in many cases a general relativistic treatment of its behavior is essential. In particular we have investigated two important areas:

- the effect of gravitational waves emitted in cataclysmic events such as the merger of two neutron stars on magnetized, relativistic *astrophysical* plasmas;
- the effect of temperature differences in the *cosmological* multi-fluid filling a FLRM Universe, in a general relativistic treatment of structure formation.

The astrophysical application is covered in most detail in Chapters 3–5. First we introduced the astronomical setting of the problem and studied the simplest case of a + polarized GW propagating perpendicular to a uniform magnetic field in Chapters 3. Note that the magnetic field is essential, since a GW does not couple to a perfect fluid to linear order (see Section 4.2).

In Chapter 4 a much more general treatment is presented in which we study a magnetized perfect fluid plasma including the gas pressure, both polarizations of the GW and arbitrary angles of the GW with respect to the ambient magnetic field. The GW are initially treated on the same footing as the plasma perturbations and we solve the Einstein-Maxwell equations self-consistently.

Only after verifying that the back-reaction of the GW on the dispersion relation is negligible under all circumstances where the geometric optics approximation is valid (Section 4.7), do we treat the GW as an external driver for the plasma perturbations. We then found for the first time that an *oblique* GW excites all three fundamental low-frequency MHD modes to linear order: the *Alfvén* mode and *slow* and *fast magneto-acoustic waves*.

Furthermore, we generalized the interaction of GW with a magnetic field to a *relativistic* plasma wind or jet that flows away from the GW source at Lorentz factors of $\gamma \sim 100$. The linearized space-time solutions of all components of the Alfvén and fast mode in both the comoving and the observer frames are calculated and only then do we specify to a magnetically (Poynting flux) dominated wind in which we can neglect the gas pressure (the sound velocity is much smaller that the generalized Alfvén velocity).

Although all three MHD modes are excited, only the fast MSW has the same dispersion relation as the GW for all angles with respect to the magnetic field (in a Poynting flux dominated outflow) and can interact coherently with the GW over significant length-scales. Hence, we only considered this mode in the remainder of this work. The analytical results of Chapters 3–4 are confirmed numerically in Duez et al. (2005a,b).

A problem with all linear perturbations excited by a GW is that the excited modes have the same $\sim$ kHz frequency as the GW which is too low to directly escape from the plasma as observational radiation. In non-linear interactions higher frequencies of the escaping mode can be obtained through the resonance condition $\omega_{\rm gw} = \omega_1 - \omega_2$. Such *parametric* excitations are discussed in Brodin and Marklund (1999) but rely on the presence of high-frequency and negative energy waves and still do not clearly lead to radiation in an observable band.

We proposed an alternative mechanism in Chapter 5 and investigated whether a form of *inverse Compton scattering* results in a sufficiently large frequency boost. In our treatment of the MSW–GW interaction in Chapters 3–4, we assumed that the fast mode is carried by relativistic but mono-energetic particles, such that we can define a rest frame comoving with the bulk of the particles in which the motions of the individual particles are non-relativistic (or zero).

In reality, however, the distribution function of the particles has a high-energy tail or there could be other inhomogeneities such as beams with a Lorentz factor different from the particles carrying the MSW. In that case, the MSW, that essentially propagates with the speed of light, can overtake and scatter on these particles. If the angle of the incident MSW with respect to the propagation direction of the particles is only slightly larger than zero, the MSW is seen to approach head-on in the frame of the scattering particles and the frequency of the radiation scattered in the forward direction can be boosted with a factor up to $\sim 2\gamma^2$.

For typical GW –and therefore MSW– frequencies of a few kHz and Lorentz factors of a few hundreds, the scattered radiation would be in the $\sim$ 100 MHz regime. This is the band that will be accessible to the low-frequency radio

array LOFAR. Because LOFAR is an all-sky monitor it is also very well suited to look for short transient events such as neutron star mergers.

A proper analysis of the scattering probabilities in a relativistic magnetized anisotropic plasma where both the incident and scattered modes are eigenmodes of the particular plasma under consideration, was presented in Chapter 5. Since the magnetic energy density is much larger than the particle energy everywhere in the wind and any transverse momentum is immediately synchrotron radiated (Section 5.7), we considered a one-dimensional intrinsically relativistic (Jüttner-Synge) distribution function where the particles are strictly confined to the magnetic field lines. To calculate the appropriate scattering probabilities we adopted the covariant gauge-independent quantum plasma dynamics formalism developed by Melrose, Gedalin et al. (Gedalin et al. 1998; Melrose et al. 1999; Melrose and Gedalin 1999; Gedalin et al. 2001; Luo and Melrose 2001; Gedalin et al. 2002) and applied it to the force-free wind well outside the light-cylinder of the system, where the magnetic field is predominantly toroidal.

Furthermore, we studied parametrically different morphologies of the wind or jet, generalizing also some of the numerical results in Chapters 3–4. Assuming an axially symmetric wind in which the radius R is given as a function of the vertical distance z from the source by $R = z^{\kappa}$, we calculated numerically the total energy in the MSW and in the scattered radio waves. We found that the volume integrated energy in the scattered mode increases with distance only when $\kappa < 1/2$. In that case both the magnetic energy density and the number density of scattering particles fall of very slowly. However, the volume integrated energy in the MSW is much smaller than in the $\kappa = 1$ case because of the smaller volume. Furthermore, we found that the scattering probability suffers from a suppression by a factor $(\gamma\omega/\Omega)^4$ resulting from the confinement of the particles to the magnetic field lines. Since the MSW is transversely polarized, the particles can not oscillate in the electric field which is always perpendicular to the ambient magnetic field. Inverse Compton scattering consequently does not seem to be an efficient radiation mechanism.

From the estimates obtained in Sections 3.6, 5.9, 5.7 it is clear that the total volume integrated energy dumped by GW in the surrounding plasma is substantial. Although the simplest radiation mechanisms, synchrotron and inverse Compton, prove inefficient it is likely that a more complicated mechanism will allow this energy to escape as observational radiation, thus providing an electromagnetic counterpart to the GW source. If such a radiation mechanism still operates in the $\sim$ 30–240 MHz band (which is the lowest observational frequency band and the closest to the original GW and MSW frequencies) the indirect detection of gravitational waves would not only be the most exciting result of this thesis work, but also one of the most interesting potential discoveries with LOFAR itself.

In the final Chapter 6 of this thesis we ventured on the quite different terrain of cosmology. Using many of the same techniques introduced in Chapter 2 and applied throughout Chapters 3–5 we investigated temperature effects in a covariant and gauge-invariant treatment of scalar perturbations on a FRW Uni-

verse. The covariant and gauge-invariant theory was developed by (Hawking 1966; Ellis and Bruni 1989; Ellis et al. 1990, 1989; Dunsby et al. 1992; Ellis and van Elst 1999a) and references therein. Many interesting problems have been studied such as a Universe consisting of radiation, matter or both in either a single fluid approach or a multi-fluid approach.

Our contribution in Chapter 6 consists of extending the theory to include pressure effects. The equations for a perfect fluid cosmology were studied before (for instance in Ellis and van Elst (1999b)) but usually the pressure terms are neglected since only the $T^{00} = \rho$ component of the stress-energy tensor governs the background evolution of the Universe. We ultimately use the same approximation for the background but study the influence of pressure (or equivalently temperature) effects on linear perturbations and the corresponding structure formation.

We constructed evolution equations for both vector and scalar perturbation quantities and derived analytical solutions in a number of limiting cases. In the long wavelength limit we can recover the results in Marklund et al. (2003) for scalar perturbations of the total density and the charge density, but we find not only the gravitational collapse and the extra oscillatory mode due to the plasma, but also the corresponding evolution of temperature perturbations. In particular, we found that when the background is in perfect thermal equilibrium the temperature perturbations are just simple plasma oscillations. A new result is that when the two plasma species have a slight temperature difference in the background this difference grows during gravitational collapse.

In the general wavelength case we neglected the evolution of the background and found that both Langmuir waves and ion-acoustic waves are excited by scalar perturbations (which will be superposed on the overall expansion of the background).

Finally, we included both the background evolution and the wavelength dependence to obtain a generalized *Jeans criterion* for gravitational collapse in a two-temperature plasma. As one would expect, the expression for the Jeans wavelength is of the same form as in a one-temperature plasma but now governed by the species with the largest sound velocity.

APPENDIX A

Auxiliary results

A.1 Explicit constants in Chapter 3

$$
\begin{aligned}
\Lambda &= \tfrac{h}{4}\tfrac{1+u_{\rm A}}{1-u_{\rm A}}\tfrac{(1-\beta)^2}{1-u_{\rm A}\beta} \simeq \tfrac{h}{4}\tfrac{\omega_{\rm g}}{\gamma^2\Delta k}\ ,\\
\Lambda_1 &= 2\tfrac{1-u_{\rm A}\beta}{(1-\beta)^3}\tfrac{\beta(1-4u_{\rm A}+\beta)+u_{\rm A}^2(2-\beta(1-\beta))}{u_{\rm A}(1+u_{\rm A})^2} = 1+\mathcal{O}[\Delta k]^2\ ,\\
\Lambda_2 &= \gamma^2\left(\tfrac{1-u_{\rm A}}{1+u_{\rm A}}\tfrac{1+\beta}{1-\beta}\right)^2\tfrac{u_{\rm A}-2\beta+u_{\rm A}\beta^2}{u_{\rm A}} = \mathcal{O}[\Delta k]^2\ ,\\
\Lambda_3 &= 2\tfrac{1-u_{\rm A}\beta}{(1-\beta)^3}\tfrac{(1+u_{\rm A}^2+2\beta^2-(1+(4-u_{\rm A})u_{\rm A})\beta}{(1+u_{\rm A})^2} = 1+\mathcal{O}[\Delta k]^2\ ,\\
\Lambda_4 &= -\gamma^2\left(\tfrac{1-u_{\rm A}}{1+u_{\rm A}}\tfrac{1+\beta}{1-\beta}\right)^2(\beta^2-2u_{\rm A}\beta+1) = \mathcal{O}[\Delta k]^2\ ,\\
\Lambda_5 &= 4\tfrac{u_{\rm A}-\beta}{(1+u_{\rm A})^2}\tfrac{1-u_{\rm A}\beta}{(1-\beta)^2} = 1-\mathcal{O}[\Delta k]^2\ ,\\
\Lambda_6 &= \left(\tfrac{1-u_{\rm A}}{1+u_{\rm A}}\tfrac{1+\beta}{1-\beta}\right)^2 = \mathcal{O}[\Delta k]^2\ ,\\
\Lambda_7 &= \tfrac{4u_{\rm A}}{(1+u_{\rm A})^2}\tfrac{1+u_{\rm A}\beta}{1-\beta} = 1+\mathcal{O}[\Delta k]\ ,\\
\Lambda_8 &= \left(\tfrac{1+u_{\rm A}}{1-u_{\rm A}}\right)^2\tfrac{\gamma^2u_{\rm A}(1+\beta)^4}{u_{\rm A}-2\beta+u_{\rm A}\beta^2} = \mathcal{O}[\Delta k]^2\ ,\\
\Lambda_9 &= 4\gamma^2\left(\tfrac{u_{\rm A}-\beta}{1+u_{\rm A}}\right)^2 = 1+\mathcal{O}[\Delta k]\ ,\\
\lambda &= \tfrac{h}{4}\tfrac{1+u_{\rm A}}{1-u_{\rm A}}\tfrac{1-\beta}{1+\beta} = \gamma^2(1-u_{\rm A}\beta)\Lambda\ ,\\
\kappa &= -\tfrac{\omega_{\rm g}}{u_{\rm A}}\tfrac{u_{\rm A}(1+\beta^2)-\beta(1+u_{\rm A}^2)}{u_{\rm A}(1+\beta^2)-2\beta} \simeq \tfrac{\omega_{\rm g}}{u_{\rm A}}\left(1+\mathcal{O}[\Delta k]\right)\ .
\end{aligned}
$$

A.2 Space-time solutions in Chapter 4

Comoving Alfvén wave components

The components of the Alfvén wave can be derived most easily by starting with it's velocity component:

$$\frac{v_y^1}{u_{\mathrm{A}\perp}} = \frac{h_\times}{4}\left[\frac{1+u_{\mathrm{A}\parallel}}{1-u_{\mathrm{A}\parallel}}\mathrm{e}^{i\phi_{\mathrm{A}}^+} - \frac{1-u_{\mathrm{A}\parallel}}{1+u_{\mathrm{A}\parallel}}\mathrm{e}^{i\phi_{\mathrm{A}}^-} - \frac{4u_{\mathrm{A}\parallel}\mathrm{e}^{i\phi_{\mathrm{g}}}}{1-u_{\mathrm{A}\parallel}^2}\right] . \tag{A.1}$$

From $\boldsymbol{E}^1 = -\boldsymbol{v}\times\boldsymbol{B}^0$ we find the electric field:

$$\frac{E_x^1(z,t)}{B_z^0} = -\frac{E_z^1(z,t)}{B_x^0} = -v_y^1(z,t) , \tag{A.2}$$

whereas the current density follows from Ampère's law:

$$j_x^1(z,t) = -\frac{i\omega}{4\pi}\frac{1-u_{\mathrm{A}\parallel}^2}{u_{\mathrm{A}\parallel}^2}E_x^1(z,t) , \tag{A.3a}$$

$$j_z^1(z,t) = \frac{i\omega}{4\pi}E_z^1(z,t) . \tag{A.3b}$$

The charge density is given by $\nabla\cdot\boldsymbol{E}^1 = 4\pi\tau^1$:

$$\frac{\tau^1(z,t)}{B_x^0\tan\theta} = \frac{i\omega h_\times}{4}\left[\frac{1+u_{\mathrm{A}\parallel}}{1-u_{\mathrm{A}\parallel}}\mathrm{e}^{i\phi_{\mathrm{A}}^+} + \frac{1-u_{\mathrm{A}\parallel}}{1+u_{\mathrm{A}\parallel}}\mathrm{e}^{i\phi_{\mathrm{A}}^-} - \frac{4u_{\mathrm{A}\parallel}^2\mathrm{e}^{i\phi_{\mathrm{g}}}}{1-u_{\mathrm{A}\parallel}^2}\right] . \tag{A.4}$$

Comoving magnetosonic wave components

The most complicated magnetosonic component is the magnetic field which clearly betrays the mixed nature (gas and electromagnetic fields) of this mode.

$$B_x^1(z,t) = \frac{B_x^0 h_+}{4(u_{\mathrm{f}}^2-u_{\mathrm{s}}^2)}[C(z,t)+D(z,t)] , \tag{A.5}$$

with:

$$C(z,t) \equiv -\left[\frac{2(u_{\mathrm{f}}^2-u_{\mathrm{s}}^2)(1+u_{\mathrm{A}}^2)\mathrm{e}^{i\phi_{\mathrm{g}}}}{(1-u_{\mathrm{f}}^2)(1-u_{\mathrm{s}}^2)} - \frac{u_{\mathrm{f}}(u_{\mathrm{f}}+u_{\mathrm{A}}^2)\mathrm{e}^{i\phi_{\mathrm{f}}^+}}{1-u_{\mathrm{f}}}\right.$$
$$\left. - \frac{u_{\mathrm{f}}(u_{\mathrm{f}}-u_{\mathrm{A}}^2)\mathrm{e}^{i\phi_{\mathrm{f}}^-}}{1+u_{\mathrm{f}}} + \frac{u_{\mathrm{s}}(u_{\mathrm{s}}+u_{\mathrm{A}}^2)\mathrm{e}^{i\phi_{\mathrm{s}}^+}}{1-u_{\mathrm{s}}} + \frac{u_{\mathrm{s}}(u_{\mathrm{s}}-u_{\mathrm{A}}^2)\mathrm{e}^{i\phi_{\mathrm{s}}^-}}{1+u_{\mathrm{s}}}\right] ,$$

and:

$$D(z,t) \equiv -u_{\rm f}u_{\rm s}\left\{\frac{2(u_{\rm f}^2-u_{\rm s}^2)\frac{1+u_{\rm A\parallel}^2}{u_{\rm A\parallel}^2}{\rm e}^{i\phi_{\rm g}}}{(1-u_{\rm f}^2)(1-u_{\rm s}^2)}\right.$$
$$-\left[\frac{1-u_{\rm A}^2}{u_{\rm A\parallel}^2}+\frac{1-u_{\rm f}}{u_{\rm f}}\right]\frac{{\rm e}^{i\phi_{\rm f}^+}}{1-u_{\rm f}}-\left[\frac{1-u_{\rm A}^2}{u_{\rm A\parallel}^2}-\frac{1-u_{\rm f}}{u_{\rm f}}\right]\frac{{\rm e}^{i\phi_{\rm f}^-}}{1+u_{\rm f}}$$
$$\left.+\left[\frac{1-u_{\rm A}^2}{u_{\rm A\parallel}^2}+\frac{1-u_{\rm s}}{u_{\rm s}}\right]\frac{{\rm e}^{i\phi_{\rm s}^+}}{1-u_{\rm s}}+\left[\frac{1-u_{\rm A}^2}{u_{\rm A\parallel}^2}-\frac{1-u_{\rm s}}{u_{\rm s}}\right]\frac{{\rm e}^{i\phi_{\rm s}^-}}{1+u_{\rm s}}\right\}\ .$$

Note that in the relativistic limit ($u_{\rm s}\downarrow 0$) D vanishes. From $\boldsymbol{E}=-\boldsymbol{v}^1\times\boldsymbol{B}^0$ we have:

$$E_y^1(z,t)=B_x^0v_z^1(z,t)-B_z^0v_x^1(z,t)\ . \tag{A.6}$$

The current density is most easily found as:

$$j_y^1(z,t)=-\frac{i\omega}{B^0\cos\theta}\frac{\gamma p^0}{c_{\rm s}^2}v_x^1(z,t)\ , \tag{A.7}$$

and the pressure is derived from (4.22):

$$\frac{p^1}{\gamma p^0}=\frac{h_+}{4}\frac{u_{\rm A\perp}^2u_{\rm s}}{u_{\rm f}^2-u_{\rm s}^2}\left[\frac{1+u_{\rm s}}{1-u_{\rm s}}\frac{{\rm e}^{i\phi_{\rm s}^+}}{u_{\rm s}}+\frac{1-u_{\rm s}}{1+u_{\rm s}}\frac{{\rm e}^{i\phi_{\rm s}^-}}{u_{\rm s}}-\frac{4{\rm e}^{i\phi_{\rm g}}}{1-u_{\rm s}^2}\right]$$
$$-\frac{h_+}{4}\frac{u_{\rm A\perp}^2u_{\rm f}}{u_{\rm f}^2-u_{\rm s}^2}\left[\frac{1+u_{\rm f}}{1-u_{\rm f}}\frac{{\rm e}^{i\phi_{\rm f}^+}}{u_{\rm f}}+\frac{1-u_{\rm f}}{1+u_{\rm f}}\frac{{\rm e}^{i\phi_{\rm f}^-}}{u_{\rm f}}-\frac{4{\rm e}^{i\phi_{\rm g}}}{1-u_{\rm f}^2}\right]\ , \tag{A.8}$$

which readily leads to the energy density:

$$\mu^1(z,t)=\frac{p^1(z,t)}{c_{\rm s}^2}\ . \tag{A.9}$$

In the limit of a Poynting flux dominated wind where $u_{\rm f}\simeq u_{\rm A}\uparrow 1$ and $p_0\downarrow 0$ so $u_{\rm s}\simeq c_{\rm s}\downarrow 0$ the fast mode can interact coherently with the GW and we find

growing amplitudes for all components:

$$\frac{B_x^1(z,t)}{B_0} = \frac{h_+}{2}\sin\theta\ \omega z\ \Im\left[\mathrm{e}^{i\phi_\mathrm{g}}\right]\ , \tag{A.10a}$$

$$v_z^1(z,t) = \frac{h_+}{2}\sin^2\theta\ \omega z\ \Im\left[\mathrm{e}^{i\phi_\mathrm{g}}\right]\ , \tag{A.10b}$$

$$v_x^1(z,t) = -\frac{h_+}{2}\sin\theta\cos\theta\ \omega z\ \Im\left[\mathrm{e}^{i\phi_\mathrm{g}}\right]\ , \tag{A.10c}$$

$$\frac{\mu^1(z,t)}{\mu^0} = \frac{h_+}{2}\sin^2\theta\ \omega z\ \Im\left[\mathrm{e}^{i\phi_\mathrm{g}}\right]\ , \tag{A.10d}$$

$$\frac{E_y^1(z,t)}{B_0} \simeq -\frac{h_+}{2}\sin\theta\ \omega z\ \Im\left[\mathrm{e}^{i\phi_\mathrm{g}}\right], \tag{A.10e}$$

$$\frac{B_x^0 j_y(z,t)}{\mu^0\omega} \simeq \frac{h_+}{2}\sin^2\theta\ \omega z\ \Re\left[\mathrm{e}^{i\phi_\mathrm{g}}\right]\ . \tag{A.10f}$$

All ultra-relativistic Alfvén wave components

First we evaluate B_y' in terms of laboratory quantities (boosted phase velocities etc.[1]):

$$B_y' = \frac{h_\times\gamma_{u_\mathrm{A}}^2 B_x^0}{4\gamma}\left\{4\left[(1+\beta^2)(1+u_{\mathrm{A}\parallel}^2) - 4\beta u_{\mathrm{A}\parallel}\right]\mathrm{e}^{i\phi_\mathrm{g}}\right.$$
$$\left.\left[\frac{1+u_{\mathrm{A}\parallel}}{1+\beta}\right]^2\frac{\mathrm{e}^{i\phi_\mathrm{A}^+}}{\gamma^4} + \left[\frac{1+\beta}{1+u_{\mathrm{A}\parallel}}\right]^2\frac{\mathrm{e}^{i\phi_\mathrm{A}^-}}{\gamma_{u_\mathrm{A}}^4}\right\}\ . \tag{A.11}$$

Now we can express all other components of the Alfvén wave in terms of (A.11) and (4.44):

$$B_y = \gamma(B_y' + \beta E_x') = \gamma B_y' - \beta\gamma B_x^0 v_y\ , \tag{A.12a}$$

$$E_x = \gamma(E_x' + \beta B_y') = \gamma\beta B_y' - \gamma B_x^0 v_y\ , \tag{A.12b}$$

$$E_z = E_z' = -B_x' v_y' = -B_x v_y\ , \tag{A.12c}$$

$$j_x = j_x' = \frac{i\omega}{8\pi\gamma^2\gamma_{u_\mathrm{A}}^2}\frac{B_z^0 v_y}{(u_\mathrm{A}-\beta)^2}\ , \tag{A.12d}$$

$$j_z = \gamma(j_z' + \beta\tau') = \frac{B_x^0}{8\pi}\left[i\omega v_y - 2\gamma\beta\frac{\partial v_y}{\partial z}\right]\ , \tag{A.12e}$$

$$\tau = \gamma(\tau' + \beta j_z') = \frac{B_x^0}{8\pi}\left[i\omega\beta v_y - 2\gamma\frac{\partial v_y}{\partial z}\right]\ . \tag{A.12f}$$

[1] We will omit the superscript on first order quantities to avoid confusion with the primes.

All ultra-relativistic MSW components

We will only consider the limit of a Poynting flux dominated ultra-relativistic wind and Lorentz transform (A.10) (with $\omega = \gamma(\omega' + \beta k') \simeq 2\gamma\omega'$):

$$B_x = \gamma(B'_x - \beta E'_y) \simeq 2\gamma B'_x = \frac{h_+}{2\gamma^2} B^0_x \omega z \, \Im\left[\mathrm{e}^{i\phi_\mathrm{g}}\right] \ , \tag{A.13a}$$

$$E_y = \gamma(E'_y - \beta B'_x) \simeq -B_x \ , \tag{A.13b}$$

$$j_y = j'_y = \frac{h_+}{8\gamma^3} \frac{\mu^0}{B^0_x} \frac{\sin^2\theta}{(1-\beta\cos\theta)^2} \omega^2 z \, \Re\left[\mathrm{e}^{i\phi_\mathrm{g}}\right] \ , \tag{A.13c}$$

$$\mu = \gamma\mu' = \frac{h_+}{4\gamma^2} \frac{\mu^0 \sin\theta}{1-\beta\cos\theta} \omega z \, \Im\left[\mathrm{e}^{i\phi_\mathrm{g}}\right] \ . \tag{A.13d}$$

A.3 Commutation relations in Chapter 6

We summarize the commutation relations that are used throughout Chapter 6 and derived in Maartens (1997) and Betschart et al. (2004). The relations are linearized about a background in which $\omega_{ab} = \sigma_{ab} = \dot{u}_a = 0$. X, X_a, X_{ab} stands for any scalar function, vector or tensor, respectively, and $\mathcal{F}$ can be any of those.

$$(\tilde{\nabla}_a \mathcal{F})^{\cdot} = \tilde{\nabla}_a \dot{\mathcal{F}} - \tfrac{1}{3}\Theta\tilde{\nabla}_a \mathcal{F} \ , \tag{A.14a}$$

$$(\tilde{\nabla}^b X_{ab})^{\cdot} = \tilde{\nabla}^b \dot{X}_{ab} - \tfrac{1}{3}\Theta\tilde{\nabla}^b X_{ab} \ , \tag{A.14b}$$

$$(\mathrm{curl} X_{ab})^{\cdot} = \mathrm{curl}\dot{X}_{ab} - \tfrac{1}{3}\Theta\mathrm{curl} X_{ab} \ , \tag{A.14c}$$

$$\tilde{\nabla}_a\tilde{\nabla}^2 X = \tilde{\nabla}^2\tilde{\nabla}_a X + \tfrac{2}{9}\left(\Theta^2 - 3\mu\right)\tilde{\nabla}_a X \ , \tag{A.14d}$$

$$\tilde{\nabla}_a\tilde{\nabla}^2 X^a = \tilde{\nabla}^2\tilde{\nabla}_a X^a - \tfrac{2}{9}\left(\Theta^2 - 3\mu\right)\tilde{\nabla}_a X^a \ , \tag{A.14e}$$

$$S\mathrm{curl}(\tilde{\nabla}^2 X^a) = \tilde{\nabla}^2(S\mathrm{curl} X^a) \ . \tag{A.14f}$$

Bibliography

Achterberg, A. (1983, October). Variational principle for relativistic magnetohydrodynamics. Phys. Rev. A *28*, 2449–2458.

Bardeen, J. M. (1980, October). Gauge-invariant cosmological perturbations. Phys. Rev. D *22*, 1882–1905.

Betschart, G., P. K. S. Dunsby, and M. Marklund (2004, April). Cosmic magnetic fields from velocity perturbations in the early universe. *Classical and Quantum Gravity 21*, 2115–2125.

Boccaletti, D., V. de Sabbata, P. Fortini, and C. Gualdi (1970). *Il Nuovo Cimento 70B*, 129.

Brodin, G. and M. Marklund (1999, April). Parametric Excitation of Plasma Waves by Gravitational Radiation. *Phys. Rev. Lett. 82*, 3012–3015.

Brodin, G., M. Marklund, and P. K. S. Dunsby (2000, November). Nonlinear gravitational wave interactions with plasmas. *Phys. Rev. D. 62*, 104008–+.

Brodin, G., M. Marklund, and P. K. S. Dunsby (2001, December). Plane-fronted parallel waves in a warm two-component plasma. *Classical and Quantum Gravity 18*, 5249–5255.

Brodin, G., M. Marklund, and M. Servin (2001, June). Photon frequency conversion induced by gravitational radiation. Phys. Rev. D *63*, 124003–+.

Challinor, A. D. and A. N. Lasenby (1998). A covariant and gauge-invariant analysis of cosmic microwave background anisotropies from scalar perturbations. *Physical Review D 58*, 023001.

Clarkson, C. A., M. Marklund, G. Betschart, and P. K. S. Dunsby (2004, September). The Electromagnetic Signature of Black Hole Ring-Down. ApJ *613*, 492–505.

Duez, M. D., Y. T. Liu, S. L. Shapiro, and B. C. Stephens (2005a, July). Excitation of magnetohydrodynamic modes with gravitational waves: A testbed for numerical codes. Phys. Rev. D *72*(2), 024029–+.

Duez, M. D., Y. T. Liu, S. L. Shapiro, and B. C. Stephens (2005b, July). Relativistic magnetohydrodynamics in dynamical spacetimes: Numerical methods and tests. Phys. Rev. D *72*(2), 024028–+.

Dunsby, P. K. S., M. Bruni, and G. F. R. Ellis (1992, August). Covariant perturbations in a multifluid cosmological medium. ApJ *395*, 54–74.

Ellis, G. F. R. (1995). Observations and Cosmological Models. *LNP Vol. 463: Galaxies in the Young Universe 463*, 51–+.

Ellis, G. F. R. and M. Bruni (1989, September). Covariant and gauge-invariant approach to cosmological density fluctuations. Phys. Rev. D *40*, 1804–1818.

Ellis, G. F. R., M. Bruni, and J. Hwang (1990, August). Density-gradient-vorticity relation in perfect-fluid Robertson-Walker perturbations. Phys. Rev. D *42*, 1035–1046.

Ellis, G. F. R., J. Hwang, and M. Bruni (1989, September). Covariant and gauge-independent perfect-fluid Robertson-Walker perturbations. Phys. Rev. D *40*, 1819–1826.

Ellis, G. F. R. and H. van Elst (1998). Cosmological models.

Ellis, G. F. R. and H. van Elst (1999a). Cosmological models. In M. Lachièze-Rey (Ed.), *Theoretical and Observational Cosmology*, Dordrecht, pp. p. 1–116. Kluwer.

Ellis, G. F. R. and H. van Elst (1999b). Cosmological Models (Cargèse lectures 1998). In *NATO ASIC Proc. 541: Theoretical and Observational Cosmology*, pp. 1–116.

Gayer, S. and C. F. Kennel (1979, February). Possibility of Landau damping of gravitational waves. Phys. Rev. D *19*, 1070–1083.

Gedalin, M., E. Gruman, and D. B. Melrose (2001, August). Low-frequency waves in asymmetric magnetized relativistic pair plasma. MNRAS *325*, 715–725.

Gedalin, M., E. Gruman, and D. B. Melrose (2002, December). Mechanism of pulsar radio emission. MNRAS *337*, 422–430.

Gedalin, M., D. B. Melrose, and E. Gruman (1998, March). Long waves in a relativistic pair plasma in a strong magnetic field. Phys. Rev. E *57*, 3399–3410.

Gedalin, M. E. and G. Z. Machabeli (1983, October). Three-plasmon processes in a magnetized electron-positron plasma. *Soviet Journal of Plasma Physics 9*, 1015–1022.

Gerlach, U. H. (1974). *Phys. Rev. Lett. 32, Nr. 18*.

Gertsenshtein, M. (1961). *Zh. Exsp. Teor. Fiz. 41*, 113.

Gurevich, A., V. Beskin, and Y. Istomin (1993, August). *Physics of the Pulsar Magnetosphere*. Physics of the Pulsar Magnetosphere, by Alexandr Gurevich and Vassily Beskin and Yakov Istomin, pp. 432. ISBN 0521417465. Cambridge, UK: Cambridge University Press, August 1993.

Harrison, E. R. (1967, October). Normal Modes of Vibrations of the Universe. *Reviews of Modern Physics 39*, 862–882.

Hawking, S. W. (1966, August). Perturbations of an Expanding Universe. ApJ *145*, 544–+.

Hawking, S. W. and G. F. R. Ellis (1973). *The large scale structure of space-time*. Cambridge Monographs on Mathematical Physics, London: Cambridge University Press, 1973.

Hulse, R. A. and J. H. Taylor (1975, January). Discovery of a pulsar in a binary system. ApJ *195*, L51–L53.

Ibrahim, A. I., J. H. Swank, and W. Parke (2003, February). New Evidence of Proton-Cyclotron Resonance in a Magnetar Strength Field from SGR 1806-20. *Astrophysical Journal Letters 584*, L17–L21.

Jackson, J. D. (1975). *Classical electrodynamics*. 92/12/31, New York: Wiley, 1975, 2nd ed.

Janka, H.-T., T. Eberl, M. Ruffert, and C. L. Fryer (1999, December). Black Hole-Neutron Star Mergers as Central Engines of Gamma-Ray Bursts. *Astrophysical Journal Letters 527*, L39–L42.

Kodama, H. and M. Sasaki (1984). Cosmological Perturbation Theory. *Progress of Theoretical Physics Supplement 78*, 1–+.

Kokkotas, K. D. (2004, March). High-frequency sources of gravitational waves. *Classical and Quantum Gravity 21*, 501–+.

Kuijpers, J. (2001a). Equatorial Pulsar Winds. *Publications of the Astronomical Society of Australia 18*, 407–414.

Kuijpers, J. (2001b). Equatorial Pulsar Winds. *Publications of the Astronomical Society of Australia 18*, 407–414.

Landau, L. D. and E. M. Lifshitz (1975). *The classical theory of fields*. Course of theoretical physics - Pergamon International Library of Science, Technology, Engineering and Social Studies, Oxford: Pergamon Press, 1975, 4th rev.engl.ed.

Lichnerowicz, A. (1967). *Relativistic Hydrodynamics and Magnetohydrodynamics*. Relativistic Hydrodynamics and Magnetohydrodynamics, New York: Benjamin, 1967.

Luo, Q. and D. B. Melrose (2001, July). Cyclotron absorption of radio emission within pulsar magnetospheres. MNRAS *325*, 187–196.

Lupanov, G. A. (1967). *Sov. Phys. JETP 25 Nr. 1*, 76–79.

Lüst, R. and A. Schlüter (1954). Kraftfreie Magnetfelder. Mit 4 Textabbildungen. *Zeitschrift fur Astrophysics 34*, 263–+.

Lyubarsky, Y. E. (1995). *Physics of pulsars*. Amsterdam: Harwood Academic Publishers, —c1995.

Maartens, R. (1997, January). Linearization instability of gravity waves? Phys. Rev. D *55*, 463–467.

Macedo, P. G. and A. H. Nelson (1983, November). Propagation of gravitational waves in a magnetized plasma. *Phys. Rev. D. 28*, 2382–2392.

Malik, K. A. and D. Wands (2005). Adiabatic and entropy perturbations with interacting fluids and fields. *JCAP 0502*, 007.

Marklund, M., G. Brodin, and P. K. S. Dunsby (2000, June). Radio Wave Emissions Due to Gravitational Radiation. *ApJ 536*, 875–879.

Marklund, M., P. K. S. Dunsby, G. Betschart, M. Servin, and C. G. Tsagas (2003, May). Charged multifluids in general relativity. *Classical and Quantum Gravity 20*, 1823–1834.

Marklund, M., P. K. S. Dunsby, and G. Brodin (2000, November). Cosmological electromagnetic fields due to gravitational wave perturbations. Phys. Rev. D *62*(10), 101501–+.

Melrose, D. B. (1986). *Instabilities in space and laboratory plasmas*. Cambridge and New York, Cambridge University Press, 1986, 290 p.

Melrose, D. B. (1997, May). Some properties of magnetized pair plasmas . *Plasma Physics and Controlled Fusion 39*, A93–A100.

Melrose, D. B. (2001). Quantum plasma dynamics. `http://www.physics.usyd.edu.au/rcfta/qpd.html`.

Melrose, D. B. and M. E. Gedalin (1999, August). Relativistic Plasma Emission and Pulsar Radio Emission: A Critique. ApJ *521*, 351–361.

Melrose, D. B., M. E. Gedalin, M. P. Kennett, and C. S. Fletcher (1999, August). Dispersion in an intrinsically relativistic, one-dimensional, strongly magnetized pair plasma. *Journal of Plasma Physics 62*, 233–248.

Mikhailovskii, A. B. (1980, June). The nonlinear generation of electromagnetic waves in a relativistic electron-positron plasma. *Soviet Journal of Plasma Physics 6*, 613–620.

Misner, C. W., K. S. Thorne, and J. A. Wheeler (1973). *Gravitation*. San Francisco: W.H. Freeman and Co., 1973.

Moortgat, J. and J. Kuijpers (2003, May). Gravitational and magnetosonic waves in gamma-ray bursts. *Astronomy & Astrophysics 402*, 905–911.

Moortgat, J. and J. Kuijpers (2004, July). Gravitational waves in magnetized relativistic plasmas. Phys. Rev. D *70*(2), 023001–+.

Moortgat, J. and J. Kuijpers (2005, March). Indirect Visibility of Gravitational Waves in Magnetohydrodynamic Plasmas. *arXiv:gr-qc/0503074*.

Moortgat, J. B. and J. Kuijpers (2006). Scattering of magnetosonic waves in a relativistic and an-isotropic magnetised plasma. MNRAS— *accepted*.

Moortgat, J. B. and M. Marklund (2006). Scalar perturbations in two-temperature cosmological plasmas. MNRAS— *submitted*.

Nelemans, G., L. R. Yungelson, and S. F. Portegies Zwart (2001, September). The gravitational wave signal from the Galactic disk population of binaries containing two compact objects. A&A *375*, 890–898.

Ohanian, H. and R. Ruffini (1994). *Gravitation and Spacetime*. New York: New York, Norton and Company, 1994. 679 p.

Papadopoulos, D. (2002, December). Acceleration and cyclotron radiation induced by gravitational waves. A&A *396*, 1045–1051.

Papadopoulos, D., N. Stergioulas, L. Vlahos, and J. Kuijpers (2001, October). Fast magnetosonic waves driven by gravitational waves. *A&A 377*, 701–706.

Paradijs, J. v., C. Kouveliotou, and R. A. M. J. Wijers (2000). Gamma-Ray Burst Afterglows. ARA&A *38*, 379–425.

Rybicki, G. B. and A. P. Lightman (1979). *Radiative processes in astrophysics*. New York, Wiley-Interscience, 1979. 393 p.

Schutz, B. F. (1996). Gravitational wave sources. *Classical and Quantum Gravity 13*, A219–238.

Schutz, B. F. (1999, December). Gravitational wave astronomy. *Classical and Quantum Gravity 16*, A131–A156.

Servin, M. (2003). *Nonlinear interaction and propagation of gravitational and electromagnetic waves in plasmas*. Ph. D. thesis, Department of Physics, Umeå University, Sweden.

Servin, M. and G. Brodin (2003, August). Resonant interaction between gravitational waves, electromagnetic waves, and plasma flows. Phys. Rev. D *68*, 44017–+.

Shibata, M. and K. Uryu (2002). Gravitational waves from the merger of binary neutron stars in a fully general relativistic simulation. *Prog. Theor. Phys. 107*, 265.

Spruit, H. C., F. Daigne, and G. Drenkhahn (2001, April). Large scale magnetic fields and their dissipation in GRB fireballs. *A&A 369*, 694–705.

Stewart, J. (1990). *Advanced general relativity*. Cambridge: Cambridge university press.

Stewart, J. M. and M. Walker (1974, October). Perturbations of space-times in general relativity. *Royal Society of London Proceedings Series A 341*, 49–74.

Thorne, K. S. (1989). Gravitational radiation: A new window onto the universe. `http://elmer.tapir.caltech.edu/ph237/`.

Thorne, K. S. and D. MacDonald (1982, January). Electrodynamics in Curved Spacetime - 3+1 Formulation. *MNRAS 198*, 339–+.

Thorne, K. S., R. H. Price, and D. A. MacDonald (Eds.) (1986). *Black holes: The membrane paradigm*.

Tsagas, C. G. (2005, January). Electromagnetic fields in curved spacetimes. *Classical and Quantum Gravity 22*, 393–407.

Wald, R. M. (1984). *General relativity*. Chicago: Chicago Press.

Weinberg, S. (1972). *Gravitation and cosmology: Principles and applications of the general theory of relativity*. New York: Wiley, —c1972.

Zel'dovich, Y. B. (1973). *Zh. Eksp. Teor. Fiz. 65*, 1311–1315.

Zhang, B. and P. Mészáros (2004). Gamma-Ray Bursts: progress, problems and prospects. *International Journal of Modern Physics A 19*, 2385–2472.

Nederlandse samenvatting

ZWAARTEKRACHT is een *getijdenkracht*: de zwaartekracht van de maan zorgt voor hoog en laag tij van onze oceanen en voor de ei-vorm van de draaiende aarde. Volgens de Algemene Relativiteitstheorie van Einstein worden deze vervormingen niet veroorzaakt door een onzichtbare *kracht* die op een afstand werkt tussen de aarde en de maan, maar door een *vervorming van ruimte en tijd* zelf, zoals geïllustreerd in Figuur 1.

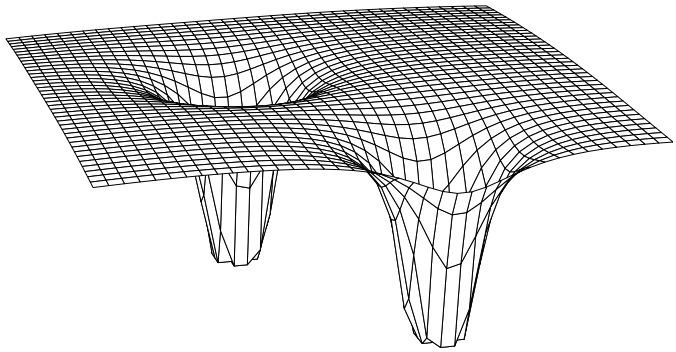

Figuur 1: Vervorming van de ruimte door de aanwezigheid van twee hemellichamen.

Einsteins relativiteitstheorie beschrijft echter niet alleen statische (tijdsonafhankelijke) getijdenkrachten, maar voorspelt ook dynamische (tijdsafhankelijke) vervormingen van ruimte en tijd: *gravitatiegolven*. Deze worden bijvoorbeeld opgewekt door de beweging van twee massa's in een dubbelsysteem, zoals de aarde en de maan of twee sterren die om elkaar heendraaien.

Veel van de eigenschappen van zwaartekracht hebben een elektromagnetische analogie. Zo heeft een stilstaand elektrisch geladen deeltje ook een statische potentiaal terwijl een versneld deeltje elektromagnetische golven uitzendt. Net zoals zulke elektromagnetische straling twee polarisaties heeft die loodrecht op elkaar staan, hebben gravitatiegolven dat ook: de + en × polarisatie. Bij elektromagnetische straling wordt de polarisatie bepaald door de oriëntatie van het elektrisch veld en bij gravitatiegolven door de twee loodrechte richtingen waarin de getijde-werking objecten uitrekt en induwt. Dit wordt in Figuur 2 geïllustreerd (in 2 en 3 dimensies) voor een ring van deeltjes vervormd tot ellipsen door een passerende gravitatiegolf.

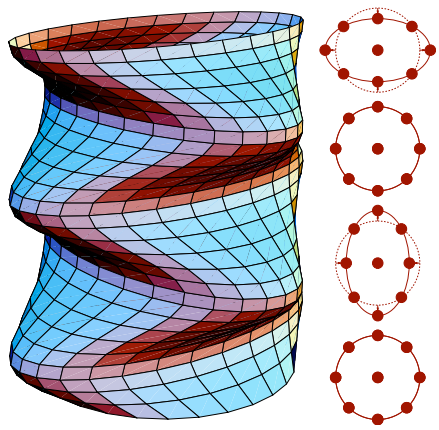

Figuur 2: Vervorming van de ruimte door een gravitatiegolf.

Zwaartekracht is de zwakste van alle fundamentele krachten en domineert alleen op grote afstanden waar de elektromagnetische kracht wordt afgeschermd doordat het heelal gemiddeld genomen neutraal geladen is. De sterkte van gravitatiegolven neemt bovendien af met de afstand tot de bron en juist de meest explosieve bronnen van gravitatiegolven, zoals de botsing van twee neutronensterren die versmelten en een zwart gat vormen, vinden typisch plaats op grote afstand van de aarde. Om enkele zulke gebeurtenissen per jaar te kunnen detecteren moet men zeker tot een afstand van circa 300 miljoen lichtjaar zoeken. Voor een dergelijke afstand is de ruimtelijke afwijking die de gravitatiegolven op aarde zouden veroorzaken ongeveer één waterstofatoomstraal op de afstand aarde–zon!

Niettemin worden er op verschillende plekken op aarde, en binnenkort ook in de ruimte, detectoren gebouwd om deze gravitatiegolven direct te meten. Dat gravitatiegolven bestaan is al indirect aangetoond door Hulse and Taylor (1975) door zeer nauwkeurig de baan van twee neutronensterren te bestuderen. Doordat een dubbelster gravitatiegolven uitstraalt, verliest het systeem

energie waardoor de baan steeds een beetje nauwer wordt en de twee sterren uiteindelijk naar elkaar toe zullen spiraliseren.

Om het onwaarschijnlijk zwakke gravitatiegolfsignaal *direct* te meten en uit de grote hoeveelheid ruis te halen is enige 'voorkennis' van hoe het signaal er waarschijnlijk uitziet van groot belang. Met name een elektromagnetisch signaal van dezelfde bron zou van onschatbare waarde zijn. In dit proefschift onderzoeken we of een dergelijke elektromagnetische puls wordt opgewekt in de nabije omgeving van een bron van gravitatiegolven.

Gravitatiegolven, ook sterke, hebben echter bijna nergens interactie mee. Een heel heelal gevuld met stof of een ideale vloeistof met een *isotrope* druk heeft nog steeds geen enkele dempende invloed op de golven. Veel bronnen van gravitatiegolven zijn echter omgeven door sterke *magneetvelden* en deze bezitten een *an-isotrope* druk die interactie mogelijk maakt (dit volgt uit Einsteins veld-vergelijkingen).

Na een behandeling van de theoretische achtergronden in Hoofdstuk 2 bestuderen we in Hoofdstuk 3 wat er gebeurt als twee neutronensterren versmelten en in minder dan een seconde bijna evenveel energie uitzenden in de vorm gravitatiegolven als de zon in heel haar leven aan licht uitstraalt. De dubbelster heeft een magneetveld dat minstens 10 miljoen maal sterker is dan het sterkste laboratoriumveld op aarde en twee jets waarin een *plasma* van elektronen en positronen (anti-elektronen) met bijna de lichtsnelheid wegstroomt langs het magneetveld. We willen onderzoeken of de gravitatiegolven gewoon ontsnappen òf een interactie hebben met het magneetveld en de deeltjes in de jets en daar een deel van hun energie aan overdragen. In het laatste geval zou dit een elektromagnetisch signaal kunnen geven tegelijk met de gravitatiegolfuitbarsting.

Eerst laten we zien hoe een gravitatiegolf die zich loodrecht op een uniform magneetveld voortbeweegt een magnetosonische golf opwekt (zie ook Figuren 3.1 en 5.1). Dit soort golven veroorzaken zowel een compressie van het gas als van het magneetveld en hebben daardoor deels eigenschappen van een geluidsgolf en deels van een elektromagnetische golf. We leiden de eigenschappen en exacte uitdrukkingen voor deze golven af (in een snel bewegend plasma) en maken een numerieke afschatting waaruit blijkt dat inderdaad een substantiële hoeveelheid energie van de gravitatiegolven wordt geabsorbeerd in het plasma via deze snelle magnetosonische golven.

Gemotiveerd door dit resultaat generaliseren we in Hoofdstuk 4 de interactie van gravitatiegolven met een gemagnetiseerd plasma door beide polarisaties van de golven te beschouwen evenals willekeurige hoeken tussen de gravitatiegolf en het magneetveld. We vinden dat afhankelijk van deze hoeken en polarisaties, alle drie de fundamentele laag-frequente golven in een gemagnetiseerd plasma opgewekt kunnen worden: de zogenaamde Alfvéngolf en de langzame en de snelle magnetosonische golven. De Alfvéngolf is vergelijkbaar met een trilling in een snaar (een magnetische veldlijn in dit geval), terwijl de magnetosonische golven zoals gezegd het karakter hebben van een compressionele magnetische drukgolf.

Wanneer de magnetische druk in de jets veel sterker is dan de gasdruk bewegen zowel de gravitatie- als de snelle magnetosonische golven in feite met de lichtsnelheid en kunnen over grote afstanden wisselwerken. Hierdoor groeien de magnetosonische golven en absorberen steeds meer energie van de gravitatiegolven. Ook onderzoeken we in Hoofdstuk 4 wat de terugkoppeling hiervan op de gravitatiegolven is en vinden dat dit nog steeds verwaarloosbaar is aangezien de energiedichtheid in de gravitatiegolven zo groot is dicht bij de bron: hier kunnen de relatieve ruimtevervormingen zo groot zijn als een millimeter op een meter!

De resultaten van Hoofstuk 3–4 betekenen helaas nog niet dat we direct met conventionele (radio) telescopen naar bronnen van gravitatiegolven kunnen gaan zoeken. De magnetosonische golven worden namelijk opgewekt bij dezelfde frequentie als die van de gravitatiegolven. Deze is twee maal de baanfrequentie van de neutronendubbelster en wordt helemaal op het eind van de inwaartse spiraalbaan van de dubbelster hoogstens een paar kilohertz. Zulke laagfrequente straling kan niet ontsnappen uit het plasma en zou overigens ook niet door onze eigen atmosfeer heendringen. Er moet dus nog een tweede proces plaatsvinden waardoor de energie in de magnetosonische golven bij een hogere frequentie kan worden uitgestraald.

Zulk een proces proberen we te vinden in Hoofstuk 5 in de vorm van inverse-Compton verstrooiing. De werking hiervan berust op enkele consequenties van de Speciale Relativiteitstheorie die enigszins tegen de intuïtie ingaan. Als er vanuit alle richtingen fotonen (licht) op een elektron afkomen dat met bijna de lichtsnelheid beweegt, ziet dit elektron vrijwel alle fotonen recht van voren komen. Dit is enigszins vergelijkbaar met hoe een wandelaar regen recht naar beneden ziet vallen terwijl een snelle fietser alle regen recht in haar gezicht lijkt te krijgen (maar nu zelfs alle regen die achter haar valt, als zij met bijna de lichtsnelheid fietst).

Bovendien ziet het elektron een hogere frequentie van deze fotonen[2]. Vervolgens verstrooit het elektron de fotonen bij deze hogere frequentie in verschillende richtingen. Een stilstaande waarnemer ziet deze verstrooide fotonen echter vrijwel allemaal in de voorwaarste richting uitgezonden worden en nog een extra keer blauw verschoven door de relativistische beweging van het elektron in de richting van de waarnemer. Het resultaat van dit proces is dat de frequentie van de verstrooide fotonen in ons geval een factor tot ongeveer 10.000 omhoog kan gaan.

Als dit gebeurt is de resulterende straling waarneembaar met de nieuwe laagfrequente radiotelescoop LOFAR die op dit moment in het noorden van Nederland wordt gebouwd. Deze telescoop bestaat uit duizenden eenvoudige radioantennes die hun gegevens met hoge snelheid door een breedband glasvezelnetwerk naar een BlueGene supercomputer in Groningen worden sturen. Daar wordt met behulp van complexe algorithmes het radiobeeld van de hemel gereconstrueerd. Een van de vele voordelen van deze telescoop is dat vrijwel

[2]De frequentie is door het Doppler effect blauw verschoven, analoog aan het hogere geluid van een sirene van een naderende ambulance.

de hele hemel tegelijk kan worden waargenomen. Dit is essentieel om kort durende gebeurtenissen te kunnen detecteren waarvan men bovendien vantevoren niet weet waar ze aan de hemel optreden, zoals de versmelting van een neutronendubbelster die maar milliseconden tot seconden lang duurt.

Een eerste eenvoudige afschatting levert verder een aanwijzing dat ook de flux van de radiostraling op aarde, indirect afkomstig van gravitatiegolven, hoog genoeg zou zijn om waar te nemen. Het grootste deel van Hoofdstuk 5 bestaat uit een meer rigoreuze afleiding die gebruik maakt van relativistische quantumplasmadynamica. Hieruit blijkt dat de inverse-Compton verstrooiing ernstig wordt beperkt, juist door het aanwezige sterke magneetveld. Het meest efficiënte stralingsmechanisme moet nog worden gevonden waardoor de grote hoeveelheid energie die door de gravitatiegolven in de plasma bundel wordt achtergelaten, kan worden uitgestraald.

Het laatste hoofdstuk van dit proefschrift, Hoofdstuk 6, is een geheel andere toepassing van dezelfde technieken als in Hoofdstukken 2–4 gebruikt worden. In plaats van te kijken naar ruimtetijd verstoringen (gravitatiegolven) op een vlakke ruimte, bestuderen we nu verstoringen van fysische grootheden als dichtheid en druk op een globaal gekromde ruimte, namelijk die van het heelal zelf. Zulke dichtheidsverstoringen zijn de oorsprong geweest van de vorming van de struktuur in het heelal zoals sterrenstelsels.

Na de Oerknal bestond het heelal uit een 'kosmische soep' van aanvankelijk quarks, fotonen, elektronen en neutrinos. Later groepeerden de quarks zich in de vorm van neutronen en protonen en nog weer later gedeeltelijk in geïoniseerd helium. Tussen ongeveer 10 seconden tot 100.000 jaar na de Oerknal werd het heelal gedomineerd door de energie van de fotonen en was het plasma zeer heet. Hierdoor was alle materie volledig geïoniseerd en werden de fotonen voortdurend sterk verstrooid als in een mist, en waren materie en straling sterk gekoppeld. Toen het heelal afkoelde tot een temperatuur van ongeveer 3000 Kelvin konden de elektronen en neutronen recombineren en zo neutraal waterstof vormen waardoor de fotonen niet meer verstrooid werden en vrij konden ontsnappen. Naarmate het heelal verder uitzette, daalde de temperatuur van de fotonen tot de 3 Kelvin kosmische achtergrondstraling (Cosmic Microwave Background, CMB) die nu in alle richtingen wordt waargenomen.

Precieze metingen van de CMB door de sateliet WMAP[3] laten zien dat de straling zeer homogeen is maar dat er relatieve temperatuurafwijkingen aan de hemel zijn van ongeveer 10^{-5}. Waarschijnlijk zijn deze afwijkingen gerelateerd aan dichtheidsafwijkingen van vergelijkbare grootte. Zulke verstoringen werden reeds voorspeld door de inflatietheorie die zegt dat bij de geboorte van het Universum de ruimte gedurende zeer korte tijd exponentieël uitzette zodat quantumfluctuaties van het vacuüm tot macroscopische proporties werden opgeblazen.

Zulke verstoringen zijn er tevens de oorzaak van geweest dat op sommige plaatsen de dichtheid in die 'kosmische soep' iets groter was dan op naburige

[3]De Wilkinson Microwave Anisotropy Probe, WMAP, website is : `http://www.gsfc.nasa.gov/`

plaatsen waardoor de materie onder de eigen zwaartekracht begon ineen te vallen om zo de eerste struktuur te vormen waaruit de (clusters van) sterrenstelsels onstonden[4].

Om deze struktuurvorming te bestuderen zijn algemeen relativistische (en *ijk-invariante*) technieken ontwikkeld om *storingsrekening* te kunnen doen op een gekromde ruimte. Wij breiden deze theorie (zie de referenties in Hoofdstuk 6) uit om ook temperatuureffecten op de struktuurvorming in het heelal te kunnen onderzoeken. Tot nu toe werd voor het gemak aangenomen dat delokale temperaturen van de verschillende deeltjessoorten in het cosmologische plasma op enig moment en plaats aan elkaar gelijk waren en dat daarvan geen invloed uitging naar de expansie van het heelal. Deze laatste aanname is zeker valide, maar temperatuur (en druk-)verschillen kunnen wel de fluctuaties in de dichtheid beïnvloeden.

We vinden verschillende interessante resultaten. Zo blijkt gravitationele ineenstorting van een dichtheidsfluctuatie in een twee-deeltjes plasma met ietwat verschillende temperaturen tevens tot een toename van dit temperatuursverschil te leiden. Wanneer we de evolutie van de expansie van het heelal zelf even verwaarlozen en op kortere tijdschalen kijken, vinden we dat zowel Langmuir- als ion-acoustische golven opgewekt kunnen worden. Dit zijn de fundamentele golven in een plasma zonder magneetvelden, waarvoor de bijdrage van de druk essentieël is. Waneer we de expansie niet verwaarlozen kunnen we een veralgemenisering van het zogenaamde *Jeans-criterium* afleiden. Dit criterium geeft een minimale lengteschaal waarboven materie gravitationeel gaat invallen. Op kleinere schalen balanceert de druk de zwaartekracht hetgeen leidt tot een *oscillerende* verstoring. Wanneer de gasdruk volledig verwaarloosd wordt, zoals in een heelal gevuld met stof, leidt elke drukverstoring tot een continue ineenstorting op alle schalen.

Afgezien van deze toepassingen is Hoofdstuk 6 een uitbreiding op een succesvolle theorie die tevens geïmplementeerd kan worden in numerieke codes die nauwkeurig de consequenties van bepaalde aannames uitrekenen en testen aan de hand van de waargenomen kosmische achtergrondstraling.

[4]Overigens blijkt uit simulaties dat de dichtheidsverstoringen zoals geïmpliceerd door WMAP niet groot genoeg zijn om op tijd alle struktuur te vormen die we nu waarnemen. Daarbij heeft ook Donkere Materie een rol moeten spelen.

Curriculum Vitae

Joachim Benedictus Moortgat was born on June 15th 1977 in Cologne, Germany, with Belgian nationality but grew up in Leiden, the Netherlands. There he went to a Montessori elementary school and subsequently to the Stedelijk Gymnasium for one year before moving to Utrecht where he continued high school at the Christelijk Gymnasium and passed the Dutch vwo examination in 1997.

After traveling for one year in Oceania and Asia he enrolled as a student at Utrecht University. In the first year he passed separate propaedeutic examinations in *geophysics* and *physics, astronomy, meteorology and physical oceanography*. For the master program he switched from geophysics to physics and later also astrophysics. During these years he was also actively involved in the student association *A-Es*^{2}, took Spanish courses at the *Volks-Universiteit Utrecht* and was teaching assistant for numerous lab- and exercise tutorials. In 2001 he completed two master programs on *theoretical physics* and *astrophysics* with a combined master thesis entitled *Watching Gravitational Waves* under the supervision of Prof. 't Hooft and Prof. Kuijpers.

After giving three colloquia in Italy on the basis of this master thesis and traveling in South America for half a year, he was offered a PhD position on the same subject by Prof. Kuijpers at the new Department of Astrophysics at the Radboud University Nijmegen. Apart from the research presented in this dissertation, a considerable amount of time was spent on teaching duties and outreach and pr for the new department. He presented his work at many international workshops, schools and conferences and in the winter of 2004 he used a Special Tuition Award and Stipend from Caltech (Pasadena, USA) to visit Prof. Phinney and the tapir group of Prof. Thorne for a period of two months.

Currently, he has taken up a postdoctoral fellowship at the Department of Physics and Astronomy at the University of Rochester with Prof. Blackman.

Index